UNIVERSITÀ DEGLI STUDI FIRENZE

DOTTORATO DI RICERCA IN FISICA

CICLO XXVII

COORDINATORE Prof. R. Livi

THE DARK SECTOR AS A METROLOGY EFFECT

effects of the trace of the extrinsic curvature of 3-space on the dark side of the Universe

Settore Scientifico disicplinare: FIS/02

Tutore
Prof. Ruggero Stanga

Dottorando
Dott. Mattia Villani

Co-Tutore
Prof. Luca Lusanna

Coordinatore
Prof. Roberto Livi

Anni 2012/2014

Per chi viaggia in direzione ostinata e contraria,
col suo marchio speciale di speciale disperazione
che tra il vomito dei respinti muove gli ultimi passi
per consegnare alla morte una goccia di splendore,
di umanità,
di verità.

Smisurata preghiera - Fabrizio De André

Butterò questo mio enorme cuore tra le stelle un giorno
giuro che lo farò
e oltre l'azzurro della tenda nell'azzurro
io volerò.
La donna cannone - Francesco de Gregori

ABSTRACT

We consider the hypothesis that Dark Matter (or at least part of it) could be explained as an effect of conventions used on the choice of the spacetime foliation into hyperplanes (the *3-space*) and time and therefore on the convention used for clock synchronization.

In recent works by L. Lusanna and D. Alba on ADM tetrad gravity and its post-Minkowskian and post-Newtonian expansion, it was found that the non local York time $^3\tilde{\mathcal{K}}_{(1)}$ gives a 0.5 PN correction (i.e. at order $O(c^{-1})$) to the particle equation of motion which can be interpreted as a correction to the particle mass depending on the foliation used (and therefore on the convention used on the clock synchronization).

In the introduction we review the modern hypothesis on Dark Matter, ADM tetrad gravity and IAU conventions.

In the following chapters we work out the effects of $^3\tilde{\mathcal{K}}_{(1)}$ on *Pulsar Timing Array* (PTA), *Very Long Baseline Interferometry* (VLBI) and on *redshift* measurements.

Exploiting some similarities between the PN form of ADM tetrad gravity metric and of $f(R)$ theories, we make the ansatz that the spatial part of $^3\tilde{\mathcal{K}}_{(1)}$ has a Yukawa form. Many different guesses can be made for the time-dependent part, we discuss three in particular: the *time-free* ansatz (in which there is no time dependece), the *linear ansatz* (in which the time dependence is assumed linear) and finally we consider the case in which the time dependece is left completely free.

In order to have an idea of the order of magnitude of the parameters

involved and how big is the effect on PTA, VLBI and redshift we fit the rotation curve of M31 (the Andromeda galaxy) which is similar to ours: in this way we will have also an idea of how much Dark Matter can be explained as an inertial effect and which of our models best describe the data.

In the last chapter, we consider other consequences of the use of ADM tg on the Tully-Fisher relation and and finally we ask ourselves if it is possible to explain also Dark Energy in terms of relativistic metrology fitting the 3rd order Taylor expansion of non homogeneous Family II Szekeres cosmological models to SNe data and confronting the results with the ΛCDM one.

CONTENTS

INTRODUCTION

That is the question

Hamlet, Act III, Scene I, W. Shakespeare

Modern cosmology must address an embarrassing question: according to observations, baryonic matter (the one we are all made of) amounts to about 5% of the energy-mass balance of the Universe and radiation to about 0.05% (see [1] and figure I.1), so:

"What is the missing 94.5% made of?"

What we "know" is that this *dark side of the Universe* is made of two different elements: *dark energy* and *dark matter*.

Dark Energy   It amounts to about 68% of the energy-mass content of the Universe [1].

The existence of Dark Energy (DE) is necessary to explain why the expansion of the Universe is accelerating (see [2, 3]); it should behave as a *fluid with negative pressure* in order to overcome gravity, which would, on the contrary, slow it down, and eventually, make the Universe recollapse.

What could DE be?

In the most widely accepted (and most succesful)[1] cosmological model (the ΛCDM model[2]), the Universe is assumed homogeneous and isotropic

---

[1]Its success is somewhat suprising given its simplicity.
[2]Also known as *Concordance Model* or *Standard Model of Cosmology.*

The content of the universe
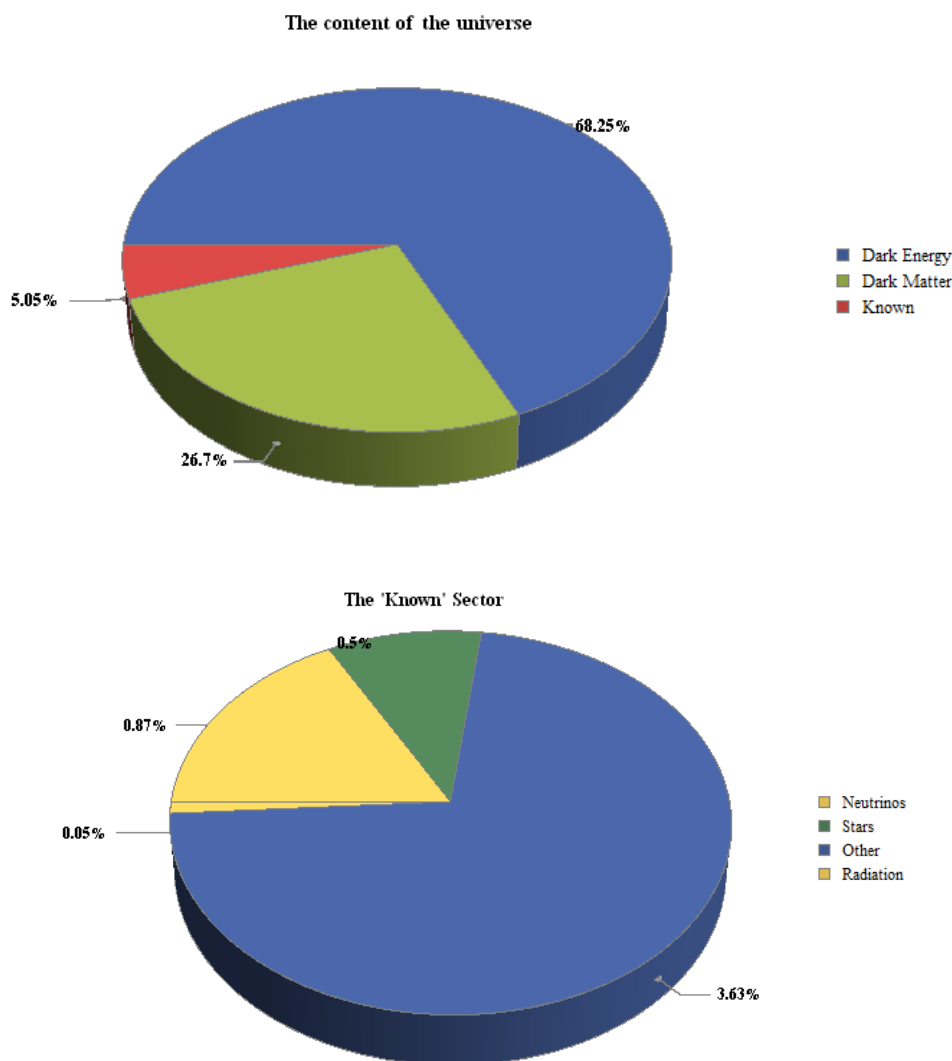
The 'Known' Sector

Figure I.1: Upper chart *The content of the Universe: dark matter (DM, dark green) amounts to 26.7%, dark energy (DE, blue) amounts to 68.25%, baryons and radiation combined (the 'Kown' Sector in red) to 5.05% [1]: we only know what the 5.5% of the universe is, the rest is* the dark side of the universe.

For clarity, in the lower pie chart the 'Known' Sector is further subdivided in **Neutrinos** *(yellow),* **Stars** *(green) and* **Other** *(blue) (the baryons) and* **Radiation** *(yellow).*

Neutrinos*. Their actual density depends on their mass: it ranges from 0.1 to 1 % [4]: we chose 0.87% in the figure, corresponding to a total mass of the three neutrinos of $\sum_\nu m_\nu c^2 = 0.39$ eV (see [5]).*

Other *Contains gas (ionized or not), planets and all other form of baryonic matter known so far (luminous or not).*

All the luminous **Stars** *in the universe amount to only 0.5 % of the total mass (this can be estimated using the mass-to-light ratio in the local universe of from simulation [6]).*

and gravity is described by General Relativity: these two hypothesis restrict the choice of the spacetime metric to the FLRW models [3]; Dark Energy is identified with the cosmological constant Λ, whose value should be given by the energy of void, but the Standard Model particle physics predicts a value which is 10^{121} times bigger than the observed dark energy density (see [16], for example).

On the other hand, an unbroken SuperSymmetry[4] gives $\Lambda \equiv 0$, in fact, for each contribution due to a Standard Model fermion there is a contribution, equal but with opposite sign, due to the corresponding bosonic partner, and viceversa, so the net effect on the void energy is zero [16, 18].

Nevertheless, if the SuperSymmetry is broken, it is possible to have a non null cosmological constant and ease the tension with observations, see [19–22] ([20], for example, reduces the tension between theory and observation by about 60 orders of magnitude).

This is not the only problem with the cosmological constant: there are also

- The *coincidence problem*. The acceleration starts only in a very recent past[5] and it is very difficult to explain why whitin ΛCDM model [16, 23, 24];

- The *initial conditions problem*. One would expect that matter, radiation and DE to have comparable initial density, but matter and radiation had a much higher initial density shortly after the Big Bang: this requires a fine tuning in the initial conditions of the Universe [24].

Other than using the cosmological constant, one could tackle the DE problem in, essentially, two different ways while keeping the hypothesis that the Universe is homogeneous and isotropic [16]: one could modifie the right hand side of the Einstein Equation and introduce a modified form of matter in the stress-energy tensor (scalar fields, such as *quintessence* or *k-essence*), or modifie the left hand side and the action of gravity (for example using

---

[3]The 3-space in FLRW models is maximally symmetric (it has the highest number of Killing vectors compatible with the dimension of the manifold, corresponding to rotational and translational symmetry): see the historical articles [7–12] and the books [13–15].

[4]SuperSymmetry is an attempt to extend the Standard Model of particle physics with the aim to resolve its issues (see [17] for an introductry review).

[5]In fact, it seems that the acceleration starts at redshifts $z \approx 0.65$: approximately when large voids start to from [23].

extended theories of gravity, with the *Galileon* field or the *Chamaleon effect*, see the recent review [25]).

In many recent works, DE and accelerated expansion are considered just a *mirage* (see [23, 24, 26–45] among the others, but literature on this argument is vast and fast growing).[6]

ΛCDM model is based on the hypothesis that the Universe is homogeneous and isotropic at least at large scales,[7] but we can see that it is definitely not true at small scales: matter is clamped in galaxies and galaxies are usually found in clusters and superclusters separated by voids ([47, 48]). These inhomogeneities can be the cause of an apparent accelerated expansion (see [32], among the others): for example, since voids (regions whose density is lower than the average) expand at a faster rate than other regions, a *local void* could explain the accelerated expansion without the need of DE ([29–31, 45], which would just be a consequence of us observers insisting on using a *wrong* homogeneous and isotropic model of the Universe (on this topic see, eg. [27] and references therein and [35, 36], but the literature on the argument is vast). We notice that this is, essentially, a metrology problem. We will come back on this topic in chapter 4.

Dark Matter   It amounts to about 26% of the mass-enegy balance of the Universe [1] and is the main topic of this work.

Dark Matter (DM) is thought to be a non-baryonic form of matter that doesn't emit radiation, which is necessary to explain some observations such as the rotation curve of spiral galaxies, the speed of the galaxies in clusters of galaxies (and therefore cluster's mass) and some aspects of structure formation.

All these topics and some of the hypothesis on DM nature are reviewed in following sections.

---

[6]Studies on inhomogeneous cosmology started many years ago: see [46] and references therein for an older review on the topic.

[7]*How large* is debated, but usually one considers > 300 Mpc [42, 43].

I.1 Why do we need Dark Matter?

The most important "proofs"[8] of the existence of a form of matter that does not interact with electromagnetic radiation are: the mass of galaxy clusters, spiral galaxies rotation curves, gravitational lenses and structure formation, as discussed in the following.

I.1.1 Virial mass of clusters of galaxies

The first evidence of the existence of some dark component of the Universe came in the 1933 when Zwicky esimated the mass of the Coma Cluster using the virial theorem, under the hypothesis that the cluster has a spherical symmetry and that it has reached equilibrium (see [49] for the original paper in german and [50] for a later review in english).

It can be shown, under those hypothesis, that a *lower limit* for the virial mass of the cluster $\mathcal{M}$ is given by:

$$\mathcal{M} > \frac{3}{5} \frac{\mathcal{R}\overline{\overline{v^2}}}{G} \tag{I.1}$$

where $\mathcal{R}$ is the virial radius and $\overline{\overline{v^2}}$ is the mean square velocity on the line of sight of the galaxies (the double overbar, $\overline{\overline{}}$, stands for a mean both in time and galaxy mass, see [49, 50]).

For the Coma Cluster, Zwicky used the measured mean squared line-of-sight velocity $\overline{\overline{v^2}} \approx 5 \times 10^{11}\,\mathrm{km^2 s^{-2}}$ and $\mathcal{R} = 2 \times 10^6$ lyr for the radius of the cluster and found:

$$\mathcal{M} > 4.5 \times 10^{13}\ \mathrm{M_\odot} \quad \text{(virial mass).} \tag{I.2}$$

Since there are about 1000 galaxies in Coma Cluster, using the mean value of $8.5 \times 10^7\ \mathrm{M_\odot}$ for the mass of the single galaxy, Zwicky found:

$$\mathcal{M}_* \approx 8.5 \times 10^{10}\ \mathrm{M_\odot} \quad \text{(luminous matter)} \tag{I.3}$$

for the visible mass of the cluster: a value about 500 times smaller that the virial mass. This means that if only the luminous matter is considered, the

---

[8]We use the quotation marks, because these are not actual proofs of the existence of DM (the *smoking gun* would be an unambiguous direct detection of a WIMP, for example, see section I.2), they are an indication that our understanding of the physics involved in these phenomena is not complete.

cluster couldn't exist, since the speed of the galaxies would be too high for them to be gravitationally bound; therefore, this was his conclusion, there must be some matter in the cluster other than the visible one.

Modern measurements that include in the mass balance also the Intra-Cluster Medium (diffuse hot gas with a temperature of the order of 10^6 K, visible in the X band of the electromagnetic spectrum) give a baryonic to dark matter ratio of the order of about $1 : 6$ (see for example [51], where it is found that $\rho_{bar}/\rho_{DM} \approx 0.17$).[9]

I.1.2   The rotation curve of spiral galaxies

Considering only the visible matter present in a spiral galaxy and calling $v_{rot}(R)$ the velocity of a star at a radius R, from Newtonian gravity, one expects the following behavior for v_{rot}: a linear growth up to a radius R_{max} at which most of the matter is contained, and then one expects $v_{rot} \propto R^{-1/2}$ (in a Keplerian fashion).

Since the works by Vera Rubin and co-workers in the 70's and 80's on the Andromeda galaxy [52] and on other spirals [53, 54], it is known that v_{rot} is actually constant, or grows at large R:[10] this means that the luminous matter is not the only one in the galaxy, there must be a dark component structured in a (almost) spherical halo that surrounds the whole galaxy and extends for hundrends of kiloparsecs, much more than the visible radius of the galaxy itstelf.

Many analytical forms for the density profile and the potential of the DM halo have been proposed in literature: we report here, for later use, the Navarro-Frenk-White (NFW) density profile and the relative potential [55]:

$$\begin{cases} \rho(R) = \rho_0 \left[\dfrac{R}{R_s} \left(1 + \dfrac{R}{R_s} \right)^2 \right]^{-1} \\[2em] \Phi(R) = -4\,\pi\,G\,\rho_0\,R_s^3\,\dfrac{\ln\left[R + R_s\right]}{R} \end{cases} \tag{I.4}$$

where ρ_0 is a parameter with the dimensions of a density and R_s is the scale

---

[9]This esimate is in agreement with the one given by the Plank mission [1], done using the CMB.

[10]See our figure 3.1 (page 76), for an example of rotation curve: blue squares and relative errors are the measured values of v_{rot} for the Adromeda Galaxy up to about 35 kpc and they show a quasi-constant behavoir at large radii (the red line is our fit).

legth of the halo. The NFW profile is in good agreement with the halos obtained in N-body simulations [56].

This profile diverges for $R \to 0$; another profile that does not diverge, but is still in good agreement with N-body simulation, is the Einasto profile [56, 57]:

$$\rho(R) = \rho_0 \, \exp\left[- \left(\frac{R}{k \, R_0} \right)^{1/N} \right]$$

where again ρ_0 is the central value of the density, R_0 is the scale length, k is a dimensionless normalizing constant.

I.1.3   Gravitational lenses

According to General Relativity, matter can act as a lense, bending light from a straight path and deforming the image of background objects [58]; if the image of a background source is highly distorted, magnified or multiplied, we have the *strong* gravitational lensing, if the background object is only slightly deformed (usually elongated) we have *weak* gravitational lensing [58, 59]. *Microlensing* is also possible: when a foreground object passes in front a background one (a star or a quasar), the luminosity of the latter spikes, due to the bending of light ray caused by the mass of the former body.

Both strong and weak lensing have been observed and both call for the existence of DM: visible matter is not enough to explain observations.

Microlensing has been observed too, but has other applications such as the discovery of very faint compact objects in our galaxy (the so-called MACHOs [60] and note 13 on page 10).[11]

I.1.4   Structure formation - Hot and Cold Dark Matter

Last, but not least, the mere existence of large scale structures (LSS) calls for the existence of DM, in the form of cold matter (already non-relativisitc when the LSS formation started).

The problem with LSS formation is twofold. On the one hand, when the collapse of the promordial H-He gas started, it was still too hot: in these conditions the collapse is not efficient and takes too much time, therefore LSS should not yet exist today; moreover, form CMB data, we know that

---

[11]It is also used to discover extrasolar planets.

the inhomogeneities were of the order of 10^{-5} at time of recombination, two orders of magnitude too small to explain the LSS we observe today.

Since DM does not interact with radiation, at the time of collapse, it was colder than baryonic matter and it worked as a potential well allowing visible matter to collapse faster.

LSS formation can also tell if the DM is cold (non relativistic) or hot (relativistic).

N-body simulations such as the *Millennium Run* (in 2005, [61])[12] and the *Bolshoi Cosmological Simulation* (in 2011, [64]) show that LSS evolved through a bottom-up process: first galaxies, then clusters and super-clusters; for this to happen, DM must be cold, since hot DM favors the top-bottom process (structures are born through successive fragmentations of the primordial gas nebula [65]).

I.2 What is Dark Matter?

What could DM be? That's a good question.

Of course, there are black holes, brown dwarves, planets, molecular hydrogen clouds and other forms of ordinary matter that do not emit radiation or that we cannot (yet?) see,[13] but observations cannot be explained with just those objects: according to the general consensus some new form of matter has to be considered, a form of matter that does not interact with electromagnetic radiation, or it would observable.

This is were particle physics, in particular *SuperSymmetry* (SUSY) theories, comes at handy, suggesting the existence of particles, called WIMPs (*Weakly Interacting Massive Particles*), that only interact with other particles through weak or gravitational force (see the reviews [66–68], for example and section 3.4 of [69]).

Depending on which particular SUSY theory is considered, WIMPs could be a *gravitino* (the supersymmetric partner of the graviton), a *neutralino* (the supersymmetric neutral partner of the Higgs boson) or a *sneutrino* (the supersymmetric partner of the neutrino).

Other possible candidates are the *axions*; originally proposed as a solu-

---

[12]And its evolutions the *Millennium II* in 2009 [62] and *Millennium XXL* in 2010 [63]

[13]Indeed, in our galaxy, compact objects were observed in the halo, the so-called MACHOs (*MAssive Compact Halo Objects*) through the microlensing effect [60].

tion to the *strong CP problem* (see [70] for an introductory review), theory predicts that if axions had low mass, the Universe would be filled by these particles produced in the first moments of life of the Universe.

The existence of *sterile neutrinos* (right handed, neutral leptons that only interacts with other particles through gravity [71–73])[14] was also considered as a possible dark matter candidate, but from Planck data it seems that there is no evidence for the existence of additional neutrinos of any kind [1].[15]

Many experiments have been carried out in order to find signals of those particles both in underground facilities or in satellites in orbit around the Earth.

Among the others we cite DAMA/NaI and DAMA/LIBRA [74], CDMS [75], PICASSO [76], PAMELA [77], AMS01 and AMS02 [78], AGILE [79], FERMI-LAT [80], LUX [81] and ICECUBE [82].

In the literature there are some claim of observations, but *none of the particles supposed to constitute DM has ever been observed directly (nor indirectly) in an* unambiguous *way.*

DAMA/NaI (at *National Laboratory of Gran Sasso*), in particular, found a highly debated signal 6.3σ over the bakground, compatible with a neutralino-antineutralino annihilation in the DM halo of our Galaxy [83], but some believe that it might be an effect due to the seasonal expansion and contraction of the atmosphere (see for example [84, 85]).

The satellite PAMELA found an excess of positrons at energy $1.5 < E < 100$ GeV that cannot be explained with the usual theory of primary cosmic rays [86]; this excess was confirmed by AMS02 [87] up to 350 GeV;[16] in [91] authors considered the possibility that the annihilation of neutralinos throught different (leptonic) channels in the DM halo could be the cause of the observed excess, but in [92] the same data are explained considering the emission of positrons from two nearby pulsars (Geminga and Monogem) finding that '*no additional exotic source is required to fit the data*', as they write.

The search for SuperSymmetric particles (not just WIMPs) and *new physics* is also one of the scientific aim of the LHC at CERN (but nothing

---

[14]The can also mix with other neutrinos and interact with the Higgs boson [71–73].

[15]The number of neutrinos is found to be 3.30 ± 0.27 [1].

[16]Similar results were found also by the baloon-borne experiment ATIC in the spectrum of e^+ and e^- [88] and by the satellites AMS01 [89] and FERMI-LAT [90].

has been found up to now [93]).

Another possible explanation for what we call Dark Matter might come from the following question:

"Is it possible that our understanding of gravity is wrong or incomplete?"

Following this line of thought, *MOdified Newtonian Dynamics* (MOND) have been proposed in 1983 by M. Milgrom[94–98] (see [99] for a relativistic version of the theory, so-called TeVeS, from *Tensor-Vector-Scalar*).

This theory suggests that Newtonian gravity is only effective at large accelerations and must be modified at small ones; the scale of acceleration at which modification to Newtonian gravity are effective is of the order of $10^{-8} \, cm \, s^{-2}$, see [95]. MOND theories are in agreement with the great part of the observations [98], but predict too high clusters densty [100].

One could also think of *extended theory of gravitation*, which include General Relativity as a special case (see [101] for a recent review).

In this work we choose:

none of the above.

We explore the idea, first suggested in [102] that what we call DM (or at least part of it) could be a relativistic inertial effect due to the choice of the *splitting of spacetime into space and time* (3+1 slicing), i.e. on the choice of clock synchronization.

A review of ADM Tetrad Gravity (ADM tg) is given in the following sections.

I.3   ADM tetrad gravity

ADM tetrad gravity (ADM tg, [102–109], first developed in [110]) is an Hamiltonian reformulation of General Relativity based on the formalism first developed by R. Arnowitt, S. Deser and C. Misner (hence the acronym ADM) in 1962 [111] (see also the chapter 21 of [112] and chapter 4 of [113], on the hamiltonian formalism for Gauge Systems see [114, 115]); unlike the latter, ADM tg considers tetrads as dynamical quantities, not the 4-metric.

We recall that in the following we use this convention for the signs of the metric: $(+; -, -, -)$; we refer to page 129 for other conventions used in this work.

I.3.1   Generalities

ADM formalism is based on a 3+1 splitting of spacetime, i.e. one foliates the spacetime into "well behaved" hypersurfaces (3-space) parametrized by a function (time); we call them Σ_τ.

As a consequence of the 3+1 splitting, the Einstein Equations also split[17] into a set of 6 dynamical equations (these are the space-space components and actually evolve the metric)[18] and 4 constraints called the Super-Hamiltonian (time-time component) and Super-Momentum constraints (time-space component) ; in addition to these, in both ADM and ADM tg there are 4 more primary constraints given by the conjugate moments to lapse (1 constraint) and shift (3 constraint) connected to the gauge freedom of the choice of the hypersurface of simultaneity (see [103, 116];[19] other (secondary) constraints arise imposing the conservation in time of the primary ones [114, 115].

In ADM tg, the four dimensional spacetime [103, 105]:

- must be globally hyperbolic: in this way the Cauchy problem is well posed (if the initial conditions on a hypersurface $\Sigma_{\tau 0}$ at a time τ_0 are given, it is possible, at least in principle, to calculate at every following time τ all the parameters that specify Σ_τ);

- must be asymptotically Minkovskian (flat);

- must not admit supertranslations; this implies that at spatial infinity, the conserved ADM 4-momentum is orthogonal to Σ_τ: this naturally defines a family of asymptotic inertial observer which can be identified with "fixed stars" (in practice far away objects whose position is known with great accuracy).

- must be topologically trivial (no singularities, no closed time-like geodetics ...) and diffeomorfic to $\mathbb{R}^3$;

- *must not* admit any kind of symmetry (Killing vector), since the Killing equations, in the Hamiltonian formalism, pose new constraints that no one has been able to solve yet.

---

[17]On this point see also [103, 112, 113].

[18]6 equations for the ten components of the metric, so there is a fourfold ambiguity: the choice of coordinate.

[19]These are called primary constraints in Hamiltonian formalism.

On Σ_τ, radar coordinates $\sigma^A = (\tau; \vec{\sigma})$ are defined;[20] the map $\sigma^A \mapsto x^\mu$ (where x^μ are cartesian coordinates in spacetime) gives the embedding of the hypersurfaces into the spacetime manifold.

Σ_τ-adapted cotetrads, ${}^4\mathring{E}_A^{(\alpha)}(\tau, \sigma^r)$, are defined by:

$$
{}^4 g_{AB}(\tau, \sigma^r) = {}^4\mathring{E}_A^{(\alpha)}(\tau, \sigma^r)\, {}^4\eta_{(\alpha)(\beta)}\, {}^4\mathring{E}_B^{(\beta)}(\tau, \sigma^r) \tag{I.5}
$$

and are given by:

$$
\begin{cases}
{}^4\mathring{E}_A^{(0)}(\tau, \vec{\sigma}) = \left(1 + n(\tau, \vec{\sigma})\right)\left(1; \vec{0}\right) = l_A(\tau, \vec{\sigma}) \\[2mm]
{}^4\mathring{E}_A^{(a)}(\tau, \vec{\sigma}) = \left(n_{(a)}(\tau, \vec{\sigma}); {}^3e_{(a)r}(\tau, \vec{\sigma})\right).
\end{cases} \tag{I.6}
$$

Tetrads are given by:

$$
\begin{cases}
{}^4\mathring{E}_{(0)}^A(\tau, \vec{\sigma}) = \dfrac{1}{1 + n(\tau, \vec{\sigma})}\left(1; -n_{(a)}(\tau, \vec{\sigma}){}^3e_{(a)}^r(\tau, \vec{\sigma})\right) = l^A(\tau, \vec{\sigma}) \\[2mm]
{}^4\mathring{E}_{(a)}^A(\tau, \vec{\sigma}) = \left(0; {}^3e_{(a)}^r(\tau, \vec{\sigma})\right).
\end{cases} \tag{I.7}
$$

In the previous equations, $l^A(\tau, \vec{\sigma})$ and its covariant version are the unit vector normal to Σ_τ.

I.3.2   The York canonical basis and the 3-orthogonal gauge

ADM tg phase space has 32 dimensions (16 configurational variables and their conjugate momenta, see [105]), but the degrees of freedom are only 4: the two gravitons' polarizations and their conjugate momenta; all other variables are Hamiltonian constraints and gauge variables.

The two gravitons polarizations and their conjugate momenta degrees of freedom are *hidden* in the triads ${}^3e_{(a)}^r$ and one can *extract* them using the canonical transformations described in [106]; at the end of the procedure the new variables are:

$\varphi_{(a)}$	$\alpha_{(a)}$	n	$\bar{n}_{(a)}$	θ^r	$\widetilde{\phi}$	$R_{\bar{a}}$
$\pi_\varphi^{(a)} \approx 0$	$\pi_\alpha^{(a)} \approx 0$	$\pi_n \approx 0$	$\pi_{\bar{n}}^{(a)} \approx 0$	$\pi_r^{(\theta)}$	$\pi_{\widetilde{\phi}}$	$\Pi_{\bar{a}}$

where:

- The gauge variables are:

  - $\varphi_{(a)}$ and $\alpha_{(a)}$: they describe the arbitrariness in the choice of the tetrad to be associated to the observer (they fix, respectively, the velocity of the observer and the orientation of the associated tetrad in the spacetime);

  - θ^r: it describes the arbitrariness in the choice of the 3-coordinates on Σ;

  - n: it is a measure of the *packing* of the 3-dimensional slices into spacetime;

  - $\bar{n}_{(a)}$ specifies which points on two different slices have the same coordinates;

  * $\pi_{\widetilde{\phi}} \propto {}^3K$: it is the trace of the extrinsic curvature tensor. It describes the arbitrariness in the choice of clock synchronization on Σ;[21][22]

- $\widetilde{\phi}$ (the square root of determinant of the 3-metric) and $\pi_r^{(\theta)}$ (the conjugate momenta of the Euler angles θ^r) are solutions, respectively of the Super-Hamiltonian and Super-Momentum constraints;

- $R_{\bar{a}}$ are the two (non-linear) gravitons and $\Pi_{\bar{a}}$ are their conjugate momenta;

- All the other variables (they are only conjugate momenta) are constraints (this is indicated as ≈ 0).

The natural gauge in this formalism is the so-called *3-orthogonal Schwinger time gauge* [121], where one imposes [108]:

$$\varphi_{(a)} \approx 0; \qquad \alpha_{(a)} \approx 0; \qquad \theta^r \approx 0. \tag{I.8}$$

No natural gauge is known for the extrinsic curvature, but we shall see in chapter 2 that at a Post-Newtonian (PN) level it is possible to make an ansatz for the mathematical form of its spatial part.

As we shall see, we cannot say anything about the time dependence so we shall make different guesses and explore their cosequences.

---

[21]This is also the *York extrinsic internal time*, hence the name of the canonical transformation (on the York time and on the problem of time in General Relativity, see [103, 106] and [119, 120]).

[22]The fact that this is the only momentum among gauge variables is a consequence of the Lorentzian signature of the metric.

I.3.3   Linearization of ADM tg - Weak field approximation

Usually, in General Relativity, the weak field approximation is carried out by postulating a metric of the form [13, 112, 122]:

$$
{}^4g_{\mu\nu} = {}^4\eta_{\mu\nu} + {}^4h_{\mu\nu}; \qquad \left(|h_{\mu\nu}| \, ; \, \left|\partial_\alpha \, {}^4h_{\mu\nu}\right| ; \, \left|\partial_\alpha\partial_\beta {}^4h_{\mu\nu}\right| \right) \ll 1, \qquad (I.9)
$$

where ${}^4h_{\mu\nu}$ is a small perturbation of the flat background.

One usually simplifies the form of the Einstein Field Equations by exploiting the gauge transformation:

$$
{}^4\bar{h}_{\mu\nu} \mapsto {}^4\bar{h}_{\mu\nu} + \partial_\mu\xi_\nu + \partial_\nu\xi_\mu \qquad (I.10)
$$

and requiring that:

$$
\Box\,\xi_\mu = 0, \qquad \partial^\mu \, {}^4\bar{h}_{\mu\nu} = 0, \qquad (I.11)
$$

where ${}^4\bar{h}_{\mu\nu}$ is the transverse traceless perturbation. This gauge is called *harmonic* or *de Donder* gauge.

In ADM tg, the weak field approximation is equivalent to a linear approximation of the theory and can be implemented imposing [108]:

$$
{}^4g_{AB} = {}^4\eta_{AB} + {}^4h_{AB}, \qquad (I.12)
$$

where now ${}^4\eta_{AB}$ is the *asymptotic* flat Minkowsky metric and, if $\zeta \ll 1$ is a smallness parameter:

$$
{}^4h_{AB} = O(\zeta) \quad \text{and} \quad {}^4h_{AB} \longrightarrow 0 \text{ at spatial infinity.} \qquad (I.13)
$$

It can be shown (see [108]) that the metric components are given by:

$$
{}^4g_{\tau\tau} = 1 + 2\,n_{(1)}; \qquad (I.14)
$$

$$
{}^4g_{\tau r} = -\bar{n}_{(1)(r)}; \qquad (I.15)
$$

$$
{}^4g_{rs} = -\delta_{rs}\left[1 + 2\left(\Gamma_r^{(1)} + 2\,\phi_{(1)} \right) \right]. \qquad (I.16)
$$

In paper [108] the weak field approximation was used to study charged particles (with a Grassmannian cut-off of self energy) with electromagnetic field in a curved spacetime: all the standard results were reproduced.

I.3.4   Post-Newtonian expansion

Whitin the weak field approximation one can study the slowly moving particle approximation ($v \ll c$): this is a Post-Newtonian (PN) approximation, [102].

Considering only uncharged particles and no electromagnetic field, in [102] it was shown that at order $O(c^{-2})$, the first PN order, one has:

$$n_{(1)} = -\frac{U}{c^2} - \frac{1}{c}\frac{\partial}{\partial t}\,^3\widetilde{\mathcal{K}}_{(1)};\tag{I.17}$$

$$\bar{n}_{(1)(r)} = \frac{\partial}{\partial\,\sigma^r}\,^3\widetilde{\mathcal{K}}_{(1)};\tag{I.18}$$

$$\phi_{(1)} = \frac{U}{2c^2};\tag{I.19}$$

$$\Gamma_r^{(1)} = O(c^{-4}),\tag{I.20}$$

where $^3\mathcal{K}_{(1)}$ is the PM approximation (at order $O(\zeta)$) of the non-local trace of the extrinsic curvature, given by:[23]

$$^3\mathcal{K}_{(1)}(\tau,\vec{\sigma}) = \frac{^3K}{\Delta} = -\frac{1}{4\pi}\int d^3\sigma_1\,\frac{^3K(\tau,\vec{\sigma}_1)}{|\vec{\sigma}_1 - \vec{\sigma}|};\tag{I.21}$$

and at first order in the PN approximation, one sets [102]:

$$^3\mathcal{K}_{(1)}(\tau,\vec{\sigma}) \mapsto {}^3\widetilde{\mathcal{K}}_{(1)}(t,\vec{\sigma}).\tag{I.22}$$

The equations of motion of the i-th particle with mass m_i at the 0.5 PN order are:

$$m_i\vec{a}_i = -m_i\,\vec{\nabla}U - m_i\,\frac{\vec{v}_i}{c}\frac{d^2}{dt^2}\,^3\widetilde{\mathcal{K}}_{(1)},\quad i = 1,\dots,N.\tag{I.23}$$

The 0.5 PN term (the one at order $O(c^{-1})$) is a damp or anti-damp force, depending on the sign of the total derivatives.

Equation (I.23) can also be recast in the following, more evocative, form:

$$\frac{d}{dt}\left[m_i\left(1 + \frac{1}{c}\frac{d}{dt}\,^3\widetilde{\mathcal{K}}_{(1)}\right)v_i\right] = -m_i\,\vec{\nabla}U.\tag{I.24}$$

This means that the particle has a (position and velocity dependent) mass whose value depends also on the non local extrinsic curvature $^3\widetilde{\mathcal{K}}_{(1)}$. *Hence the particle's mass depends on the choice of the 3+1 splitting and*

---

[23]Δ is the Laplacian in flat metric, Δ^{-1} its Green function. It is possible to use the flat operator, since $^3\widetilde{\mathcal{K}}_{(1)}$ is already at first order in PM expansion (linearization).

on the choice of the clock synchronization: this leads to a violation of the equivalence principle *only in 3-space, not* in the spacetime [102, 109].

The additional 0.5 PN term can therefore be interpreted as DM, which would be, in this case, only an *inertial relativistic effect* [109].

I.3.5 DM signatures in ADM tg

In paper [102], some of the observational signatures of DM were studied.

- One can show that the *Virial theorem*, used, for example, by Zwicky in his estimate becomes:

$$\frac{1}{2} m \langle v^2 \rangle = -\frac{1}{2} \langle U \rangle + \frac{m}{2c} \left\langle (\vec{r} \cdot \vec{v}) \frac{d^2}{dt^2} {}^3\widetilde{\mathcal{K}}_{(1)} \right\rangle. \qquad (I.25)$$

  This leads to:

$$M = M_{\text{baryon}} + M_{DM}, \qquad M_{DM} = \frac{\mathcal{R}G}{c^2} \left\langle (\vec{r} \cdot \vec{v}) \frac{d^2}{dt^2} {}^3\widetilde{\mathcal{K}}_{(1)} \right\rangle. \ (I.26)$$

  Here, $\langle \dots \rangle$ stands for a time average over a time longer than any internal dynamical time scale.

- *Weak gravitational lensing* The deviation angle is given by:

$$\alpha = M \frac{4G}{c^2} \frac{\vec{\xi}}{|\xi|}, \qquad (I.27)$$

  where $\vec{\xi}$ is the impact parameter of the light ray. This equation leads to:

$$M = M_{\text{baryon}} + M_{DM}, \qquad M_{DM} = -2 \frac{c^2}{G} \partial_t {}^3\widetilde{\mathcal{K}}_{(1)} |\vec{\sigma}|. \qquad (I.28)$$

- *Rotation curve of spiral galaxies*[24] From the equation of motion (I.23), under the hypothesis that the particle is moving on a circular orbit ($R = $ constant), we can get the rotation curve of the galaxy by equating (I.24) to the cetrifugal force and imposing:

$$v = v_0 + v_{(1)},$$

---

[24]This is different from the procedure used in [102], which leads to a formula (equation (6.16) section VI.D) valid only at large distance $R > R_{max}$ where R_{max} is the distance of the farthest particle. Our equation (I.30), on the contrary, is valid for every galactic distance.

where v_0 is given by the gravitational potential and $v_{(1)}$ is a first order (i.e. $v_{(1)}/v_0 \ll 1$) correction.

The final result is:[25]

$$v^2 = v_0^2 \left(1 - \frac{R}{v_0} \frac{1}{c} \frac{d^2}{dt^2} \widetilde{\mathcal{K}}_{(1)} \right) ; \qquad (\text{I.29})$$

$$v = v_0 \left(1 - \frac{1}{2} \frac{R}{v_0} \frac{1}{c} \frac{d^2}{dt^2} \widetilde{\mathcal{K}}_{(1)} \right) , \qquad (\text{I.30})$$

where in the second line we took the square root and used the fact that the second term between parethesis is *small*.

As seen in section I.3.4, the conventions used in astronomy and metrology are of paramount importance, since the function $^3\widetilde{\mathcal{K}}_{(1)}$ and the amount of DM depend on them, therefore in the following section we review the current conventions.

I.4   A review on relativistic metrology

In General Relativity, there is no preferred coordinate system, but astronomy, astrophysics, satellite tracking and high precision positioning ask questions like *'Where is this planet right now?', Where will it be in ten years from now?, 'Where is the ISS?'* (the International Space Station), and so on. To answer this kind of questions one is forced to introduce a definite coordinate system and this procedure necessarily involves the use of conventions defining the reference system (axis orientation and their origin) and the reference frame (the practical realization of the reference system, i.e. a set of objects whose position is known with great accuracy).[26]

In recent years, General Relativity has become important in high precision positioning (in missions like GAIA[27] for example, in which microar-

---

[25]As proven in [108], $^3\widetilde{\mathcal{K}}_{(1)}$ has the dimension of a distance, so the dimensional analysis is correct.

[26]In Newtonian theory the problem of choosing a reference system does not exist since there are preferred systems and observables are easily related to it.

[27]GAIA (Global Astrometric Interferometer for Astrophysics) is an ESA satellite devoted primarily to the creation of a catalogue of about 10^9 stars, measuring with high precision their position and its change in time (i.e. the peculiar motionof the star), brigthness and other astrophysical parameters [123].

GAIA was launched on December 2013, but the first data won't be available until 2017.

cosecond precision can be achieved) and in high precision time measurements (Pulsar Timing Array, PTA [124], and Very Long Baseline Interferometry, VLBI [125], see also chapter 1), therefore it is necessary to give an explicit definition of the metric, the gauges and the coordinate system to be used and tranformation functions between different coordinate systems.

It is also necessary to specify *what* to measure, since, when General Relativity is involved, great care must be used, and, especially in time and velocity measurements, one has to be careful to point out which quantity is referred to which observer and reference system: observer independent quantities are, therefore, to be preferred.

The International Astronomical Union (IAU[28]) is in charge of these conventions; here we review their resolutions on reference systems and frames and the convention on measurements (the resolutions reviewed here were adopted in 2000 [126] and updated in 2006 [127]).

I.4.1   Reference systems and frames

ICRS *The International Celestial Reference System.* A kinematically non-rotating reference system (its axis are fixed with respect objects whose position is known with great accuracy); its origin is set in the Solar System Barycenter.

Its realization is the ICRF (*International Celestial Reference Frame*): until 2009 the ICRF1 was used (it was a catalogue of 608 extragalactic radio sources evenly distributed on the celestial vault [125]) and since 2009 the ICRF2 (a caltalogue of 3414 compact radio sources) is used [128].

ICRS is the reference system to be used in cosmological observations and, for example, tests on the *Cosmological Principle*.

BCRS *BariCentric Reference System.* A kinematically non rotating reference system whose origin is set at the Solar System Barycenter.

---

[28]http://www.iau.org/

Its metric is defined as follows:

$$^4g_{00} = 1 - 2\,\frac{w}{c^2} + 2\,\frac{w^2}{c^4};$$
$$^4g_{i0} = -4\,\frac{w^i}{c^3};$$
$$^4g_{ij} = -\delta_{ij}\left(1 + 2\,\frac{w}{c^2}\right);$$

(I.31)

with:

$$w(t,x) = G\int d^3x'\,\frac{\sigma(t,x')}{|x-x'|} + \frac{G}{2c^2}\,\frac{\partial^2}{\partial t^2}\int d^3x'\,\sigma(t,x')\,|x-x'|, \quad \text{(I.32a)}$$

$$w^i(t,x) = G\int d^3x'\,\frac{\sigma^i(t,x')}{|x-x'|}, \quad \text{(I.32b)}$$

where σ and σ^i are, respectively, the mass density and current density.

Time is *coordinate time*, and is denominated TCB.

The de Donder gauge has to be used.[29]

BCRS is the reference system used for ephemeris measurements, satellite tracking within the Solar System, ...

Moreover, IAU recommends that all measurements (of position, velocity, ...) are to be referred to this reference system.

Its axes are directed as the ICRS' ones [127].

In BCRS Solar System is supposed to be isolated, but one can show that the acceleration due to the galaxy is negligible and so are cosmological effects (see [129, 130]).

GCRS *GeoCentric Reference System*. BCRS is not convenient for the modelling of the Earth and its surroundings since in this reference system the Earth moves, and therefore it experiences a Lorentz contraction in the direction of the motion; moreover the Earth's speed is not constant during the year (because the orbit is not circular and because of the interaction with other planets) so the contraction changes: this means that the distance between two point would change with time[30] and the description of satellite orbits would be a very, very hard task. This is why a new reference is introduced: the GCRS.[31]

---

[29]Because, quoting, 'considerable work has been done with this gauge' [126].

[30]As we will see this is important for VLBI.

[31]Similar reference systems are introduced also for other planets and are used, mostly, when describing the orbits of deep space satellites.

GCRS is a kynematically non-rotating reference system with respect to BCRS and whose origin is set at the center of the Earth.

Its metric is defined to be:

$$G_{00} = 1 - 2\,\frac{W}{c^2} + 2\,\frac{W^2}{c^4};$$
$$G_{i0} = -4\,\frac{W^i}{c^3};$$
$$G_{ij} = -\delta_{ij}\left(1 + 2\,\frac{W}{c^2}\right);$$

(I.33)

where the potential W is split into a terrestrial component W_E (due only to the Earth mass) and an external tidal component due to the presence of the rest of the Solar System W_{ext}:

$$W = W_E + W_{\text{ext}}.$$

(I.34)

The same goes for W^i; Earth potentials are defined in the same way as (I.32).

Time is *coordinate time* and is denominated TCG.

The de Donder gauge has to be used.

GCRS is a local reference system for Earth-based measurements.

Its axes are oriented as the BCRS' one.

One goes from TCG to TCB, using the formula (valid at first PN order):

$$T = t\,(1 + L_C) - \frac{1}{c^2}\left[\vec{v}_E \cdot \vec{r}_E + \int dt'\left(\frac{1}{2}\,v_E^2 + w_{\text{ext}}\right)\right]$$

(I.35)

where:

$$L_C = \frac{TCG}{TCB};$$

it is a constant that is a combination of Earth rotational speed and of the gravitational potential W_E at its surface (see section 1.6 for details).

Last, but not least, if the observer is a satellite with a negligible mass, one has to consider a different reference system, called the *Local* one. Again the metric is similar in form to the previous two, but in the potentials one has to consider only the *external* (tidal) term in (I.34).

I.4.2 Conventions on measurements

Six quantities are needed to define the phase space of an object: its position and its velocity.

If, in the BCRS, the position of an object is written as:

$$\vec{r}_* = \widehat{u}\, r_*,$$

the astrometric parameters are [131]:

- The position of the object on the celestial sphere (the direction of $\widehat{u}$) given by two angles: the *right ascension*, α and the *declination*, δ;[32]

- *Parallax* $\Pi = \dfrac{A}{r_*}$, where A is the Astronomical Unit (the mean radius of Earth orbit).
  Parallax gives the third spatial coordinate;

- The *proper motion* of the object $\vec{\mu} = \dfrac{d\widehat{u}}{dt_B}$ (where t_B is the time in the BCRS);

- The *astrometric radial velocity* is the last of component of the velocity of the object and is defined as $\rho = \dfrac{dr_*}{dt_B} = d\left(\dfrac{A}{\Pi}\right)/dt_B$.

The case of spettroscopy

Often, the radial velocity is measured using spettroscopic techniques, measuring the redshift of the object and inverting the formula (valid in the BCRS, [131]):

$$1 + z = \left(1 + \frac{\rho}{c}\right)\left(1 + \frac{U}{c^2} + \frac{1}{2}\frac{v^2}{c^2}\right). \tag{I.36}$$

At first order, one has, indeed:

$$\rho = cz, \tag{I.37}$$

but there are too many unknowns in the higher order terms (see references [131–134])[33]: the potential U at the source position is given by numeric simulations of stellar dynamics and gives corrections of the order of 100 m/s

---

[32]They are respectively a 'longitude' and a 'latitude'.

[33]Gaining control over these unknows is highly desirable (but not feasiblein the near future [131]) if the spectroscopic measurements of the radial velocity have to rival with the astrometric ones, which can have an accuracy of the order of 1 m/s [131].

(gravitational redshift), but one should also consider the effects of convective motions on the surface of the star which gives corrections of the order -1000 m/s (it is a blueshift, but its actual value strongly depends on the source), atmospheric oscillations and other phenomena[34]; the v^2 term, which contains transverse Doppler effect, is not well known either [133].

All those unknowns are summed up in a $X-$term, and (I.36) is rewritten as [133]:

$$1 + z = \left(1 + \frac{\rho}{c}\right) \left(1 + \frac{U}{c^2} + \frac{1}{2} \frac{v^2}{c^2}\right) (1 + X) \qquad \text{(I.38)}$$

Because of the $X-$term, typically, the spectroscopically determined radial velocity differs from the *correct* astrometric one by several hundrends of m/s [132].

---

[34]See [131, 132] for the exaustive list of all the phenomena that contribute to the uncertainty of the radial velocity

I.5 This work & ADM tg vs IAU conventions

In this work we will use the PN metric defined by eqs. (I.14) to (I.20) given in section I.3.4; it has the from:

$$^4g_{\tau\tau} = 1 - \frac{2}{c}\,\partial_t\,^3\widetilde{\mathcal{K}}_{(1)} - \frac{2}{c^2}\,U \qquad (I.39)$$

$$^4g_{\tau r} = -\partial_r\,^3\widetilde{\mathcal{K}}_{(1)} \qquad (I.40)$$

$$^4g_{rs} = -\delta_{rs}\left(1 + 2\,\frac{U}{c^2}\right) \qquad (I.41)$$

This metric is the one to be used to define the reference systems within the ADM tg formalism.

Confronting this one with the metric of IAU conventions, we have additional terms depending on the the non-local extrinsic curvature $^3\widetilde{\mathcal{K}}_{(1)}$ and its derivatives: this correspond to a *redefinition of the proper time* of the observer and to the introduction of *frame dragging effects*.[35]

Usually it is assumed that a metric of the form:

$$ds^2 = \left(1 - 2\,\frac{U}{c^2}\right)c^2\,dt^2 - \left(1 + 2\,\frac{U}{c^2}\right)dx^i\,dx^j \qquad (I.42)$$

where U is the potential, will describe the propagation of light in the galaxy at order $O(c^{-2})$. One can show that this metric has an extrinsic curvature tensor of order $O(c^{-3})$, so the metric is, at the considered order, *flat.*

We will calculate explicitly the extrinsic curvature tensor of our metric in chapter 2 and we will see that it has additional terms at the highest order: we will see, in fact that it has the form:

$$^3K_{rs} = \partial_r\partial_s\,^3\widetilde{\mathcal{K}}_{(1)} + \delta_{rs}\left(\frac{1}{3}\,^3K_{(1)}\right) + O(c^{-3})$$

where $^3K_{(1)}$ is the trace of the extrinsic curvature, while $^3\widetilde{\mathcal{K}}_{(1)} = \dfrac{^3K_{(1)}}{\Delta}$ is the non-local York time.

We notice that using a *Constant Mean Curvature*-like gauge (CMC-like), in which $^3K_{(1)} = constant$,[36] in particular $^3K_{(1)} \equiv 0$, we recover the metric

---

[35]The frame dragging effect is present also in the usual formalism but apperas at the order $O(c^{-3})$.

[36]This is not an "exact" CMC gauge, since we are only fixing the first order of ^3K.

and the results of the usual treatment (losing at the same time the chance to explain the DM phenomenon as a relativistic inertial effect).

We are *not* using the de Donder gauge, but the 3-orthogonal one, because, as explained in section I.3.2 the 3-orthogonal gauge is the natural one in ADM tg.

Astrometric quantities do not depend on the extrinsic curvature, and therefore are carried over in ADM tg without modifications.

On the contrary, we will see that additional terms depending on derivatives of ^3K will appear (see chapter 2): in a perfect world, confronting the spectroscopic radial velocity and the one predicted by ADM tg would give an idea of the mathematical form of $^3\widetilde{\mathcal{K}}_{(1)}$, but as we saw in section I.4.2 there are too many unknowns in the redshift formula, so this is not feaseble (at least in the near future), in contrast to what was stated in [102], section IV.A.1.

I.6 Plan of the work

In the following chapter, we will calculate analytically at the first PN order the effects of the extrisic curvature on Pulsar Time Array (PTA) and on Very Long Baseline Interferometry (VLBI) and on redshift.

Since we are not using all of the IAU conventions, in particular, since our metric is different than the recommended one, we shall also give an explicit expression of the Lorentz transformations that link two different coordinate system: this is necessary since measurements are often done on the Earth within the GCRS system, but, conventionally, have to be reported in the BCRS.

In chapter 2 we shall exploit some similarities between our PN metric and the one given by PN expansion of $f(R)$ theories in order to guess the spatial part of $^3\widetilde{\mathcal{K}}_{(1)}$. Time dependence is still unknown, so we shall discuss different ansatz for the time-dependent part and, finally, we shall rewrite the results of chapter 1 using these ansatz.

In chapter 3, we shall fit the rotation curve of M31 and estimate the value of the parameters involved: in this way we can have an idea of how much DM can be explained as an inertial effect under different hypothesis on the time dependence.

With these values, we shall calculate the order of magnitude of the expected delay in the time of arrival of light from some of the isolated pulsars quoted in [124].

In chapter 4 we shall study the effect of the non-local York time on the Tully-Fisher relation (we shall find that it changes the behavior of the relation at small velocities, as is often observed) and we will ask if it is possible to explain also the acceleration of the universe and the DE in terms of relativistic metrology.

CHAPTER 1

CALCULATIONS

In the introduction, we gave our definition of the metric at the PN order: the presence of 0.5 PN terms proportional to ${}^{3}\widetilde{\mathcal{K}}_{(1)}$ will affect the propagation of light in the spacetime; therefore, in this chapter we shall give the general expression of the null geodetics in PN ADM tg metric.

Looking for some observational signature of the effects of our additional 0.5 PN term, we shall calculate the correction to Pulsar Timing Array (PTA), Very Long Baseline Interferometry (VLBI) and to redshift due to the presence of ${}^{3}\widetilde{\mathcal{K}}_{(1)}$.

Finally, measurements are usually carried out on the Earth (or on satellites), but, by convention, they must be referred to the BCRS (see [126, 127] and section I.4.1); since we are not using the metric recommended by the IAU, we shall also calculate our transformation law between two different inertial reference systems (at PN order) and compare it to equation (I.35) as given by IAU.

1.1   The embedding of the hypersurface

As said in the introduction, section I.3.1, on the hypersurface Σ_τ, we define radar coordinates σ^A;[1] the embedding of Σ_τ into the spacetime manifold is given by the map:

$$\sigma^A \mapsto x^\mu = z^\mu(\tau, \vec{\sigma}).$$

Now, if we define the 4-coordinates x^μ to be centered on the world line $x^\mu(\tau) = \left(x^0(\tau); \vec{0}\right)$, the world line of a time-like observer fixed at position 0, Σ_τ is given by the condition $x^0(\tau) = const$: in this way Σ_τ are hypersurfaces of simultaneity.

Finally, if the aforementioned world line is the one of an asymptotic observer, the embedding of Σ_τ into the spacetime manifold is given by [102]:

$$z^\mu(\tau, \vec{\sigma}) = x_0^\mu + \epsilon_A^\mu \, \sigma^A, \tag{1.1}$$

where:

$$\epsilon_\tau^\mu = (1; \vec{0}) \quad \text{and} \quad \epsilon_r^\mu = (0; \delta_r^i) \tag{1.2}$$

are the flat asymptotic tetrads.

Equations (1.1) and (1.2) define the embedding that we shall use in the following.

1.2   Null geodetics

In this section we shall give the expression of the Post-Newtonian expansion of the null geodetics, written as $y^\mu(s) = \epsilon_A^\mu \, \sigma^A(s) + y^\mu(0)$.

We call s the affine parameter; it is defined in such a way that the observer is at $s = 1$ and the source is at $s = 0$.

We define $p_A(s) = d\sigma_A(s)/ds$, and we set $b_A = p_A(0)$, in this way $k^\mu(s) = \epsilon_A^\mu \, p^A(s)$ is the (null) tangent vector to the geodetic.

Geodesic equations are [102, 112, 122]:

$$\frac{dp^A(s)}{ds} = \frac{d^2\sigma^A(s)}{ds^2} = -{}^4\Gamma_{BC}^A \, p^B \, p^C. \tag{1.3}$$

The relevant PM Christoffel symbols can be calculated with the formula [102, 112, 122]:

$$\Gamma_{BC}^A = \frac{1}{2} \, {}^4\eta^{AD} \left[{}^4g_{(1)\,DB,C} + {}^4g_{(1)\,DC,B} - {}^4g_{(1)BC,D} \right]$$

---

[1]With the caveats described in [107, 117, 118].

where ${}^4 g_{(1)\,AB}$ is the first PM order of the metric; their explict expression is given in [102], section 2.F.

1.2.1 Post Minkowskian expansion

Post Minkowskian null geodesics in ADM tg were first calculated in [102], here we briefly review the result: in the following subsection we shall calculate the Post Newtonian expansion.

We have to impose the condition that the geodetics are light-like, so we have to write:

$$
{}^4 g_{AB}\, b^A\, b^B = 0, \tag{1.4}
$$

where the PM metric ${}^4 g_{AB}$ is given in (I.14)-(I.16). This means that only three of the four components of b^A are free parameters: we choose the spatial ones, which represent the direction of emission of the light ray.

Substituting the definition of the metric (eqs. (I.14) to (I.16)) in equation (1.4) leads, therefore, to a condition on b^τ, which, at PM order, can be written as:[2]

$$
b^\tau = \pm \sqrt{\vec{b}^2} + c_{\pm(1)}(\tau_0, \vec{\sigma}_0), \tag{1.5}
$$

$$
\begin{aligned}
c_{(1)\pm}(\tau_0,\vec{\sigma}_0) =\; &\mp \sqrt{\vec{b}^2} \left[n_{(1)}(\tau_0,\vec{\sigma}_0) + \sum_r (b^r)^2 \left(\Gamma_r^{(1)} + 2\,\phi_{(1)} \right)(\tau_0,\vec{\sigma}_0) \right] + \\
&+ \sum_r b^r\, \bar{n}_{(1)(r)}(\tau_0,\vec{\sigma}_0),
\end{aligned} \tag{1.6}
$$

where the plus sign is for future oriented geodetics, while the minus sign is for past oriented ones.

In the following we will only consider future oriented geodesics (as seen from the source).

---

[2]We take the opportunity to correct the wrong formula (4.1) for the definition of $c_{(1)\pm}(\tau_0, \vec{\sigma}_0)$ in [102].

Integrating equation (1.3), we find:

$$\sigma^r(s) = \sigma^r(0) + b^r s + \tag{1.7}$$

$$- \int_0^s ds_1 \int_0^{s1} ds_2 \, \vec{b^2} \left[\partial_r \, n_{(1)} + \partial_\tau \bar{n}_{(1)(r)} \right] (\sigma_0 + b_0 s_2) +$$

$$- \int_0^s ds_1 \int_0^{s1} ds_2 \, 2\sqrt{\vec{b^2}} \sum_u b^u \Big[\delta_{ur} \, \partial_\tau \left(\Gamma_r^{(1)} + 2\phi_{(1)} \right) +$$

$$- \frac{1}{2} \left(\partial_r \, \bar{n}_{(1)(u)} - \partial_u \, \bar{n}_{(1)(r)} \right) \Big] (\sigma_0 + b_0 \, s_2) +$$

$$- \int_0^s ds_1 \int_0^{s1} \sum_{uv} b^u \, b^v \Big[2\delta_{ru} \, \partial_v \left(\Gamma_r^{(1)} + 2\,\phi_{(1)} \right) +$$

$$- \delta_{uv} \, \partial_r \left(\Gamma_u^{(1)} + 2\,\phi_{(1)} \right) \Big] (\sigma_0 + b_0 s_2)$$

for space components, while for the time one, we have:

$$\tau(s) = \tau_0 + \left(\sqrt{\vec{b^2}} + c_{(1)+}(\tau_0, \vec{\sigma}_0) \right) s + \tag{1.8}$$

$$- \int_0^s ds_1 \int_0^{s1} ds_2 \left(\vec{b^2} \, \partial_\tau n_{(1)} + 2\sqrt{\vec{b^2}} \sum_u b^u \, \partial_u n_{(1)} \right) (\sigma_0 + b_0 \, s_2) +$$

$$- \int_0^s ds_1 \int_0^{s1} \sum_{uv} b^u b^v \left[-\frac{1}{2} \left(\partial_u \, \bar{n}_{(1)(v)} + \partial_v \, \bar{n}_{(1)(u)} \right) \right] (\sigma_0 + b_0 s_2) +$$

$$- \int_0^s ds_1 \int_0^{s1} ds_2 \, \vec{b^2} \, \partial_\tau \left(\Gamma_r^{(1)} + 2\phi_{(1)} \right) (\sigma_0 + b_0 s_2).$$

1.2.2 Post Newtonian expansion

Substituting eqs. (I.17) to (I.20) in (1.6), we find:

$$c_{(1)\pm}(\tau_0, \vec{\sigma}_0) = \mp \sqrt{\vec{b^2}} \Bigg[-\frac{1}{c} \, \partial_t \, {}^3\widetilde{\mathcal{K}}(\tau_0, \vec{\sigma}_0) - \frac{U(\tau_0, \vec{\sigma}_0)}{c^2} +$$
$$+ \sum_r (b^r)^2 \, \frac{U(\tau_0, \vec{\sigma}_0)}{c^2} \Bigg] + \sum_r b^r \, \partial_r \, {}^3\widetilde{\mathcal{K}}(\tau_0, \vec{\sigma}_0) \tag{1.9}$$

while equation (1.7) gives:

$$\sigma^r(s) = \sigma^r(0) + b^r s + \frac{2}{c^2} \int_0^s ds_1 \int_0^{s_1} ds_2 \, \vec{b^2} \, (\partial_r U) \, (\sigma_0 + b_0 s_2) + \tag{1.10}$$

$$- \frac{2}{c^2} \int_0^s ds_1 \int_0^{s_1} ds_2 \, b^r \, b^v \, (\partial_v U) \, (\sigma_0 + b_0 \, s_2).$$

Multiplying the last equation by b^r,[3] integrals simplify, so we can find a simple relation between the affine parameter s (and its differential and

---

[3] b^r are constant vectors and can go in and out of the integrals.

derivative) and σ^r:

$$b_r \left[\sigma^r(s) - \sigma^r(0)\right] = \vec{b}^2 s$$

$$\Downarrow$$

$$s = \frac{b_r}{\vec{b}^2} \left[\sigma^r(s) - \sigma^r(0)\right], \tag{1.11}$$

$$ds = \frac{b_r}{\vec{b}^2} d\sigma^r, \tag{1.12}$$

$$b^r \frac{\partial}{\partial \sigma^r} = b^r \frac{\partial s}{\partial \sigma^r} \frac{\partial}{\partial s} = \frac{d}{ds}. \tag{1.13}$$

More over, at the highest order one finds:[4]

$$\frac{\vec{\sigma}(s) - \vec{\sigma}(0)}{|\vec{\sigma}(s) - \vec{\sigma}(0)|} = \frac{\vec{p}(s)}{|\vec{p}(s)|} = \frac{\vec{b}}{|\vec{b}|} + O(\zeta; c^{-2}), \tag{1.14}$$

so $-\widehat{p}(s) \approx -\widehat{b}$ is the unit vector that gives the direction of observation and all previous equations (1.9)-(1.13) simplify:

$$c_{(1)\pm}(\tau_0, \vec{\sigma}_0) = \pm \frac{1}{c} \partial_t \, {}^3\widetilde{\mathcal{K}}_{(1)}(\tau_0, \vec{\sigma}_0) + \sum_r b^r \, \partial_r \, {}^3\widetilde{\mathcal{K}}_{(1)}(\tau_0, \vec{\sigma}_0); \tag{1.15}$$

$$\sigma^r(s) = \sigma^r(0) + b^r s + \frac{2}{c^2} \int_0^s ds_1 \int_0^{s_1} ds_2 \, (\partial_r U) \, (\sigma_0 + b_0 s_2) + \tag{1.16}$$
$$- \frac{2}{c^2} \int_0^s ds_1 \int_0^{s_1} ds_2 \, b^r \, b^v \, (\partial_v U) \, (\sigma_0 + b_0 \, s_2);$$

$$s = b_r \left[\sigma^r(s) - \sigma^r(0)\right] \quad \Rightarrow \quad s = |\vec{\sigma}(s) - \vec{\sigma}(0)|; \tag{1.17}$$

$$ds = b_r \, d\sigma^r = d\sigma; \tag{1.18}$$

$$b^r \frac{\partial}{\partial \sigma^r} = b^r \frac{\partial s}{\partial \sigma^r} \frac{\partial}{\partial s} = \frac{d}{ds}. \tag{1.19}$$

The time component of the future oriented geodetics at a generic point

---

[4]The notation $O(\zeta; c^{-2})$ stands for term at the first PM order further expanded at the first PN order.

s becomes:

$$\tau(s) - \tau(0) - \tau_{3K} = s \left(\sqrt{\vec{b^2}} + c_{(1)+} \right)_0 + \tag{1.20}$$
$$+ 2 \int_0^s ds_1 \int_0^{s_1} ds_2 \sqrt{\vec{b^2}} \, b^r \, \partial_r U =$$
$$= \pm \, |\vec{\sigma}(s) - \vec{\sigma}(0)| \left(1 \mp c_{(1)\pm} \right)_0 +$$
$$+ \frac{2}{c^2} \int_0^s ds_1 \int_0^{s1} ds_2 \left(b^r \, \partial_r \, U \right) (\sigma_0 + b_0 \, s_2)$$

where (see [102]):

$$\tau_{3K}(s) = \int_0^s ds_1 \int_0^{s1} ds_2 \left(\frac{1}{c^2} \partial_t^2 \, {}^3\widetilde{\mathcal{K}}_{(1)} \right) (\sigma_0 + b_0 \, s_2) + \tag{1.21}$$
$$+ \frac{2}{c} \int_0^s ds_1 \int_0^{s1} ds_2 \left(b^r \, \partial_r \partial_t \, {}^3\widetilde{\mathcal{K}}_{(1)} \right) (\sigma_0 + b_0 s_2) +$$
$$+ \sum_{uv} b^u b^v \int_0^s ds_1 \int_0^{s1} ds_2 \left(\partial_u \partial_v \, {}^3\widetilde{\mathcal{K}}_{(1)} \right) (\sigma_0 + b_0 s_2)$$

is a term that collects all the integral contributions due to ${}^3\widetilde{\mathcal{K}}_{(1)}$.

Using the embedding given in section 1.1 (equations (1.1) and (1.2)), we define:

$$r^i := \epsilon_r^i \, \sigma^r(1), \tag{1.22}$$

the observer position (with respect to the origin of the coordinates),

$$R^i := \epsilon_r^i \, \sigma^r(0), \tag{1.23}$$

the source position (with respect to the origin of the coordinates), and:

$$\widehat{k}_\oplus^r := -\epsilon_s^r \, p^s(s) \approx -\epsilon_s^r \, b^s, \tag{1.24}$$

the direction of observation.

One now has to integrate the last line of (1.20); each body will give a logarithmic contribution; only the bodies which are close to the geodetic will give a non negligible contribution, and this will be maximum at the distance of maximum approach $\left| \vec{d_i} \right|$ (on this point, see also [135, 136]).

With all this, we find the equation of Time Of Arrival (TOA) of a signal in PN ADM tg:

$$c\,t = c\,t_0 + \tau_{3K} + \left[1 + \left(\frac{1}{c}\,\partial_t{}^3\widetilde{\mathcal{K}} - \sum_r \widehat{k}_{\oplus}^r\,\partial_r{}^3\widetilde{\mathcal{K}}\right)\right]_0 \left|\vec{R} - \vec{r}\right| + \qquad (1.25)$$

$$- 2\,\frac{G}{c^2} \sum_i \log\left[\frac{(\vec{r} - \vec{d_i}) \cdot \widehat{k}_{\oplus} + \left|\vec{d_i} - \vec{r_i}\right|}{\left(\vec{R} - \vec{d_i}\right) \cdot \widehat{k}_{\oplus} + \left|\vec{d_i} - \vec{R}\right|}\right]\,m_i.$$

Where m_i is the mass of the $i - th$ body.

Equation (1.25) will be the basis for the future calculations.

The usual formulation gives (see [135, 136], for example):

$$c\,t = c\,t_0 + \left|\vec{R} - \vec{r}\right| - 2\,\frac{G}{c^2} \sum_i \log\left[\frac{(\vec{r} - \vec{d_i}) \cdot \widehat{k}_{\oplus} + \left|\vec{d_i} - \vec{r_i}\right|}{\left(\vec{R} - \vec{d_i}\right) \cdot \widehat{k}_{\oplus} + \left|\vec{d_i} - \vec{R}\right|}\right]\,m_i. \quad (1.26)$$

In both equations eqs. (1.25) and (1.26), the logarithmic term is the *Shapiro time delay* [137]; in the first line of equation (1.25) we have two corrections given by the presence of the extrinsic curvature:

A *local one*, to be calculated at the source position:

$$\frac{1}{c}\,\partial_t{}^3\widetilde{\mathcal{K}}_{(1)} - \sum_r \widehat{k}_{\oplus}^r\,\partial_r{}^3\widetilde{\mathcal{K}}_{(1)}$$

This is due to the modification of the proper time due to the choice of the 3+1 splitting of spacetime.

And an *integral one*, τ_{3K}, whose expression is given in (1.21), its value depends on the actual path of the light ray in the spacetime and on the extrinsic curvature of the hypersufaces.

In a Euclidean hypersurface, all these corrections are zero.

In this section we used a general argument and we didn't specify which reference system we were using. In the following, unless otherwise specified, we assume that the observer is set on the Earth and that the reference system is the BCRS, following the IAU convention [126, 127].

1.3   Pulsar Timing Array - PTA

1.3.1   Generalities

A Pulsar is a neutron star which emits very regular pulses in the radio range with a short period (from millisecond to seconds) [138, 139].

It is thought that the pulses are beams of radiation emitted along the magnetic axis of the pulsar and that their regular and fast emission is due to the star's rotation: every time the magnetic axis is oriented in our direction we register a pulse.[5]

In *Pulsar Timing Array* (PTA), one measures the time of arrival for many pulses for each one of the pulsar in the considered set evenly distributed on the celestial vault; then one fits the signal with a theoretical function derived from a model for the astrometric properties of the pulsar (position and velocity) and of the details of the propagation of the pulse in the galaxy. Using this model it is possible to calculate the TOA of future pulses; this expectation is confronted again with the actual pulse: deviations between the two are called *residuals*; if these residuals are not a white noise (for example if the model is constantly ahead the measured TOA), something is not modeled correctly.

For many pulsars, in the measurement process, one can reach a precision of the order of 100 ns and residuals are of the same order [140], but for the millisecond pulsars it is possible to reach a precision of the order of a few tens of nanoseconds [141].[6]

There are three main aspects that can be investigated with the PTA:

* Check the stability and the presence of errors in the reference system; in this case the signature is a monopole: if the reference time is runnig fast, pulses will be running slow, and vice versa [124];

• Check for errors in ephemeris: if the Earth position is wrong there will be a dipole-like effect in the time of arrival of the pulses in the array [124];

---

[5]Neutron star are the collapsed nucleus of a star exploded as a Supernova: the high rotation speed comes from the conservation of angular momentum (this is not valid for the *recicled pulsars*, pulsars in binary systems whose spin rate has been speeded up by accretion of matter from the companion).

[6]For pulsar PSR J0437-4715 the TOA is known with a precision of 30ns and (root mean squared) residuals are 200ns [140, 141].

- Detection of gravitational waves (GWs): in this case the signature is a quadrupole, due to the GW nature [124, 140, 141].

In this work, we are only interested in the first point, marked with a star: since the effects of the choice of the 3-space hypersurface on the time of propagation is always ignored, this should appear as a monopole signature in the time of arrival.

We notice that in principle, if all the parameters in the time of arrival equation are known with acceptable accuracy, it is possible to test different mathematical form for the $^{3}\widetilde{\mathcal{K}}_{(1)}$ (see chapter 2).

We shall try to esimate at least the order of magnitude of the effect of the non-local York time in PTA in chapter 3.

1.3.2 Mathematical derivation of the time of arrival of the pulse

Usually (see [135, 136, 142] for example), it is assumed that the pulsar has constant velocity $\vec{V}$, so its position at time t_n of the emission of the $n-$th pulse is given by:

$$\vec{R}_n = \vec{R}_0 + \vec{V}\,(\bar{t}_n - \bar{t}_0) \tag{1.27}$$

where $\vec{R}_0$ and $\tilde{t}_0$ are reference initial position and time. Moreover it is assumed that the pulsar is very far from the observer, so:

$$\left|\vec{V}\right|(t_n - t_0) \ll \left|\vec{R}_0\right|. \tag{1.28}$$

One now has to substitute equation (1.27) in (1.25) for the ADM tg time of arrival, or (1.26) for the *usual* one, and expand the logarithmic term and the distance term keeping in mind (1.28): since in this calculation the extrinsic curvature is not involved, nothing changes from the usual calculation.[7]

The direction of observation

The direction of observation becomes:

$$\widehat{k}_{\oplus} \approx \frac{\vec{R}_0}{\left|\vec{R}_0\right|} \tag{1.29}$$

---

[7]See also figure 2.1 for the definitions of the vectors.

The logarithmic term

Nothing changes in the numerator; in the denominator on the contrary, one has:

$$\widehat{k}_{\oplus} \cdot \left[\vec{R}_0 + \vec{V}\ (t_n - t_0)\right] + \left|\vec{R}_0 + \vec{V}\ (t_n - t_0)\right| \approx$$

$$\approx R_0 + R_0 \left|1 + \frac{V}{R_0}\ (t_n - t_0) - \frac{\vec{d}_i}{R_0}\right| \approx 2R_0$$

where we used the definition of $\widehat{k}$ and the fact that $d_i \ll R_0$.

So we have:

$$-2\,\frac{G}{c^2} \sum_i \log\left[\frac{(\vec{r} - \vec{d}_i) \cdot \widehat{k}_{\oplus} + |\vec{d}_i - \vec{r}_i|}{\left(\vec{R} - \vec{d}_i\right) \cdot \widehat{k}_{\oplus} + |\vec{d}_i - \vec{R}|}\right] m_i \approx$$

$$\approx -2\,\frac{G}{c^2} \sum_i \log\left[\vec{r} \cdot \widehat{k}_{\oplus} + |\vec{d}_i - \vec{r}|\right] m_i + 2\,\frac{G}{c^2} \sum_i m_i \log\left[2R_0\right]$$

Modulo term

We have to substitute equation (1.27) in $\left|\vec{R} - \vec{r}\right|$:

$$\left|\left(\vec{R}_0 + \vec{V}\ (t_n - t_0) - \vec{r}\right)\right| \approx |R_0| \sqrt{\left(\widehat{k}_{\oplus} + \frac{\vec{V}}{|R_0|}\ (t_n - t_0)\right)^2 - \left(\frac{\vec{r}}{|R_0|}\right)^2}$$

and expand it in Taylor series.

Only the inner product in the 3-space is needed because of the smallness of the terms involved, therefore the extrinsic curvature is not involved in this calculations and Euclidean approximation is enough at this order (see eqs. (I.16), (I.19) and (I.20)).

This all means that the standard result as quoted in [135, 136, 142] is still valid.

Final result

Putting it all togheter, we have the *PTA time of arrival in ADM tg*:

$$c\,(t_n - t_0) = c\,\left(\tilde{t}_n - \tilde{t}_0\right) - 2\,\frac{G}{c^2}\,\sum_i \log\left[\vec{r}\cdot\hat{k}_\oplus + |\vec{d}_i - \vec{r}|\right]\,m_i +$$

$$+\,\tau_{3K} + \left(1 + \frac{1}{c}\,\partial_t\,^3\widetilde{\mathcal{K}} - \sum_r \hat{k}_\oplus^r\,\partial_r\,^3\widetilde{\mathcal{K}}\right)_{\text{sor}}\,\times$$

$$\times\left\{\left[\left(\hat{k}_\oplus\,\cdot\,\vec{V}\right)\Delta t_n - \left(\hat{k}_\oplus\,\cdot\,\vec{r}\right)\right] + \frac{1}{2\,R_0}\left[r^2 - \left(\hat{k}\,\cdot\,\vec{V}\right)^2\right] +\right.$$

$$-\,\frac{1}{R_0}\left[\vec{V}\cdot\vec{r} - \left(\hat{k}_\oplus\,\cdot\,\vec{V}\right)\left(\hat{k}_\oplus\,\cdot\,\vec{r}\right)\right](\Delta t_n) +$$

$$\left.+\,\frac{1}{2R_0}\left[V^2 - \left(\hat{k}_\oplus\,\cdot\,\vec{V}\right)^2\right]\Delta t_n^2\right\}$$

$$(1.30)$$

where we set:

$$t_0 = \tilde{t}_0 + 2\,\frac{G}{c^3}\,\sum_i m_i\,\log\left[2R_0\right] + \frac{R_0}{c}, \qquad (1.31)$$

the reference 'initial' time.

The usual treatment gives the expression (see [135, 136, 142]):

$$c\,(t_n - t_0) = c\,\left(\tilde{t}_n - \tilde{t}_0\right) - 2\,\frac{G}{c^2}\,\sum_i \log\left[\vec{r}\cdot\hat{k}_\oplus + |\vec{d}_i - \vec{r}|\right]\,m_i +$$

$$+\,\left[\left(\hat{k}_\oplus\,\cdot\,\vec{V}\right)\Delta t_n - \left(\hat{k}_\oplus\,\cdot\,\vec{r}\right)\right] + \frac{1}{2\,R_0}\left[r^2 - \left(\hat{k}_\oplus\,\cdot\,\vec{V}\right)^2\right] +$$

$$-\,\frac{1}{R_0}\left[\vec{V}\,\cdot\,\vec{r} - \left(\hat{k}_\oplus\,\cdot\,\vec{V}\right)\left(\hat{k}_\oplus\,\cdot\,\vec{r}\right)\right](\Delta t_n) +$$

$$+\,\frac{1}{2R_0}\left[V^2 - \left(\hat{k}_\oplus\,\cdot\,\vec{V}\right)^2\right]\Delta t_n^2.$$

$$(1.32)$$

Again, confronting (1.30) and (1.32), we have the local and integral corrections (second line of equation (1.30)) coming from the extrinsic curvature.
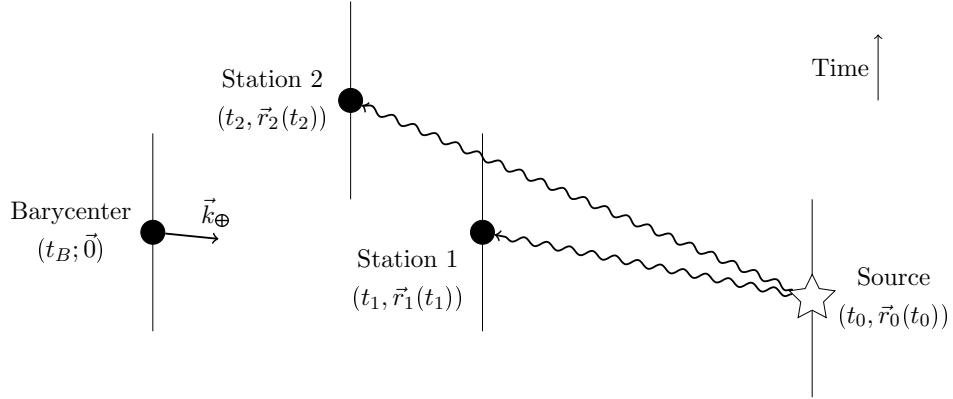
Figure 1.1: *Scheme for VLBI in the BCRS with the definition of the various quantities needed in equation (1.33).*
Vertical lines represent schematically the line of universe of the object they pass through.
The baseline vector in the BCRS is $\vec{b} = \vec{x}_1(t_1) - \vec{x}_2(t_2)$.
The unit vector $\hat{n}$ is not drawn: it is the unit vector from the Solar System Barycenter to the center of the Earth.

1.4   Very Long Beseline Interferometry - VLBI

In Very Long Baseline Interferometry, one measures the time of arrival from the same source in two different, Earth-based and far away stations and subtracts the results (see figure 1.1): in this way it is possible to obtain very accurate measurements of position of celestial bodies that can be used for the construction of reference frames (see [125, 128] for the construction of the ICRF1 and ICRF2 with this technique). At the same time, VLBI gives unmatched informations on the Earth orientation and position and also on plate tectonics [143].

VLBI are interesting also in Black Hole physics: the *Event Horizon Telescope* is the project to use existing and planned VLBI structures to study the environment of a black hole, its spin, its accretion rate and more [144].

For each station, one gets a result similar to equation (1.30) (or (1.32) in the usual treatment) and, after subtracting, various terms simplify, in particular, in our case, *the local correction drops out*, since it has to be calculated at the source position in both cases.

As far as the integral correction is concerned, the limits of integration are not the source and the Earth anymore, but the positions of the two stations: so this corrective term is completely negligible, since the integral has to be

made only on continental distances.

This means that in ADM tg there is no substatantial corrections due to the extrinsic curvature and the equation of time delay is the usual one as given, for example, in [135, 136]:

$$
\begin{aligned}
c\,(T_1 - T_2) = &-\left(\widehat{k}_\oplus \cdot \vec{b}\right)\left[1 + \frac{\widehat{k}_\oplus \cdot (\vec{v}_e + \vec{\omega}_2)}{c}\right]^{-1} \times \\
&\times \left[1 - 2\,U - \frac{1}{2}\frac{\langle v_\oplus^2 \rangle}{c^2}\right] + \\
&- \frac{\vec{v}_\oplus \cdot \vec{b}}{c} - \frac{1}{2}\frac{\left(\widehat{k}_\oplus \cdot \vec{v}_\oplus\right)\left(\vec{b} \cdot \vec{v}_\oplus\right)}{c^2} + \\
&- 2\,\frac{GM_\odot}{A\,c^2}\frac{\left(\widehat{k}_\oplus + \widehat{n}\right) \cdot \vec{b}}{1 + \widehat{k}_\oplus \cdot \widehat{n}}
\end{aligned}
\tag{1.33}
$$

where $\vec{b}$ is the baseline vector, $\widehat{k}_\oplus$ is the direction of observation, $\vec{\omega}_2$ is the geocentric rotational speed of the second antenna, $\vec{v}_\oplus$ is the BCRS Earth speed, U is the potential of the Solar System at the center of the Earth plus the potential of the Earth at the equator and $\widehat{n}$ is the Sun-Earth unit vector (see figure 1.1).[8]

1.5 Redshift

Redshift can be calculated from the definition:

$$
1 + z := \frac{d\widetilde{t}_{obs}}{d\widetilde{t}_{sor}},
\tag{1.34}
$$

where, $\widetilde{t}_{obs}$ and $\widetilde{t}_{sor}$ are, respectively the proper time at the observer and at the source position. This must be expanded in the following way:

$$
1 + z = \frac{d\widetilde{t}_{obs}}{dt_{obs}}\frac{dt_{obs}}{dt_{sor}}\frac{dt_{sor}}{d\widetilde{t}_{sor}}
\tag{1.35}
$$

where the t_{obs} and t_{sor} are the coordinate time at the source and observer position.

In PN ADM tg metric, the proper time (at PN order) is given by (see (I.14)):

$$
d\widetilde{t}_i = dt_i\left(1 - \frac{U}{c^2} - \frac{1}{c}\,\partial_{t_i}\,{}^3\widetilde{\mathcal{K}}_{(1)}\right) \qquad i = \{obs,\ sor\},
\tag{1.36}
$$

---

[8]Only the Sun is considered because other bodies in the Solar System give corrections that are too small.

and t_{obs} is given by equation (1.25), while t_{sor} is linked to the latter by [131]:

$$t_{obs} = t_{sor} + \frac{R}{c} + \log\left(\frac{2R}{A}\right)\frac{2G\,M}{c^3}. \tag{1.37}$$

where R is the distance between source and observer and A is a reference distance ([131] uses the astronomical unit).

Substituting everything in (1.34), we find (ρ is the radial velocity of the source, and v is the magnitude of its velocity):

$$
\begin{aligned}
1 + z =\ & \left(1 + \frac{1}{2}\frac{v^2}{c^2} + \frac{U}{c^2} + \frac{1}{c}\,\partial_t{}^3\widetilde{\mathcal{K}} - \frac{v^r}{c}\,\partial_r{}^3\widetilde{\mathcal{K}}\right)_{\text{sor}} \times \\
& \times \left(1 + \frac{d\tau_{3k}}{dt}\frac{1}{c} + \frac{\rho}{c}\right) \times \\
& \times \left(1 - \frac{v_\oplus}{c}\right) \times \\
& \times \left(1 - \frac{1}{2}\frac{v^2}{c^2} - \frac{U}{c^2} - \frac{1}{c}\,\partial_t{}^3\widetilde{\mathcal{K}} + \frac{v^r}{c}\,\partial_r{}^3\widetilde{\mathcal{K}}\right)_{\oplus}
\end{aligned}
\tag{1.38}
$$

where we omitted the derivative of the logarithmic term of (1.37) since, tipically it gives correction of the order 0.3 mm/s [131] while stellar velocities are of the order of hundrends of km/s and modern measurements precision is about 1m/s [131];[9].

The usual formula for redshift as measured by an observer on the Earth is [131]:

$$
\begin{aligned}
1 + z =\ & \left(1 + \frac{1}{2}\frac{v^2}{c^2} + \frac{U}{c^2}\right)_{\text{sor}}\left(1 + \frac{\rho}{c}\right) \times \\
& \times \left(1 - \frac{v_\oplus}{c}\right)\left(1 - \frac{1}{2}\frac{v^2}{c^2} - \frac{U}{c^2}\right)_{\oplus}
\end{aligned}
\tag{1.39}
$$

In order to get the redshift at the Solar System barycenter, one just has to repeat the whole procedure with an observer fixed in the barycenter where the potential is zero by definition, see [133]; the results, respectively

---

[9]Nevertheless, there are cases in which this term might become important: for example when microlensing is involved [133].

on ADM tg and in the usual case are:[10]

$$1 + z = \left(1 + \frac{1}{2} \frac{v^2}{c^2} + \frac{U}{c^2} + \frac{1}{c} \partial_t{}^3\widetilde{\mathcal{K}} - \frac{v^r}{c} \partial_r{}^3\widetilde{\mathcal{K}} \right)_{\text{sor}} \times$$
$$\times \left(1 + \frac{d\tau_{3k}}{dt} \frac{1}{c} + \frac{\rho}{c} \right) \tag{1.40}$$

$$1 + z = \left(1 + \frac{1}{2} \frac{v^2}{c^2} + \frac{U}{c^2} \right)_{\text{sor}} \left(1 + \frac{\rho}{c} \right) (1 + X) \tag{I.36}$$

Confronting equation (1.38) and (1.39) (or (1.40) and (I.36)), we see that we have various corrections coming from the extrinsic curvature, both at the source and at the observer position (first and last line of (1.38)): these corrections arise from the change in the definition of the proper time and from the frame dragging effect due to the ${}^4g_{0r}$ term; furthermore, we have a correction in the second line of (1.38) (or (1.40)), coming from the integral term τ_{3K} (see equation (1.21)), that *directly influences the radial velocity* of the source.

All these corrections are currently "hidden" in the $X-$term of equation (I.36), and won't be observable until all the other sources of uncertanties (convective motion at the surface of the star, atmospheric oscillations, ..., see [131–134] for the exhaustive list) will be under control.

---

[10]In the last case we include all the unknown in the $X-$term (see section I.4.2) and references [131–134].

1.6   Lorentz transformation

Measurements are usually carried out on Earth (using GCRS), while
IAU recommends to report them in BCRS, so we need a the Lorentz trans-
formation between the two reference systems; the transformation of time
coordinate between the two systems is of course of utmost importance for
the arguments of the previous sections.[11]

Here $\vec{v}$ is the relative speed between the two reference systems (the ve-
locity of the Earth in the BCRS); $(T, \vec{\xi})$ are the GCRS, while $(t, \vec{x})$ are the
BCRS one; the metrics of the reference systems have the form described in
sections I.3.3 and I.3.4 other conventions used here are listed in the table at
page 129.

All calculations will be at the order $O(c^{-2})$.

1.6.1   Calculations

We start by considering the following coordinate transformation from
the BCRS and a primed system in which the metric is (locally) flat (see
[112] and also [135, 136]):[12]

$$
\begin{cases}
dt' = \left(1 - \dfrac{U}{c^2} - \dfrac{1}{c}\dfrac{\partial}{\partial t}\,{}^3\widetilde{\mathcal{K}}_{(1)}\right) dt - \dfrac{1}{c}\,\partial_r\,{}^3\widetilde{\mathcal{K}}_{(1)}\,dx^r \\[4mm]
dx'^r = \left(1 + \dfrac{U}{c^2}\right) dx^r
\end{cases}
\tag{1.41}
$$

At order $O(c^{-2})$, the Lorentz transformation between the primed refer-
ence system and the Earth one is given by:

$$
\begin{cases}
dT = \left(1 + \dfrac{1}{2}\dfrac{v^2}{c^2}\right)\left(dt' - \dfrac{v^r}{c^2}\,dx'^r\right) \\[6mm]
d\xi^r = dx'^r + \dfrac{1}{2}\dfrac{v^r v^s}{c^2}\,dx'^s - \left(1 + \dfrac{1}{2}\dfrac{v^2}{c^2}\right) v^r\,dt'
\end{cases}
\tag{1.42}
$$

Substituting the definition of primed coordinates (1.41) in the Lorentz
transformation (1.42), we find the transformation from GCRS coordinates

---

[11]See also [145] on this topic.

[12]This primed coordinate system is actually a (co)tetrad, since it transforms the metric
given by eqs. (I.14) to (I.16) into a flat metric (see [112], section 39.10, on this point).

to BCRS ones:

$$
\begin{cases}
dT = \left(1 + \dfrac{1}{2}\dfrac{v^2}{c^2}\right)\left[\left(1 - \dfrac{U}{c^2} - \dfrac{1}{c}\partial_t{}^3\widetilde{\mathcal{K}}_{(1)}\right)dt + \right. \\[2ex]
\qquad \left. - \dfrac{1}{c}\partial_r{}^3\widetilde{\mathcal{K}}_{(1)}\,dx^r - \dfrac{v_r}{c}\left(1 + \dfrac{U}{c^2}\right)dx^r\right] \\[4ex]
d\xi^r = \left[\left(1 + \dfrac{U}{c^2}\right)\delta^r_s + \dfrac{1}{2}\dfrac{v^r v_s}{c^2} + \dfrac{1}{2}\dfrac{v^2}{c^2}\partial_s{}^3\widetilde{\mathcal{K}}_{(1)}\dfrac{v^r}{c}\right]dx^s + \\[2ex]
\qquad + \left(1 + \dfrac{1}{2}\dfrac{v^2}{c^2}\right)\dfrac{v^r}{c}\partial_s{}^3\widetilde{\mathcal{K}}_{(1)}\,dx^s + \\[2ex]
\qquad - \left(1 + \dfrac{1}{2}\dfrac{v^2}{c^2}\right)\left(1 - \dfrac{U}{c^2} - \dfrac{1}{c}\partial_t{}^3\widetilde{\mathcal{K}}_{(1)}\right)v^r\,dt
\end{cases}
\tag{1.43}
$$

At order $O(c^{-2})$, we have the *transformation rule from the BCRS* $\left(T,\vec{\xi}\right)$ *to the GCRS* $(t,\vec{x})$ *in ADM-tg:*

$$
\begin{cases}
dT = \left(1 + \dfrac{1}{2}\dfrac{v^2}{c^2} - \dfrac{U}{c^2} - \dfrac{1}{c}\partial_t{}^3\widetilde{\mathcal{K}}_{(1)}\right)dt - \left(\dfrac{1}{c}\partial_s{}^3\widetilde{\mathcal{K}}_{(1)} + \dfrac{v_s}{c^2}\right)dx^s \\[4ex]
d\xi^r = \left[\left(1 + \dfrac{U}{c^2}\right)\delta^r_s + \dfrac{1}{2}\dfrac{v^r v_s}{c^2} + \dfrac{1}{2}\dfrac{v^2}{c^2}\partial_s{}^3\widetilde{\mathcal{K}}_{(1)}\dfrac{v^r}{c}\right]dx^s + \\[2ex]
\qquad + \left(1 + \dfrac{1}{2}\dfrac{v^2}{c^2}\right)\dfrac{v^r}{c}\partial_s{}^3\widetilde{\mathcal{K}}_{(1)}\,dx^s + \\[2ex]
\qquad - \left(1 + \dfrac{1}{2}\dfrac{v^2}{c^2} - \dfrac{U}{c^2} - \dfrac{1}{c}\partial_t{}^3\widetilde{\mathcal{K}}_{(1)}\right)v^r\,dt
\end{cases}
\tag{1.44}
$$

Inverting the relations (1.43) and keeping only terms linear in U and at most at order $O(c^{-2})$, we have the *transformation rule from the GCRS* $(t,\vec{x})$ *to the BCRS* $\left(T,\vec{\xi}\right)$ *in ADM-tg:*

$$
\begin{cases}
dt = \left(1 + \dfrac{1}{2}\dfrac{v^2}{c^2} + \dfrac{U}{c^2} + \dfrac{1}{c}\partial_t{}^3\widetilde{\mathcal{K}}_{(1)} - \dfrac{v^s}{c}\partial_s{}^3\widetilde{\mathcal{K}}_{(1)}\right)\left(dT - \dfrac{v_s}{c}d\xi^s\right) \\[4ex]
dx^r = \left(1 - \dfrac{U}{c^2}\right)\left[\left(\delta^r_s + \dfrac{1}{2}\dfrac{v^r v_s}{c^2}\right)d\xi^s + v^r\left(1 + \dfrac{1}{2}\dfrac{v^2}{c^2}\right)dT\right].
\end{cases}
\tag{1.45}
$$

We notice that, at this order, in the transformation from the GCRS to the BCRS only the time-time transformation involves the non-local York time $^{3}\widetilde{\mathcal{K}}_{(1)}$, while in the inverse relation 1.44 it is involved in a more complicated way.

With the usual treatment, the Lorentz transformation from the GCRS to the BCRS is [145]:

$$
\begin{cases}
dt = \left(1 + \dfrac{1}{2}\dfrac{v^2}{c^2} + \dfrac{U}{c^2}\right)\left(dT - \dfrac{v_s}{c}\,d\xi^s\right) \\[4mm]
\\
dx^r = \left(1 - \dfrac{U}{c^2}\right)\left[\left(\delta^r_s + \dfrac{1}{2}\dfrac{v^r\,v_s}{c^2}\right)d\xi^s + v^r\left(1 + \dfrac{1}{2}\dfrac{v^2}{c^2}\right)dT\right].
\end{cases}
\tag{1.46}
$$

1.6.2   Time transformation rule

For a clock at rest on the Earth, we have $d\xi^r \equiv 0$ ($r = \{1,2,3\}$), therefore, the time-transformation from GCRS to BCRS and the inverse from the BCRS to GCRS are given respectively by:

$$
dt = \left(1 + \dfrac{1}{2}\dfrac{v^2}{c^2} + \dfrac{U}{c^2} + \dfrac{1}{c}\,\partial_t\,^3\widetilde{\mathcal{K}}_{(1)} - \dfrac{v^s}{c}\,\partial_s\,^3\widetilde{\mathcal{K}}_{(1)}\right)dT
\tag{1.47}
$$

$$
dT = \left(1 - \dfrac{1}{2}\dfrac{v^2}{c^2} - \dfrac{U}{c^2} - \dfrac{1}{c}\,\partial_t\,^3\widetilde{\mathcal{K}}_{(1)} + \dfrac{v^s}{c}\,\partial_s\,^3\widetilde{\mathcal{K}}_{(1)}\right)dt
\tag{1.48}
$$

The difference with respect the usual transformation rule (see [145]) arise from the modification of the proper time and from the frame dragging efffect given by $^{4}g_{0r}$.

Now, following closely the usual treatment of [135, 136], the potential at the clock position on the Earth, $U(\vec{\xi}_C)$, can be split into a component due to the Earth mass $w_E(\vec{\xi}_C)$ and one due to the rest of the Solar System $w_{ext}(\vec{\xi}_C)$; the latter can be further decomposed with a Taylor series, into:[13]

$$
w_{ext} = w_{ext}(\vec{\xi}_C) + \vec{\nabla}w_{ext}\Big|_{\vec{\xi}_C} \cdot \vec{\xi}_C = w_{ext}(\vec{\xi}_C) + \vec{a}_\oplus \cdot \vec{\xi}_C.
\tag{1.49}
$$

More over, one needs to take into account the rotation of the Earth, so:

$$
\vec{v} = \vec{v}_{\mathrm{rot}} + \vec{v}_\oplus \quad \Rightarrow \quad v^2 = v^2_{\mathrm{rot}} + v^2_\oplus + 2\,\vec{v}_\oplus \cdot \vec{v}_{\mathrm{rot}}
\tag{1.50}
$$

---

[13]$\vec{a}_\oplus$ is the acceleration of the Earth in the BCRS.

Substituting back into (1.47), we find:

$$
dt = dT \left[1 + L_C + \frac{\vec{a}_\oplus \cdot \vec{\xi}}{c^2} + \frac{w_{ext}}{c^2} + \frac{1}{2} \frac{v_\oplus^2}{c^2} + \right. \\
\left. + \frac{1}{c} \, \partial_T \, {}^3\widetilde{\mathcal{K}}_{(1)} - \left(\frac{v_{rot}^r}{c} + \frac{v_\oplus^r}{c} \right) \partial_r \, {}^3\widetilde{\mathcal{K}}_{(1)} \right]
$$

(1.51)

where:

$$
L_C := \frac{w_E}{c^2} + \frac{1}{2} \frac{v_{rot}^2}{c^2}
$$

(1.52)

this must be compared with the one given by IAU, which we rewrite here (I.35) (see also [135, 136]):

$$
dt = dT \left[1 + L_C + \frac{\vec{v}_\oplus \cdot \vec{\xi}}{c^2} + \frac{w_{ext}}{c^2} + \frac{1}{2} \frac{v_\oplus^2}{c^2} \right]
$$

In the second line of (1.51), we separated out the additional terms due to the extrinsic curvature. L_C is the same in both equations (see page 129).

1.7   Summary of the chapter and discussion

In this chapter we calculated the time of arrival (TOA) of a light signal from a source to the Earth and found that there are two different contributions due to the extrinsic curvature (see equations (1.26), (1.25)): a *local one* (to be valuated at the source position) coming from the redefinition of the proper time in ADM tg and an *integral one* given by equation (1.21) which depends on the path followed by the light and by the extrinsic curvature of the 3-hypersurface (all these corrections are zero for an Euclidean 3-space).

Then, in order to find some observational signature for the effects of the 0.5 PN terms, we applied our formula to the case of PTA and VLBI:

- We found no (significant[14]) contribution in the VLBI due to the extrinsic curvature: this means that the catalogues already in use are not affected by the choice of the hypersurface and can still be used to define a reference frame.

  Even if the reference frame built through VLBI does not depend on the convention used for the splitting, the reference system it defines, does: a careful choice of this latter can be used to get rid of part of the DM and possibly DE (see also [109]).

- We found two different contributions in the PTA depending on the extrinsic curvature: in principle one could use our formula (1.30) to calculate the time delay and compare it with the measured one to gain some information on ${}^{3}\widetilde{\mathcal{K}}_{(1)}$.

  Usually the needed astrometric parameters for the pulsars (position and velocity) are fitted with the time delay formula, but in [146], authors suggest the use of VLBI to determine the astrometric parameters of pulsars, since it would improve dramatically the precision of the procedure and reduce the time of observation.[15]

  The problem, here, is that VLBI measurements are done in ICRS,[16] while the PTA measurements are done in BCRS, so a tranformation

---

[14]We remind that the integral correction survives, but the integration limit are the positions of the two receivers on the Earth.

[15]A pulsar has to be observed for many years before the errors on parameters and the residuals become accepatble (in [147], authors use observations made over a span of 10 years).

[16]They actually define it! (see [125] and section 1.4)

function between the two reference systems has to be defined. In [146] this is done supposing that the two systems are simply rotated by a small angle, so one can define a tranformation matrix of this kind:

$$\mathbf{\Omega} = \mathbf{I} + \begin{pmatrix} 0 & A_z & -A_y \\ -A_z & 0 & A_x \\ A_y & -A_x & 0 \end{pmatrix}$$

where $\mathbf{I}$ is the identity matrix and the parameters A_i are fitted with a minimization procedure. It is possible to show that the error on the rotation parameters scales as $\propto \dfrac{1}{\sqrt{N}}$, where N is the number of the pulsars considered, so the bigger the sample the smaller the statistical error.

In our case, since the VLBI does not depend on ${}^3\widetilde{\mathcal{K}}_{(1)}$, one should rather use this method to deduce astrometric parameters for the pulsars, then try to fit the other parameters, in particular the non-local York time, keepeng the astrometric ones fixed, since this might resolve possilbe degeneracy among ${}^3\widetilde{\mathcal{K}}_{(1)}$ and other parameters.

One should, nevertheless, be careful in this process, since even if the VLBI measurements do not depend on the choice of ${}^3\widetilde{\mathcal{K}}_{(1)}$, the PTA measurements do, so in the transformation matrix $\mathbf{\Omega}$ there is a hidden dependence on the non-local York time and on the choice of hypersurface of simultaneity.

We also showed that the redshift formula is modified by the non-local York time (equation (1.38)), in particular the (derivative of the) integral correction *directly* affects the definition of radial velocity: in a perfect world, confronting the radial velocity as measured with spectroscopy with the astrometric one, would be a very good and clean way to determine the effects of the non-local York time, but, as we discussed in the introduction (section I.4.2, see also references [131–134]), there are too many uncertanties in the redshift formula for it to be useful in the determination of the ${}^3\widetilde{\mathcal{K}}_{(1)}$: our correction must be added to the error budget.

Finally, IAU recommends that all measurements must be referred to the BCRS [126], but many are done on the Earth in the GCRS, therefore the Lorentz transformation between the two reference system is needed and we calculated it in section 1.6. Since we are not using the IAU-recommended

metric, the transformation is different from the one reported in [126], in particular, we found that for a clock fixed on the Earth[17] only the time transformation depends on $^3\widetilde{\mathcal{K}}_{(1)}$, and we explicitly gave its expression in equation (1.51).

We explicitly considered the case of an observer on the Earth, when the observer is a satellite (GAIA, for example), another level of transformation must be added to connect the *local reference system* to the GCRS and then to the BCRS: equations (1.45) and (1.44) are completely general and can be used to derive the needed transformations, remembering that the satellite has negligible mass and so it gives no contribution to the potential; it is now easy to show that the transformation between the satellite time T_{sat} and the GCRS one, T, is given by an epression similar to (1.47) and (1.48):

$$dT_{sat} = \left(1 - \frac{1}{2}\frac{v_{sat}^2}{c^2} - \frac{U_{ext}}{c^2} - \frac{1}{c}\,\partial_T\,^3\widetilde{\mathcal{K}}_{(1)} + \frac{v_{sat}^s}{c}\,\partial_s\,^3\widetilde{\mathcal{K}}_{(1)}\right)dT \qquad (1.53)$$

where now U_{ext} is only the tidal potential on the satelltite and $\vec{v}_{sat}$ is the satellite orbital velocity.

Without an explicit mathematical form for the $^3\tilde{\mathcal{K}}_{(1)}$, *one can only go this far.*

In the next chapter we will make the guess that its spatial part has a Yukawa-like form along with different ansatz for the time dependent part and study their effect.

Later on (chapter 3) we shall estimate the order of magnitude of the effects of $^3\widetilde{\mathcal{K}}_{(1)}$.

---

[17]This is the case for PTA measurements , for example.

CHAPTER 2

AN ANSATZ FOR $^3\widetilde{\mathcal{K}}_{(1)}$

In this chapter we shall make the guess that the spatial part of $^3\widetilde{\mathcal{K}}_{(1)}$ has a Yukawa-like form and then rewrite the results of the previous chapter using this function in section 2.4

This ansatz comes from a similarity between our PN metric and the PN metric of $f(R)$ theories, so we shall first briefly review these modified gravity theories in section 2.1.

Our guess only fixes the spatial part of the non-local York time, but the time-dependence is left unknown so we will discuss two different possible choices (the most straightforward ones) for this part and their effects on PTA and redshift: we will consider a *linear ansatz* in which the time dependence is linear and a *time free ansatz* in which there is no time dependence ($^3\widetilde{\mathcal{K}}_{(1)}$ is constant in time).

The consequences of a general time dependence will be explored in chapter 3 when we shall fit the rotation curve of the Andromeda galaxy, M31, with the intent to estimate how much DM can be considered as a relativistic inertial effect under different hypothesis on $^3\widetilde{\mathcal{K}}_{(1)}$.

In section 2.3 we shall also give an analytical expression for the tensor of extrinsic curvature $^3K_{rs}$ at order $O(c^{-3})$.

2.1 $f(R)$ Post Newtonian expansion

$f(R)$ theories, where R is the Ricci scalar, are *extended theories of gravity* whose lagrangian is given by:

$$L_f = \frac{c^4}{16\pi G} \int d^4\sigma \sqrt{-g}\, f(R). \tag{2.1}$$

This is meant to replace the Hilbert-Einstein one:

$$L_{HE} = \frac{c^4}{16\pi G} \int d^4\sigma \sqrt{-g}\, R \tag{2.2}$$

that gives the usual Einstein Field Equations (see [13, 112, 122]. In both the previous equation $-g$ is the determinat of the spacetime metric.

From the theoretical point of view, the function f is constrained by the fact that the above lagrangian (2.1) must contain the Hilbert-Einstein one, so:[1]

$$f(R) \approx R + \frac{R^2}{2}\, f''(0) + \dots; \tag{2.3}$$

more over, the Principle of Equivalence must be respected, but $f(R)$ is otherwise completely free. $f(R)$ is nevertheless constrained from the experimental point of view, in particular the Solar System and stellar dynamics impose strong constraints on its derivatives (see for example the review [148]).

Recent reviews on $f(R)$ and extended theories of gravity can be found in [101, 149–153]; we are primarily interested in its PN expansion; this can be found in [148] (see also the references therein).

The metric (written in spherical coordinates) in the PN approximation

---

[1]If one considers a Taylor expansion of the type:

$$f(R) \approx a + R + \frac{R^2}{2}\, f''(0) + \dots;$$

the constant a behaves like a cosmological constant: this can be seen by comparing the former equation with the action:

$$L_{HE\,\Lambda} = \frac{c^4}{16\pi G} \int d^4\sigma \sqrt{-g}\, (R - 2\,\Lambda)$$

which gives the correct Einstein Equations with a cosmological constant Λ.

can be written as [148]:

$$g_{tt} = 1 - 2\frac{GM}{c^2}\frac{1}{r(1+\delta)} - 2\frac{GM}{c^2}\frac{\delta}{1+\delta}\frac{1}{r}\exp\left(-\frac{r}{L}\right);$$ (2.4)

$$g_{rr} = -\left[1 + \frac{2GM}{c^2\,r(1+\delta)} + 2\frac{GM}{c^2\,r}\left(\frac{1}{L} + \frac{1}{r}\right)\exp\left(-\frac{1}{r}\right)\left(\frac{\delta}{1+\delta}\right)\right];$$ (2.5)

$$g_{\theta\theta} = -r^2;$$ (2.6)

$$g_{\varphi\varphi} = -r^2\sin^2\theta.$$ (2.7)

Yukawa-like terms appear in equations (2.4) and (2.5);[2] we notice they are of the same order as the usual Newtonian potential ($O(c^{-2})$). In particular, from the former equation, one can read off a new effective gravitational potential:

$$\Phi_{eff}(r) = -\frac{GM}{(1+\delta)}\left[1 + \delta\exp\left(-\frac{r}{L}\right)\right]\frac{1}{r}.$$ (2.8)

In this potential, the mass is corrected in the following way:

$$M \mapsto \frac{M}{1+\delta}$$ (2.9)

and δ is a measure of the importance of the Yukawa-like term (if $\delta = 0$ one recovers the usual Newtonian potential; in [148, 152], $\delta \equiv 1/3$ is used when fitting rotation curves of spiral galaxies or the profile of clusters of galaxies respectively).

δ is actually an arbitrary function of time (see [148]), but is assumed constant: in this way M and L are a constants too; as a consequence, in particular, L can be interpreted as a lenght scale of the additional Yukawa interaction.

In [148], the authors review the effect of the Yukawa term on Jeans instability and stellar structure, rotation curves of spiral galaxies and on the dynamics of elliptical galaxies and study the observational constraint imposed by the Equivalence Principle and the Solar System.

---

[2]They are a consequence of the presence of quadratic term in the action(2.1) (see [148]).

In particular they show that it is possible to explain the behavior of rotation curves without a DM halo, using only the Yukawa term and the modified potential (2.8).[3]

2.2   An ansatz for $^3\widetilde{\mathcal{K}}_{(1)}$

First of all, we assume that $^3\widetilde{\mathcal{K}}_{(1)}$ can be separated into an explicitly time-dependent and a space-dependent functions:

$$^3\widetilde{\mathcal{K}}_{(1)}(t,\vec{r}) = \Delta(t)\,Y(\vec{r}). \tag{2.10}$$

We will now explain our ansatz for the two functions.

2.2.1   The spatial part $Y(\vec{r})$

Our ansatz for the spatial function $Y(\vec{r})$, comes from a comparison between the time-time component of the metric (2.4) and ours as given in equation (I.14) with the lapse given in (I.17); we rewrite them both here:

$$g_{\tau\tau} = 1 - 2\,\frac{U}{c^2} - \frac{2}{c}\,\partial_t\,^3\widetilde{\mathcal{K}}_{(1)}; \tag{1.51}$$

$$g_{tt} = 1 - 2\,\frac{GM}{c^2}\,\frac{1}{r\,(1+\delta)} - 2\,\frac{GM}{c^2}\,\frac{\delta}{1+\delta}\,\frac{1}{r}\,\exp\left(-\frac{r}{L}\right). \tag{2.4}$$

So we impose that the time derivative of the non-local York time has a Yukawa-like form:

$$\partial_t\,^3\widetilde{\mathcal{K}}_{(1)} \mapsto \partial_t\,\Delta(t)\,\frac{1}{|\vec{r}|}\,\exp\left(-\frac{|\vec{r}|}{L}\right) = \delta(t)\,Y(\vec{r}). \tag{2.11}$$

2.2.2   The time-dependent part $\Delta(t)$

We have no information on the time-dependent term $\Delta(t)$; we can anyway make different choices:

(a) We make no real hypothesis and leave $\Delta(t)$ as a free function. We will not consider this in this chapter, but only in chapter 3, when we will fit the rotation curve of the M31 galaxy.[4]

It can be seen that $[\Delta(t)] = [L]^2$.

---

[3] They use simulated galaxies.

[4] Only time averaged values of the derivatives of δ can be found in this way, as we shall see in chapter3.

(b) $\delta(t)$ is quasi constant or constant,[5] so that $\partial_t^2\, ^3\widetilde{\mathcal{K}}_{(1)} \approx 0$[6] and $\Delta \approx \tau\, \delta = c\, t\, \delta$.

With this choice, the non-local York time becomes:

$$^3\widetilde{\mathcal{K}}_{(1)}(t,r) = \tau\, \frac{\delta}{r}\, \exp\left(-\frac{r}{L}\right) =$$
$$= c\, t\, \frac{\delta}{r}\, \exp\left(-\frac{r}{L}\right). \tag{2.12}$$

As shown in [108], $^3\widetilde{\mathcal{K}}_{(1)}$ has the dimension of a length: simple dimensional analysis shows that: $[\delta] = [L]$.

We will call this ansatz the "linear ansatz".

(c) The ansatz:

$$^3\widetilde{\mathcal{K}}_{(1)}(t,r) = \frac{\delta'}{r}\, \exp\left(-\frac{r}{L}\right), \tag{2.13}$$

in which the time does not appear at all, would simplify greatly the calculations and the interpretation of our results,[7] but we remind that,[8] for example, the weak lensing formula depends on $\partial_t\, ^3\widetilde{\mathcal{K}}_{(1)}$ which would be zero in this ansatz and therefore, in this case, weak gravitational lensing would be a real effect of actual DM.

We shall also see in chapter 3 that the fit of the M31 (the Andromeda galaxy) rotation curve is much worse in this case and a greater amount of "real" DM is needed (actually almost all of it is needed, see table 3.7).

It can be shown that $[\delta'] = [L]^2$.

We will call this ansatz the "time free ansatz".

We shall see in chapter 3 that, depending on which of the previous hypothesis on the time dependent part we choose, different amounts of DM can be described as an inertial effect.[9]

---

[5]This is similar to what authors did in [148, 152], fixing $\delta = 1/3$ when fitting rotation curves and density profile of clusters with $f(R)$ theories.

[6]This derivative appears in τ_{3K} (1.21) and on the rotation curve (I.30).

[7]We shall see that time appears in rotation curves and in redshift expression using the linear ansatz and in the general case: this will require a time average.

[8]See the introduction, section I.3.5, equation (I.28).

[9]In fact, we will see in chapter 3, that, in the case (a) with no hypothesis on the mathematical form of $\Delta(t)$, one can dispense with the DM halo in the case of M31, while in case (c), only about 3% of DM can be eliminated (at least for radii < 35 kpc), see table 3.7.

2.2.3 A consideration on the space coordinate

We notice here that, since our aim is to give an explanation to the phenomenon of DM, the 'r' that appears in (2.11) must be the *distance from the source to the galactic center*, and not from the the barycenter of the Solar System, so in our reference system (the BCRS), we must actually write (we use a generic time dependence):

$$^3\widetilde{\mathcal{K}}_{(1)}(t,R) = Y(R)\,\Delta(t) =$$
$$= \frac{\Delta(t)}{\left|\left(\vec{R}-\vec{r}\right)-\vec{R}_\odot\right|}\,\exp\left[-\frac{\left|\left(\vec{R}-\vec{r}\right)-\vec{R}_\odot\right|}{L}\right] \qquad (2.14)$$

at the source position, while at the Earth position we have:

$$^3\widetilde{\mathcal{K}}_{(1)}(t,r) = Y(r)\,\Delta(t) =$$
$$= \frac{\Delta(t)}{\left|\vec{r}-\vec{R}_\odot\right|}\,\exp\left[-\frac{\left|\vec{r}-\vec{R}_\odot\right|}{L}\right] \approx$$
$$\approx \frac{\Delta(t)}{\left|\vec{R}_\odot\right|}\,\exp\left[-\frac{\left|\vec{R}_\odot\right|}{L}\right] \qquad (2.15)$$

where $\vec{R}$ and $\vec{r}$ are the positions of the source and of the Earth in BCRS, and $\vec{R}_\odot$ is the distance of the Solar System from the galactic center (≈ 7.6 kpc [154], see the figure 2.1 for all the definitions); it is usually directed as the y axis both in ICRS and BCRS (see [131], for example).

One last note: modules in the previous equation can be calculated in the usual (Euclidean) fashion, since $^3\widetilde{\mathcal{K}}_{(1)}$ is already at PM order; we will see that this will be useful in the next chapters, when we will need to calculate angles between vectors, since trivial geometry and trigonometric relations such as the *Law of Cosines* will be the only things needed.[10]

Before we move to the calculation of the effect of our ansatz on the PTA and on redshift, we give the analytical expression of the extrinsic curvature tensor.

---

[10]At higher orders, this will not do, since we are *not* making any hypothesis on the geometry of the 3-space.
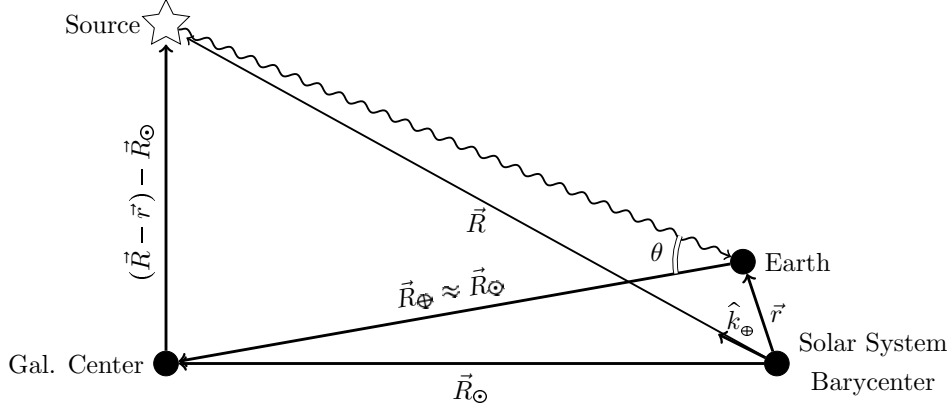
Figure 2.1: *Scheme and definitions for the calculations that follow.*
$\vec{R}_\odot$, the distance of the Solar System barycenter from the galactic center, and
$\vec{R}_\oplus$, the distance of the Earth from the galactic center, are approximately equal,
the difference being 1 astronomical unit over distances of the order of 10 kpc
(one astronomical unit is about 5×10^{-9} Kpc).

2.3 Analytical form of the tensor of extrinsic curvature at 1st PN order and its trace $^3K_{(1)}$

From the definition of the non-local York time $^3\widetilde{\mathcal{K}}_{(1)}$, we can calculate the analytical form of the trace of the extrinsic curvature of the hypersurfaces at the first PN order:[11]

$$^3\widetilde{\mathcal{K}}_{(1)} = \frac{^3K_{(1)}}{\Delta} \quad \Rightarrow \quad {}^3K_{(1)} = \Delta \, {}^3\widetilde{\mathcal{K}}_{(1)}. \tag{2.16}$$

This gives (we consider a generic time dependence, the case (a) in section 2.2.2):

$$^3K_{(1)} = \frac{\Delta(t)}{L^2} \, Y(r). \tag{2.17}$$

With trivial dimensional analysis, it can be checked that in all of the cases considered in the previous section, $\left[^3K_{(1)}\right] = [L]^{-1}$, as was stated in [108].

The extrinsic curvature tensor of the hypersurfaces at the first PN order is [102]:

$$\begin{aligned}
^3K_{rs} &= \partial_r \, \partial_s \, {}^3\widetilde{\mathcal{K}}_{(1)} + \delta_{rs} \left(\frac{1}{3} \, {}^3K_{(1)} \right) + O(c^{-3}) \\
&= \Delta(t) \left(\partial_r \, \partial_s \, Y(r) + \frac{1}{3} \delta_{rs} \frac{Y(r)}{L^2} \right) + O(c^{-3}).
\end{aligned} \tag{2.18}$$

---

[11]Δ is the flat Laplacian and Δ^{-1} is its Green function, see [102, 108, 109].

As we mentioned in the introduction (section I.5), while the usual metric gives ${}^{3}K_{rs} \approx O(c^{-3})$, in our case we have additional terms at the higher order; only in the particular CMC-like gauge ${}^{3}K_{(1)} \equiv 0$, we have ${}^{3}K_{rs} = O(c^{-3})$ (we remind that in this gauge all the usual results are recovered).

This (extrinsic) curvature of the 3-manifold is the source of the Dark Matter phenomenon: we conventionally impose that the 3-space is flat and, as a consequence, we *see* the DM; instead, if we changed the conventions, we could get rid of it.

2.4 Reformulation of previous results

In this section we rewrite the results of chapter 1 using the ansatz given in the previous section.

We will only consider the linear and the time free ansatz.

We notice that, since we interpret the 0.5PN terms depending on the non-local York time as 'Dark Matter', when calculating these terms we are basically *trying to evaluate the effect of DM on both the PTA and the redshift.*

In the next chapter's section 3.5.2, we shall estimate the effect of "actual" DM distributed in a halo with the profile described in [155] (see our equation (3.24)) and of the average potential of the galactic disc on this kind of measurements in order to have a comparison between the two different interpretations.[12]

2.4.1 The integral correction τ_{3K}

We found in section 1.2.2 that the integral correction was given by:

$$
\begin{aligned}
\tau_{3K}(s) &= \int_0^s ds_1 \int_0^{s1} ds_2 \left(\frac{1}{c^2} \partial_t^2 \, {}^{3}\widetilde{\mathcal{K}}_{(1)} \right) (\sigma_0 + b_0 \, s_2) + \\
&+ \frac{2}{c} \int_0^s ds_1 \int_0^{s1} ds_2 \left(b^r \, \partial_r \partial_t \, {}^{3}\widetilde{\mathcal{K}}_{(1)} \right) (\sigma_0 + b_0 s_2) + \qquad (1.21) \\
&+ \sum_{uv} b^u b^v \int_0^s ds_1 \int_0^{s1} ds_2 \left(\partial_u \partial_v \, {}^{3}\widetilde{\mathcal{K}}_{(1)} \right) (\sigma_0 + b_0 s_2)
\end{aligned}
$$

---

[12]We shalll find that the effect of actual Dark Matter is actually negligible (it is of the order of $10^{-15} \div 10^{-12}$ s), unlike our 0.5 PN correction (which is of the order of 10 ns), see section 3.5.

In order to calculate the previous integrals, one should remember the relations given in section 1.2.2: section 1.2.2):

$$\frac{d}{ds} = b^r \, \partial_r \qquad ds = d\sigma.$$

More over, the following formulae prove to be useful:

$$\int_a^s ds_1 \int_a^{s_1} ds_2 \, \frac{d^2 \, F(s_2)}{ds_2{}^2} = -F(a) + F(s) + (a - s) \, \frac{d \, F}{d \, s} \qquad (2.19)$$

$$\frac{d}{ds} \int_a^s ds_1 \int_a^{s_1} ds_2 \, \frac{d^2 \, F(s_2)}{ds_2{}^2} = -\frac{dF}{ds}\Big|_a + \frac{dF}{ds}\Big|_s \qquad (2.20)$$

The linear ansatz

If we consider the first case of the previous section (the linear ansatz), the first line of equation (1.21) is null, while for the third line one should use the equation (2.19); at the end we have:

$$\tau_{3K}(R) = 2\,\delta \int_{|r|}^{|R-r|} Y(r) \, dr+$$
$$- \delta\,\tau \left[Y(R) - Y(r) + \left(\left| \vec{R} - \vec{r} \right| - |\vec{r}| \right) \left(\widehat{k}_\oplus^r \, \partial_r Y(r) \right)_{sor} \right]. \qquad (2.21)$$

The first line comes from the mixed derivative $\partial_t \, \partial_r$, while the second from the double derivative in space; integration always start at the Earth position in BCRS since measurements are done on the Earth.

At the highest order,[13] $\tau \approx \left| \vec{R} - \vec{r} \right|$, so:

$$\tau_{3K}(R) = 2\,\delta \int_{|r|}^{|R-r|} Y(r) \, dr+ \qquad (2.22)$$
$$- \delta \left| \vec{R} - \vec{r} \right| \left[Y(R) - Y(r) + \left(\left| \vec{R} - \vec{r} \right| - |\vec{r}| \right) \left(\widehat{k}_\oplus^r \, \partial_r Y(r) \right)_R \right]$$

The time-free ansatz

If we use the time-free ansatz, both the first and the second line in (1.21) are zero, and we are left with:

$$\tau_{3K}(R) = -\delta' \left[Y(R) - Y(r) + \left(\left| \vec{R} - \vec{r} \right| - |\vec{r}| \right) \left(\widehat{k}_\oplus^r \, \partial_r Y(r) \right)_R \right] \qquad (2.23)$$

---

[13]We consider only the highest order, since ${}^3\widetilde{\mathcal{K}}_{(1)} = \delta \, Y(R)$ is already at PM order (see equations (1.8) and (1.20)).

2.4.2   Redshift and radial velocity

The linear ansatz

In our redshift formula (1.38), we had the time derivative of the integral correction. Going back to equations from (1.16) to (1.20), in section 1.2.2, we have (at the highest order):

$$\frac{1}{c}\frac{d}{dt} = \frac{1}{c}\frac{\partial s}{\partial t}\frac{d}{ds} = -\left(\frac{\vec{v}_{sor}}{c} - \frac{\vec{v}_\oplus}{c}\right)\cdot\widehat{k}_\oplus\,\frac{d}{ds} \qquad (2.24)$$

where the minus sign comes from equation (1.24) so we can use (2.20) in the third line of (1.21), and then transform back to the $\vec{R}$ and $\vec{r}$ variables. The result is:[14]

$$\frac{1}{c}\frac{d\tau_{3K}}{dt} = 2\,\widehat{k}_\oplus\cdot\left(\frac{\vec{v}_{sor}}{c} - \frac{\vec{v}_\oplus}{c}\right)\delta\,Y(R)+$$

$$-\delta\left(\frac{\vec{v}_{sor}}{c} - \frac{\vec{v}_\oplus}{c}\right)\cdot\widehat{k}_\oplus\left[Y(R) - Y(r)+\right.$$

$$\left.+\left(\tau\,\widehat{k}_\oplus\cdot\vec{\nabla}Y\right)_R - \left(\tau\,\widehat{k}_\oplus\cdot\vec{\nabla}Y\right)_r\right] =$$

$$= 2\,\widehat{k}_\oplus\cdot\left(\frac{\vec{v}_{sor}}{c} - \frac{\vec{v}_\oplus}{c}\right)\delta\,Y(R)+$$

$$-\delta\left(\frac{\vec{v}_{sor}}{c} - \frac{\vec{v}_\oplus}{c}\right)\cdot\widehat{k}_\oplus\left[Y(R) - Y(r)+\right.$$

$$-\left|\vec{R} - \vec{r}\right|\left(\frac{1}{\left|\vec{R} - \vec{R}_\odot\right|} + \frac{1}{L}\right)Y(R)\,\widehat{k}_\oplus\cdot\widehat{k}_{sor}+$$

$$\left.+\left|\vec{r}\right|\left(\frac{1}{\left|\vec{r} - \vec{R}_\odot\right|} + \frac{1}{L}\right)Y(r)\,\widehat{k}_\oplus\cdot\widehat{k}_{obs}\right]$$

The first lines comes from the second line of (1.21), while all the others come from the third line; $\vec{v}_{sor}$ and $\vec{v}_\oplus$ are respectively the velocity of the source and of the Earth with respect the BCRS, and where we put:

$$\widehat{k}_{sor} = \frac{\vec{R} - \vec{R}_\odot}{\left|\vec{R} - \vec{R}_\odot\right|} \qquad \widehat{k}_{obs} = \frac{\vec{r} - \vec{R}_\odot}{\left|\vec{r} - \vec{R}_\odot\right|} \approx \frac{\vec{R}_\odot}{\left|\vec{R}_\odot\right|}. \qquad (2.25)$$

---

[14]In the last two lines the terms $\left|\vec{R} - \vec{r}\right|$ and $\left|\vec{r}\right|$ arise from the time dependence of the $^3\widetilde{\mathcal{K}}_{(1)}$ and the fact that at the highest order $\tau \approx \left|\vec{R} - \vec{r}\right|$.

the direction of the source and of the Earth with respect the Galaxy canter; $\widehat{k}_\oplus$ is the direction of observation and is given in (1.24).

In the case the observer is set in the barycenter of the Solar System, $\vec{v}_\oplus \equiv 0$ and $\vec{r} \equiv 0$, so:[14]

$$
\frac{1}{c} \frac{d\tau_{3K}}{dt} = 2 \, \widehat{k}_\oplus \cdot \frac{\vec{v}_{sor}}{c} \, \delta \, Y(R) +
$$
$$
- \delta \, \frac{\vec{v}_{sor}}{c} \cdot \widehat{k}_\oplus \left[Y(R) - Y(0) + \left| \vec{R} \right| \, \widehat{k}_\oplus \cdot \vec{\nabla}Y \Big|_R \right]
$$
$$
\frac{1}{c} \frac{d\tau_{3K}}{dt} = 2 \, \widehat{k}_\oplus \cdot \frac{\vec{v}_{sor}}{c} \, \delta \, Y(R) +
$$
$$
- \delta \, \frac{\vec{v}_{sor}}{c} \cdot \widehat{k}_\oplus \left[Y(R) - Y(r) + \right.
$$
$$
\left. - \left| \vec{R} \right| \left(\frac{1}{\left| \vec{R} - \vec{R}_\odot \right|} + \frac{1}{L} \right) Y(R) \, \widehat{k}_\oplus \cdot \widehat{k}_{sor} \right] \tag{2.26}
$$

We notice that, in the first and in the second lines, $\vec{v}_{sor} \cdot \widehat{k} = \rho$, the radial velocity of the source with respect the BCRS.

We can finally write *the redshift in the Solar System barycenter with the linear ansatz as:*

$$
1 + z = \left(1 + \frac{1}{2} \frac{v^2}{c^2} + \frac{U}{c^2} + \frac{\delta}{c} Y(r) - \delta \frac{\tau}{c} v^r \, \partial_r Y(r) \right)_{\text{sor}} \times
$$
$$
\times \left[1 + \frac{\rho}{c} \left(1 + \delta \, Y(R) + \delta \, Y(0) + \left| \vec{R} \right| \delta \, Y'(R) \right) \right] \tag{2.27}
$$

where we used the notation:

$$
Y'(a) = \widehat{k}_\oplus \cdot \vec{\nabla}Y \Big|_a \tag{2.28}
$$

We see that the integral correction gives rise to a *direct correction to the radial velocity* (second line) depending on the value of the Yukawa-like function at the source position and its derivative evaluated both at the source and at the observer position; there is also a correction in the first line given by the change in the definition of proper time.

For completeness, the redshift as measured on the moving Earth is given

by:

$$
1 + z = \left(1 + \frac{1}{2}\frac{v^2}{c^2} + \frac{U}{c^2} + \frac{\delta}{c}\,Y(r) - \delta\,\frac{\tau}{c}\,v^r\,\partial_r\,Y(r) \right)_{\text{sor}} \times
$$

$$
\times \left[1 + \frac{\rho}{c}\left(1 + \delta\,Y(R) + Y(r) + \left|\vec{R} - \vec{r}\,\right|\,\delta\,Y'(R) - |\vec{r}\,|\,\delta\,Y'(r) \right) + \right.
$$

$$
\left. - \delta\,\widehat{k}_\oplus \cdot \frac{\vec{v}_\oplus}{c}\left(Y(R) + Y(r) + \left|\vec{R} - \vec{r}\,\right|\,Y'(R) - |\vec{r}\,|\,Y'(r) \right) \right] \times
$$

$$
\times \left(1 - \frac{1}{2}\frac{v^2}{c^2} - \frac{U}{c^2} - \frac{\delta}{c}\,Y(r) + \delta\,\frac{\tau}{c}\,v^r\,\partial_r\,Y(r) \right)_\oplus \tag{2.29}
$$

We notice that in the third line there is a correction depending on the Earth motion proportional to the Yukawa-like function and its derivatives: these kind of term is absent in the usual redshift function.

We notice further that in both cases there is an *explicit dependence on time* τ: we can get rid of it if we remember that at the highest order, we have $\tau = \left|\vec{R} - \vec{r}\,\right|$ at the source (first line of both (2.27) and (2.29)) and $|\vec{r}\,|$ at the Earth position (last line of (2.29)).

The time free ansatz

With the time free ansatz, we can repeat all the previous calculations using equations (1.21) and (2.20), keeping in mind that in the former only the last line is non null.

For an observer in the Solar System barycenter, we have (using again the notation (2.28)):

$$
1 + z = \left(1 + \frac{1}{2}\frac{v^2}{c^2} + \frac{U}{c^2} - \delta'\,\frac{v^r}{c}\,\partial_r\,Y(r) \right)_{\text{sor}} \times
$$

$$
\times \left[1 + \frac{\rho}{c}\left(1 + \delta'\,Y'(R) - \delta'\,Y'(0) \right) \right] \tag{2.30}
$$

while for an observer on the Earth:

$$
1 + z = \left(1 + \frac{1}{2}\frac{v^2}{c^2} + \frac{U}{c^2} - \delta'\,v^r\,\partial_r\,Y(r) \right)_{\text{sor}} \times
$$

$$
\times \left[1 + \frac{\rho}{c}\left(1 + \delta'\,Y'(R) - \delta'\,Y'(r) \right) - \delta\,\widehat{k}_\oplus \cdot \frac{\vec{v}_\oplus}{c}\left(Y'(R) - Y'(r) \right) \right] \times
$$

$$
\times \left(1 - \frac{1}{2}\frac{v^2}{c^2} - \frac{U}{c^2} + \delta'\,v^r\,\partial_r\,Y(r) \right)_\oplus \tag{2.31}
$$

In both cases, no difficult to explain residual time dependence is left.

2.4.3   PTA

Linear ansatz

In order to show the effect of our ansatz on the equation for PTA in the case of the linear ansatz, we have to substitute (2.22) in (1.30), and expand the term $\left| \vec{R} - \vec{r} \right|$ like we did in section 1.3.2. The result is:[15]

$$
c\,(t_n - t_0) = c\,\left(\tilde{t}_n - \tilde{t}_0\right) - 2\,\frac{G}{c^2}\sum_i \log\left[\vec{r}\cdot\hat{k}_\oplus + |\vec{d}_i - \vec{r}|\right]\,m_i +
$$

$$
+\,2\,\delta\int_{|r|}^{|R-r|} Y(r')\,dr' +
$$

$$
+\left[1 + \delta\,Y(r) - \delta\left(1 + \left|\vec{R}-\vec{r}\right| - |\vec{r}\,|\right)Y'(R)\right]\times
$$

$$
\times\left\{\left[\left(\hat{k}_\oplus\cdot\vec{V}\right)\Delta t_n - \left(\hat{k}_\oplus\cdot\vec{r}\right)\right] + \frac{1}{2\,R_0}\left[r^2 - \left(\hat{k}\cdot\vec{V}\right)^2\right] + \right.
$$

$$
-\frac{1}{R_0}\left[\vec{V}\cdot\vec{r} - \left(\hat{k}_\oplus\cdot\vec{V}\right)\left(\hat{k}_\oplus\cdot\vec{r}\right)\right](\Delta t_n) +
$$

$$
\left.+\frac{1}{2R_0}\left[V^2 - \left(\hat{k}_\oplus\cdot\vec{V}\right)^2\right]\Delta t_n^2\right\} \tag{2.32}
$$

Time free ansatz

In this case, we have to substitute equation (2.23) in (1.30), remembering that in this case $\partial_\tau{}^3\widetilde{\mathcal{K}}_{(1)} \equiv 0$; the result is:

$$
c\,(t_n - t_0) = c\,\left(\tilde{t}_n - \tilde{t}_0\right) - 2\,\frac{G}{c^2}\sum_i \log\left[\vec{r}\cdot\hat{k}_\oplus + |\vec{d}_i - \vec{r}|\right]\,m_i +
$$

$$
-\,\delta'\left[Y(R) - Y(r) + \left(\left|\vec{R}-\vec{r}\right| - |\vec{r}\,|\right)Y'(R)\right] +
$$

$$
+\left(1 - \delta'\,Y'(R)\right)\times
$$

$$
\times\left\{\left[\left(\hat{k}_\oplus\cdot\vec{V}\right)\Delta t_n - \left(\hat{k}_\oplus\cdot\vec{r}\right)\right] + \frac{1}{2\,R_0}\left[r^2 - \left(\hat{k}\cdot\vec{V}\right)^2\right] + \right.
$$

$$
-\frac{1}{R_0}\left[\vec{V}\cdot\vec{r} - \left(\hat{k}_\oplus\cdot\vec{V}\right)\left(\hat{k}_\oplus\cdot\vec{r}\right)\right](\Delta t_n) +
$$

$$
\left.+\frac{1}{2R_0}\left[V^2 - \left(\hat{k}_\oplus\cdot\vec{V}\right)^2\right]\Delta t_n^2\right\} \tag{2.33}
$$

---

[15]One should also remember that at the highest order $\tau = |\vec{R}-\vec{r}\,|$

2.5 Summary of the chapter and discussion

In this chapter, we exploited a similarity between the form of the ADM tg PN expansion of the metric and the PN expansion of the metric in $f(R)$ theories making the ansatz that the spatial part of the $^3\widetilde{\mathcal{K}}_{(1)}$ has a Yukawa form.

We notice that even if the two metrics (1.51) and (2.4) have a similar form (at least in the time-time component), the interpretation of the Yukawa-like terms and the origin of Dark Matter is completely different:

- In the $f(R)$ theories, the Yukawa correction comes as a consequence of the modification of the Hilbert-Einstein action, in particular as a consequence of the quadratic terms in the Taylor expansion of $f(R)$ (see [148] and reference therein, where it is shown that the length scale L of the Yukawa interaction is proportional to the second derivative of the $f(R)$ function): this is an *actual potential* that modifies the Newtonian action (they are of the same order, $O(c^{-2})$).

  The consequence of this additional real potential is DM: when fitting the rotation curves using Newtonian gravity,[16] *we are using the wrong theory* of gravity and as a consequence we *see* DM;

- In our case, the Yukawa-like term is *a choice* for the gauge fixing of the trace of the extrinsic curvature of the 3-space in the 3+1 splitting formalism.[17] This is not a true potential, but a relativistic inertial effect, and so is DM.

  In all the present measurements, even if it is never mentioned explicitly, we conventionally use a flat 3-space and as a consequence we *see* DM.

  We notice that the choice we made of the Yukawa-like $^3\widetilde{\mathcal{K}}_{(1)}$ is just a possibility among others: as pointed out in [102, 109] one should choose the form that cancels out most of the DM.

Since we have no clue of its actual form, we made two different guesses for the time dependent part $\Delta(t)$:

---

[16]According to the general consensus Newtonian gravity is enough when describing the dynamics of galaxy (see also [155]).

[17]We mentioned in the introduction, section I.3.2, that the ^3K is the only gauge variable for which there isn't a natural gauge fixing.

(b) The *linear ansatz*:

$$^3\widetilde{\mathcal{K}}_{(1)} = c\, t\, \delta\, \frac{1}{|\vec{r}\,|}\, \exp\left(-\frac{|\vec{r}\,|}{L}\right) \tag{2.12}$$

(c) The *time free* ansatz:

$$^3\widetilde{\mathcal{K}}_{(1)} = \delta'\, \frac{1}{|\vec{r}\,|}\, \exp\left(-\frac{|\vec{r}\,|}{L}\right) \tag{2.13}$$

We also mentioned that it is possible to consider the more general case in which we make no hypothesis on the form of $\Delta(t)$, but we will do this in the next chapter when fitting the Andromeda rotation curve.

As was stressed in subsection 2.2.3, in the two equations (2.12) and (2.13), the spatial coordinate $\vec{r}$ is the distance from the center of the galaxy, since the 0.5 PN term is meant to describe (at least part) of the Dark matter.

Using (2.12) and (2.13), we recalculated the TOA for the PTA and the redshift formula:

- In the redshift formulae (equations (2.27) and (2.30)) there are two corrections: the one in the first line due to the change in the definition of proper time and then there is a direct contribution to the radial velocity coming from the derivative of τ_{3K}.

  In the case of the linear ansatz, in the next chapter we will see that the direct contributions to the radial velocity is of the order of few percent, so the absolute effect is of the order of a few kilometers per second (we notice that this is of the same order of magnitude of the effects due by the convective motions on the star surface [132–134] and, therefore, are hidden by the latters).[18]

- In PTA The results for the linear and the time free ansatz are given in equations (2.32) and (2.33); the usual form is given in (1.32). In both equations the 0.5PN corrections are in the second and third line.

  We shall see in the next chapter that the contribution of the 0.5 PN terms in the case of the linear ansatz are of the order of ≈ 10 ns[19] and possibly observable in the future using millisecond pulsars (see section 1.3 and references [140, 141]).

---

[18]The time free ansatz gives results out of scale: see chapter 3.

[19]Also in this case the time free ansatz gives corrections out of scale, see chapter 3.

Enough with calculations!

In the next chapter we shall use the ansatz described i this chapter to fit the rotation curve of the Andromeda galaxy: we shall try to find out wich ansatz best describes the data and how much Dark Matter can be eliminated and considered a relativistic inertial effects.

Then we will come back to our Galaxy and estimate the effects of the 0.5 PN terms on PTA and redshift.

CHAPTER 3

FITS AND NUMBERS

In this chapter we shall fit the rotation curve of M31 (the Andromeda galaxy) with our function (I.30).

Using the three different hypothesis for the time dependence of $^{3}\tilde{\mathcal{K}}_{(1)}$ described in section 2.2, we shall find in section 3.2 which form fits better the data and how much DM can be considered as an inertial effect in M31.

In order to do this, we fit 7 different models:

- The "*usual model*", mutuated from [156], in which there is an actual Dark Matter halo and no Yukawa-like terms (we use this as a basis for comparison with the other models);

- Three models in which there is no DM halo at all (and accordingly called "*no DM*"): we use the ansatz described in the previous chapter to substitute it;

- Three "*hybrid models*" in which we admit the possible existence of an actual DM halo along side with the Yukawa terms: these are a mix of the previous two.

Our models of rotation curve are fitted to data taken from [157] using a Markov Chain MonteCarlo (MCMC) code.

We then come back to our galaxy in section 3.5 and, only for the linear and time free ansatz, we use parameters estimated before to have at least an idea of the order of magnitude of the effect of the 0.5PN term on PTA

and on redshift measurements. We shall also use the thick disk + bulge + actual DM halo models for our Galaxy described in [155] to calculate the effect of the average galactic potential and "actual" DM on PTA.

The rationale for using M31 also in the estimate of the 0.5PN effects on the PTA and redshift in our Galaxy is that M31 is similar to ours and this should suffice for an order of magnitude estimate.

3.1 M31 rotation curve

In this section we build the model for the M31 rotation curve given by the formula (I.30), which we rewrite here:[1]

$$v(R) = v_0(R) \left(1 - \frac{1}{2} \frac{R}{v_0(R)} \frac{1}{c} \frac{d^2}{dt^2} \tilde{\mathcal{K}}_{(1)} \right) \quad {}^3\widetilde{\mathcal{K}}_{(1)} = \frac{\Delta(t)}{r} \exp\left(-\frac{r}{L} \right)$$

under one of the three guesses for $\Delta(t)$ discussed in the previous chapter (section 2.2.2):

(a) No hypothesis on the form of $\Delta(t)$;

(b) The linear ansatz (2.12);

(c) The time free ansatz (2.13).

As already said in the introduction of this chapter, at the end we will have 7 models:

1. The "usual model", mutuated from [156], in which there is an actual NFW halo of DM (we use this as a basis for comparison with the other models);

2. Three models in which there is no DM halo at all. We use the ansatz described in the previous chapter. We will call these models "no DM" (a), (b) and (c) depending on which guess for the non-local York time we are considering (see the list above);

3. Three "hybrid models" ((a), (b), (c), depending on which guess for the $\Delta(t)$ we are using) in which we admit the possible existence of an actual DM halo together with the Yukawa terms: these are an intermediate case between the previous two.

---

[1]$v_0(R)$ is the usual "Newtonian" rotational velocity, see the introduction I.3.5 and the following sections.

We use the usual case estimate for comparison when calculating how much DM can be explained as an inertial effect in the hybrid case and to fix the disk and bulge parameters.

In the next subsections, we first present the mathematical functions we used for Bulge, Disk and DM halo (mutuated from [156]) and for the 0.5PN term.

3.1.1 The bulge, the disk and the Dark Matter halo

For the bulge, we consider a *Hernquist profile* [155, 156]:[2]

$$M_b(R) = M_b \frac{R^2}{(L_b + R)^2} \tag{3.1}$$

$$\Phi_b(R) = -\frac{GM_b}{L_b + R} \tag{3.2}$$

$$v_b^2(R) = GM_b \frac{R}{(L_b + R)^2} = \frac{GM_b}{L_b} \frac{R}{L_b} \left(\frac{R}{L_b} + 1\right)^{-2} \tag{3.3}$$

where M_b is the bulge total mass and L_b is its scale length.

For the disk, we consider a *flat disk model* [155, 156]:

$$M_d(R) = 2\pi \Sigma_0 L_d^2 \left[1 - \left(1 + \frac{R}{L_d}\right) \exp\left(-\frac{R}{L_d}\right)\right] \tag{3.4}$$

$$\Phi_b(R) = -\frac{2\pi G \Sigma_0 L_d}{R} \left(\frac{R}{2L_d}\right)^2 \times \tag{3.5}$$
$$\times \left[I_0\left(\frac{R}{2L_d}\right) K_0\left(\frac{R}{2L_d}\right) - I_1\left(\frac{R}{2L_d}\right) K_1\left(\frac{R}{2L_d}\right)\right]$$

$$v_d^2(R) = 4\pi G \Sigma_d L_d \left(\frac{R}{2L_d}\right)^2 \times \tag{3.6}$$
$$\times \left[I_0\left(\frac{R}{2L_d}\right) K_0\left(\frac{R}{2L_d}\right) - I_1\left(\frac{R}{2L_d}\right) K_1\left(\frac{R}{2L_d}\right)\right]$$

---

[2]A central black hole is usually considered too, but its mass, estimated to be $(5.6 \pm 0.7) \times 10^7$[158] is important for the dynamics of the galaxy only at radii < 20 pc [156], so we neglect it in the following.

where Σ_0 is the disk superficial mass density, L_d is the disk scale length and I_n and K_n are the modified Bessel functions, respectively of the first and second kind of order n.

We estimated the four parameters of bulge and disk only in the case of the usual model: in all the other cases they were kept fixed at the value we obtained (we only want to compare the 'DM halos').

We consider a DM halo with a NFW profile (see equation (I.4) in the introduction) whose squared-velocity field is given by:

$$v_h^2(R) = \frac{4\,\pi\,G\,\rho_h\,L_h^3}{R}\left[-\frac{R}{R+L_h} + \ln\left(\frac{R+L_h}{R}\right)\right] \qquad (3.7)$$

The parameters are the density of the halo ρ_h and its scale length L_h.

3.1.2   The 0.5 PN term

We can write the 0.5PN term as:

$$\frac{d^2}{dt^2}\,^3\tilde{\mathcal{K}}_{(1)} = \ddot{\Delta}(t)\,Y(R) + \dot{\Delta}(t)\,v_0{}^u\,\partial_u\,Y(R) + \Delta(t)\,v_0{}^u\,v_0^s\,\partial_u\,\partial_s\,Y(R) \quad (3.8)$$

where $Y(R)$ is the Yukawa function.

We need to average over time to eliminate the explicit dependence over t:[3]

$$\left\langle \frac{d^2}{dt^2}\,^3\tilde{\mathcal{K}}_{(1)} \right\rangle = \delta_1\,Y(R) + \delta_2\,v_0{}^u\,\partial_u\,Y(R) + \delta_3\,v_0{}^u\,v_0^s\,\partial_u\,\partial_s\,Y(R) \qquad (3.9)$$

This is for the "no prior" (a) case.

For the linear (case (b)) and the time free ansaz (case (c)), we have, respectively:[4]

$$\left\langle \frac{d^2}{dt^2}\,^3\tilde{\mathcal{K}}_{(1)} \right\rangle = \delta\,c\,v_0{}^u\,\partial_u\,Y(R) + \delta_4 c\,v_0{}^u\,v_0^s\,\partial_u\,\partial_s\,Y(R) \qquad (3.10)$$

$$\frac{d^2}{dt^2}\,^3\tilde{\mathcal{K}}_{(1)} = \delta'\,v_0{}^u\,v_0^s\,\partial_u\,\partial_s\,Y(R) \qquad (3.11)$$

The velocity $\vec{v}_0$ that appears in these equations is the speed at order zero, given only by the total Newtonian potential:

$$v_0{}^2 = v_b{}^2(R) + v_d{}^2(R) + v_h{}^2(R) \qquad (3.12)$$

---

[3]We have to consider a time scale much longer than the typical dynamical time scale (longer than the galactic year, for example).

[4]No time average is needed for the time free ansatz.

3.1.3   Data for the M31 rotation curve

The rotational velocity as a function of the galactic radius up to about 35 kpc used in this work is listed in table 3.1.

Data are taken from [157], where the authors measure the rotational velocity of the Andromeda Galaxy using HI regions assuming an angular distance of 780 kpc from the Sun[5] and a bulk velocity of -300 km/s.[6]

Table 3.1: *Rotation curve of M31 up to 35 kpc, data from [156].*

R (kpc)	V_{rot} km/s	δV_{rot} km/s	R (kpc)	V_{rot} km/s	δV_{rot} km/s
5.68	235.5	17.8	21.45	227.6	28.8
6.81	242.9	0.8	22.47	226.0	28.8
7.95	251.1	0.7	23.50	225.7	28.8
9.08	262.0	2.1	24.52	227.5	28.8
10.22	258.9	6.9	25.54	227.4	28.8
11.35	255.1	5.7	26.56	225.6	28.8
12.49	251.8	5.7	27.58	224.4	28.8
13.62	252.1	7.4	28.60	222.3	28.8
14.76	251.0	18.6	29.62	222.1	28.8
15.89	245.5	28.8	30.65	224.9	28..8
17.03	232.8	1.0	31.67	228.1	28.8
18.16	232.0	14.2	32.69	231.1	28.8
19.30	235.7	4.6	33.71	230.4	28.8
20.43	229.3	13.8	34.73	226.8	28.8

---

[5]In photometric measurements, distances between two objects are given by the separation angle: if one knows the (angular diameter) distance from the two objects and the receiver, one can calculate the actual distance (in kpc) of the two objects.

[6]The bulk velocity of the whole galaxy must be subtracted from the measured velocity of the HI region if one wants its rotational velocity.

3.2   The Markov Chain MonteCarlo (MCMC)

In every case, the fit is done with a *random-walk Metropolis-Hastings MCMC* (Markov Chain Monte Carlo with gaussians priors on parameters [159, 160]), written with Python 2.7: see appendix B for a description of MCMC method and generalities on Bayesian approach.

In each model, we considered two chains 1.5×10^6 elements long[78]. In MCMC simulations, there is a so-called *burn in* phase in which the code is looking for the region of the parameter space where the maximum of the likelihood lies, therefore the initial part has to be eliminated from the final chains: it is just a matter of choice how long the burn in phase is, therefore we eliminated 90% of elements (in this way we were in the maximum area and also we could deal with much smaller files): our final chains were therefore 3×10^5 elements long.

We used the Gelman and Rubin test to check the convergence of our parameters: in every model and for each parameter the index $R - 1$ less then 0.01, only in the no DM (c) model we had $R - 1 \approx 0.1$ for the δ' and δ_1 parameters.

The acceptance rate for our models was between 0.2 and 0.4 (if the acceptance rate is too high, the code does not sweep fast enough through the parameter space, if it is too low, then the convergence is too slow; this is just *rule of thumb*, but in random walk MCMC code an acceptance rate between 0.2 and 0.5 is considered desiderable [159, 160].)

3.2.1   Our likelihood

We now call $\mathbf{V}_{rot}$ the vector of the measured rotational velocities as a function of the galactic radius (from table 3.1) and $\mathbf{Vth}(par)$ the vector of our rotational velocities as calculated with equation (I.30) depending on the parameters *par* that define our model. We also introduce the (covariance) matrix:

$$\mathbf{C} = (\mathrm{diag}\,\{\delta V_{rot}\})^2$$

---

[7]The convergence was very slow for models other than the usual one: we did not investigate this issue: using other MCMC codes instead of the Metropolis-Hastings, such as the Gibbs sampler [159, 160] could solve this problem.

[8]Even if the convergence was much faster then the other cases, we used 1.5×10^6 elements long chains also in the usual case.

where the δV_{rot} are given in table 3.1. Then, for each model, our likelihood is given by:

$$\mathcal{L} \propto \exp\left[-\frac{1}{2}\ (\mathbf{V}_{rot} - \mathbf{Vth})^T \cdot \mathbf{C}^{-1} \cdot (\mathbf{V}_{rot} - \mathbf{Vth}) \right]$$

where n is the number of parameters and ^{T} stands for vector trasposition.

Likelihood are defined less than a multiplicative constant (the normalization factor): Central Limit Theorem guarantees that in many cases (and ours is one of them) it is well approximated by a multivariate Gaussian [161], so we set:

$$\mathcal{L} = \frac{1}{\sqrt{(2\,\pi)^n \det \mathbf{C}}}\ \exp\left[-\frac{1}{2}\ (\mathbf{V}_{rot} - \mathbf{Vth})^T \cdot \mathbf{C}^{-1} \cdot (\mathbf{V}_{rot} - \mathbf{Vth}) \right]$$

3.2.2 Constraints on parameter space

Since MCMC sweeps the whole parameter space, we have to impose some constraint in order to avoid non physical results. The number of constraints cannot be greater than the number of parameters.

In the 'usual case', we impose that all the parameters are positive definite, since they are densities and length scales.

In all the other cases, we impose that the lenght scale L of the Yukawa function, the central density of actual DM halo and its scale length (when considered) are all positive definite. Since we know nothing on δ, δ' ..., in these cases we are free to set other constraints: we choose to impose that $v_{rot}^2 > 0$.

3.2.3 Error estimate

We estimate the errors on parameters assuming each element (c_j) of our final chains is an independent measurement of the parameter; in this way the (aspectation) value of the parameter p_i is given by the average:

$$p_i = \frac{1}{N} \sum_{j=0}^{N} c_j \tag{3.13}$$

where N is the length of ou final chains (3×10^5 elements); the relative error is given by the square root of the variance:

$$\delta p_i = \sqrt{\frac{1}{N-1} \sum_{j=0}^{N} (p_i - c_j)^2} \tag{3.14}$$

3.3 Results

In this section, we describe the results of our fits.

First, we consider the usual case and we make a comparison between this and the model by [156] calculating the masses of the various M31 components.

Then we discuss separately the cases (a), (b) and (c); for the hybrid models we also use our halo parameters to calculate the mass of the Dark Matter component within 35 kpc (these values are summed up in table 3.7 and in figure 3.10, we plot the halo masses for each model in function of the galactic radius).

A comparison among the models is done in the following section 3.4.

3.3.1 The usual case

In table 3.2 we list the parameters obtained in our fit; for comparison, in the same table, we write the results of the fit by [156] (authors do not consider the same dataset as our: they use velocity dispersion from [162], rotational velocity data from [163] and surface brightness data from [164]).

Figure 3.1 displays the fitted rotation curve for this case as a full black line together with the separated contribution given by the bulge (purple dash-dotted line), the disk (red dash-dotted line) and the halo (blue dash dotted line); finally, the thick red line is the model from [156].

The total Dark Matter inside a sphere of radius R is given by the equation:

$$M(< R) = \int_0^R 4\,\pi\,\rho_h(r)\,r^2\,dr \tag{3.15}$$

where ρ_h is given in (I.4).

With the parameters given in table 3.2, we find:

$$M_{us}(< 35) = 1.75 \,\times\, 10^{11}\,M_\odot. \tag{3.16}$$

In figure 3.2 we plot the mass of the luminous part (bulge+disk, respectively from equations (3.1) and (3.4)), the halo and of the total mass of M31 as a function of the radius, for our model (thick lines) and for the [156] one (dashed lines); in figure 3.3, we plot the ratio between the total mass in the two models extrapolated up to 300 kpc.

A few comments on the table 3.2 and on figures 3.2 and 3.3:

- The two bulges are about of the same dimensions;

- Our disk is more dense then in [156], but we have a smaller length scale; as a result:

- *The luminous part of the galaxy has the same dimension in both the models (see the almost overlapping red thick and red dashed lines in figure* 3.2);

- Our Halo is less dense and has a longer length scale; as a result:

- *Within a radius of 35 kpc, our halo is about* 20% *smaller then the one obtained in* [156] (see the purple thick and dashed lines in 3.2).

- *Considering the total mass within a radius of 35 kpc, our M31 is about* 25% *smaller than in* [156] (see figure 3.3);

- Up to 300 kpc the mass of the two models differ of about 17 %.

Table 3.2: *Results from our fit for the usual case and comparison with the fit done by [156].*

OUR FIT					
M_b $(\times 10^{10}\ M_\odot)$	L_b (kpc)	Σ_0 $(10^8\ M_\odot\ kpc^{-2})$	L_d (kpc)	ρ_h $(10^7\ M_\odot\ kpc^{-3})$	L_h (kpc)
3.3 ± 0.1	0.7 ± 0.1	5.00 ± 0.03	5.1 ± 0.1	2.6 ± 0.04	8.65 ± 0.07
FIT BY GEEHAN ET AL. [156][a]					
M_b $(\times 10^{10}\ M_\odot)$	L_b (kpc)	Σ_0 $(10^8\ M_\odot\ kpc^{-2})$	L_d (kpc)	$\rho_h{}^b$ $(10^7\ M_\odot\ kpc^{-3})$	L_h (kpc)
3.3	0.61	4.6	5.4	3.8	8

[a] Authors report the confidence ellipses for the parameters, but do not write explicitly the errors.

, [a] The authors actually write $\rho_h = \rho_{cr}\,\delta_h$, where $\rho_{cr} = 277.72 h^2\ M_\odot\ kpc^{-3}$ is the critical density and $\delta_h = 27.0 \times 10^4$ is a dimensionless parameter (they use the value $h = 0.71$ km/s/Mpc).
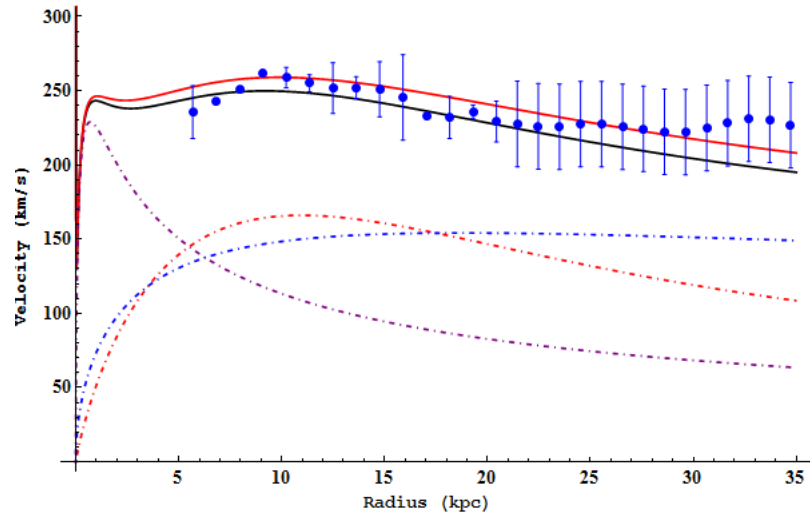

Figure 3.1: *The fit of the rotational velocity of the M31 galaxy in the usual case. The black thick line is the result of the fit, the dot-dashed lines are the single contributions of bulge (purple), disk (red) and halo (blue). The blue dots with their errors bars are the data reported in table 3.1. Finally, the red thick line is the fit from[156].*
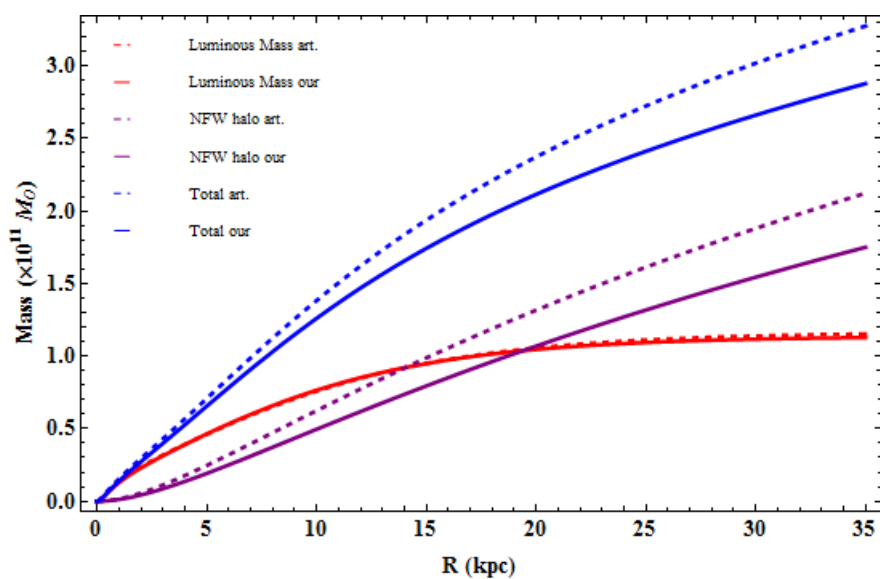
Figure 3.2: *Mass of the various components of M31 and the total mass as a function of R, up to 35 kpc: in red the luminous components (bulge+disk), in purple the halo and in blue the total mass of the galaxy; thick lines are our model, dahed lines are [156] model.*
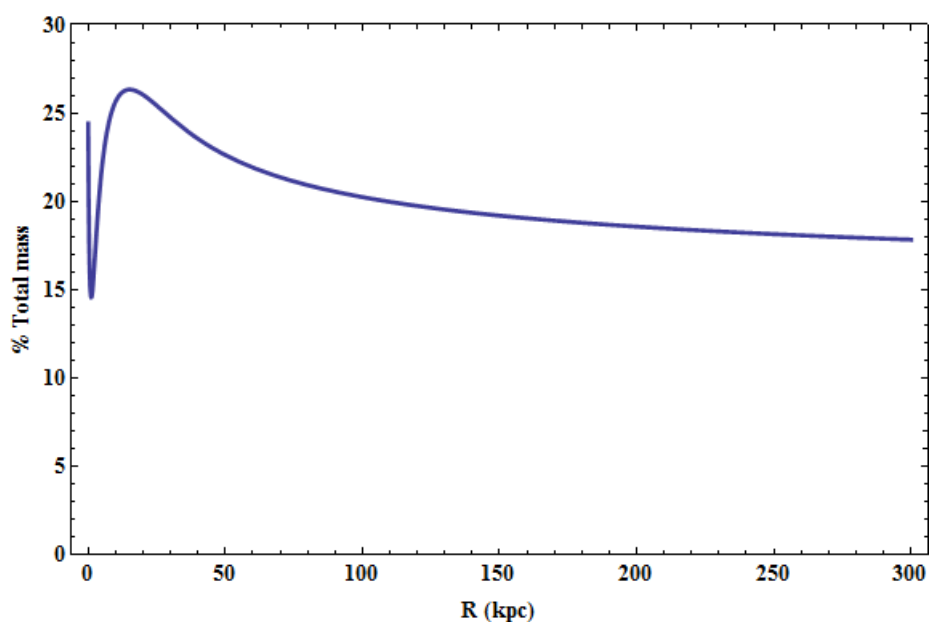

Figure 3.3: *Difference between the total masses of our model and the one from [156] as a function of the galactic radius.*

3.3.2   No priors on δ (case (a))

In table 3.3 we list the parameters obtained in our fits for the case (a) (no priors on $\Delta(t)$) both in the "no DM" and in the "hybrid" case.

Figure 3.4 displays the fitted rotation curves: the full black line is for the hybrid case, the dashed black line is for the case of no 'real' DM.

In the hybrid case, the total DM within 35 kpc is:

$$M_{(a)}(< 35kpc) = 2.5 \times 10^{10} \, M_\odot. \tag{3.17}$$

Table 3.3: *Results from our fit with no priors on $\Delta(t)$. We list the results of our fit for the case in which no DM is considered (first line) and the case in which the DM halo is considered (second line).*

Model	0.5 PN term				DM	
	$\delta_1{}^a$ $(10^5 \text{ kpc}^2/\text{s}^2)$	$\delta_2{}^a$ $(10^5 \text{ kpc}^2/\text{s})$	$\delta_3{}^a$ (10^4 kpc^2)	L (kpc)	ρ_h $(\times 10^7 \, M_\odot)$	L_h (kpc)
No DM (a)	5.8 ± 37.1	1.02 ± 0.29	0.98 ± 0.08	117.3 ± 20.8	//	//
Hybrid (a)	-7.8 ± 45.0	1.00 ± 0.05	0.99 ± 0.01	85.9 ± 20.3	0.95 ± 0.27	5.8 ± 2.9

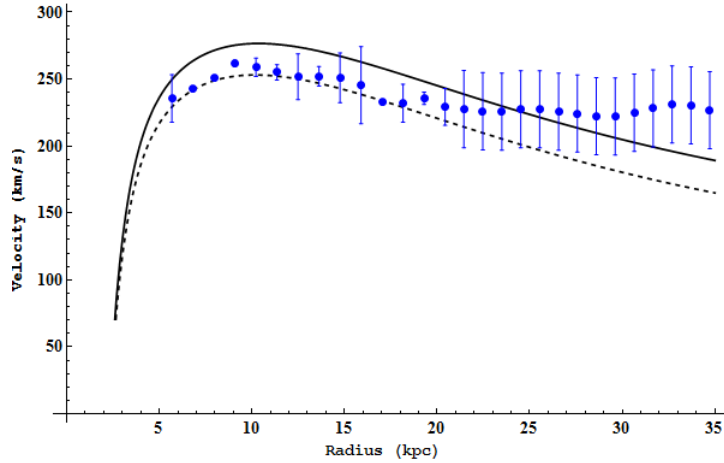^{a} Time dependence is a consequence of the derivations and the time average.

Figure 3.4: *We report here our fit of the M31 rotation curve for the case (a), calculated with the parameters listed in table 3.3. The thick black line is the hybrid case (a), the dashed black line is the 'no DM' case. The blue dots and relative errors are the measured rotation curve (from table 3.1).*

3.3.3 The linear ansatz (case (b))

In table 3.4 we list the parameters obtained in our fit for the case (b) (time free ansatz) both in the "no DM" and in the "hybrid" case.

Figure 3.5 displays the fitted rotation curves: the full black line is for the case with the 'real' DM halo, the dashed black line is for the case of no 'real' DM.

In the hybrid case, the total DM within 35 kpc is:

$$M_{(b)}(< 35kpc) = 1.0 \times 10^{11} \, M_\odot. \tag{3.18}$$

Table 3.4: *Results from our fit for the linear ansatz, with and without DM halo. We list the results of our fit for the case in which no DM is considered (first line) and the case in which the DM halo is considered (second line).*

Model	0.5 PN term			DM	
	δ	$\delta_4{}^a$	L	ρ_h	L_h
	(kpc)	(kpc s)	(kpc)	($\times 10^7 \, M_\odot$)	(kpc)
No DM (b)	0.057 ± 0.004	0.46 ± 0.02	16.7 ± 1.3	//	//
Hybrid (b)	0.031 ± 0.004	0.23 ± 0.03	8.6 ± 1.3	3.3 ± 0.2	6.2 ± 0.4

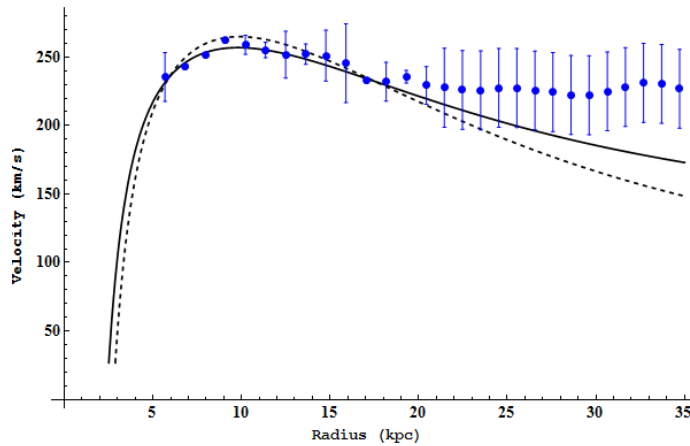^{a} Time dependence is a consequence of the time average.

Figure 3.5: *We report here our fit of the M31 rotation curve for the case (b), calculated with the parameters listed in table 3.4. The thick black line is the hybrid case (b), the dashed black line is the 'no DM' case. The blue dots and relative errors are the measured rotation curve (from table 3.1).*

3.3.4   The time free ansatz (case (c))

In table 3.5 we list the parameters obtained in our fit for the case (c) (time free ansatz) both in the "no DM" and in the "hybrid" case.

Figure 3.6 displays the fitted rotation curve: the full black line is for the case with the 'real' DM halo, the dashed black line is for the case of no 'real' DM.

In the hybrid case, the total DM within 35 kpc is:

$$M_{(c)}(< 35kpc) = 1.7 \times 10^7 \, M_\odot. \tag{3.19}$$

Table 3.5: *Results form our fit for the time free ansatz, with and without DM halo. We list the results of our fit for the case in which no DM is considered (first line) and the case in which the DM halo is considered (second line).*

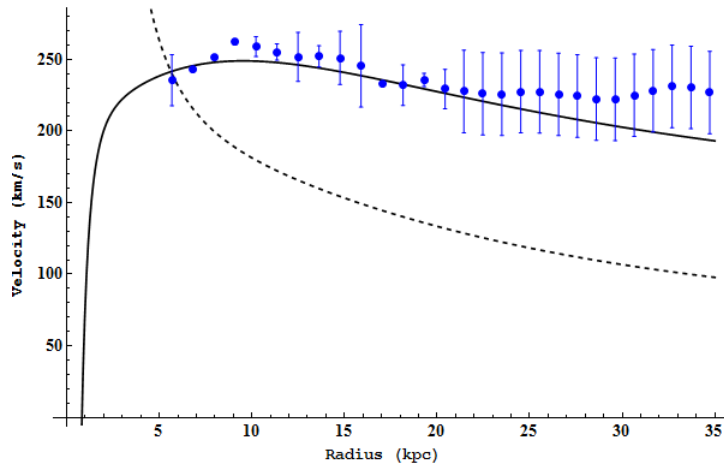| Model	0.5 PN term		DM	
	δ'	L	ρ_h	L_h
	(kpc^2)	(kpc)	$(\times 10^7 \, M_\odot)$	(kpc)
No DM (c)	$(-1.77 \pm 0.02) \times 10^4$	82.3 ± 13.5	//	//
Hybrid (c)	664 ± 247	10.2 ± 1.4	3.3 ± 0.1	8.0 ± 0.2

Figure 3.6: *We report here our fit of the M31 rotation curve for the case (c), calculated with the parameters listed in table 3.4. The thick black line is the hybrid case (c), the dashed black line is the 'no DM' case. The blue dots and relative errors are the measured rotation curve (from table 3.1..*

3.4 Models comparison and comments on the results of our fits

In this section we will make a comparison between our models and then consider the hybrid cases to see how much actual Dark Matter is still needed.

3.4.1 Model comparison

Since we are not dealing with nested models,[9] the comparison between the models cannot be done with the usual *likelihood-ratio test*,[10] therefore we use the *Akaike test* (see [165, 166]): among a set of models i describing the same data set,[11] each with *maximum likelihood* $\mathcal{L}_i$ and p_i parameters, the model for which the quantity (the *Akaike Information Criterion*):

$$AIC_i = -2\ln\mathcal{L}_i + 2p_i \tag{3.20}$$

is a minimum is the best one to describe the considered data set.

As pointed out in [165], *this is not a null hypothesis test*: it says that the model describes the data better thant the others, no confidence level is given.[12]

In table 3.6 we sum up the number of parameters, the logarithm of the maximum likelihood and the AIC value for each model and in the figure 3.7, we report the results of our test.

We see that the one with the minimum AIC value is the hybrid (b) (linear ansatz with a NFW halo). The second and third best are the No DM (a) and hybrid (a) (no hypothesis on the $\Delta(t)$ function). It must be said that

---

[9]Two models A and B are nested if, say, all the parameters A are contained in the set of parameters B.

In our case this is true for the hybrid and no DM models (the latter is nested in the former), but this is not true in the other cases: .

[10]In this test, one calculates the ratio B the likelihood of the considered model with a reference model (the null hypothesis, which in our case would be the Usual model), then the quantity $-2\ln B$ behaves approximately as a χ^2 distribution with a number of degrees of freedom equal to the difference of the paramters of the two models (see [161, 165]).

In our case, the null hypothesis would be the usual case and it is not nested with the others, this is why we cannot use the test ratio.

[11]This is fundamental [165].

[12]This is on contrast to the ratio test, which gives selects the model which best describes the data and gives information on the confidence levels.

these three model describe quite well data at small radii, but describe quite
poorly the data at larger radii.

We notice further that the case No DM (c) (the time free ansatz) is the
worst (its AIC is 3386, while the AIC of the best model is 53, see table 3.6).

The fact that the usual case gives such a bad result in confront with
our models (except the cases (c)) might be a hint that the NFW halo was
too *naïve* a choice: more complicated models might give better results and
challenge ours.

Table 3.6: *In this table we sum up number of parameters p_i, the maximum
likelihood $\mathcal{L}_i$ ant the AIC value for each model cosidered in this chapter.*
*Since we are only interested in the DM models, the maximum likelihood for the
Usual case is the one after the marginalization over bulge and disk parameters.*

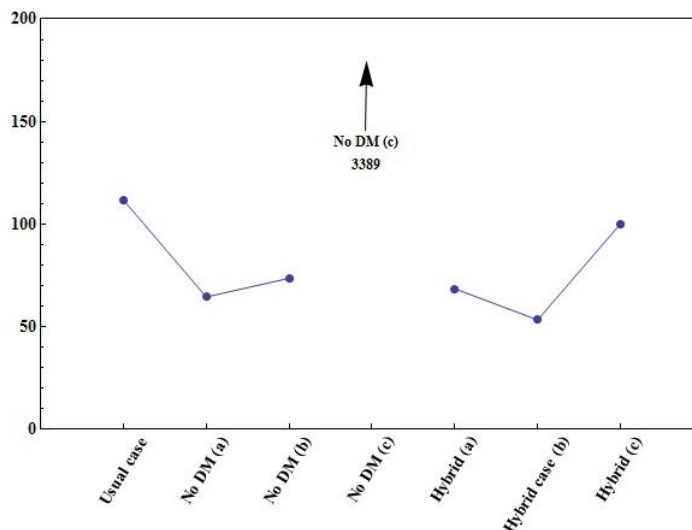| Model	p_i	$\ln \mathcal{L}_i$	AIC	Model	p_i	$\ln \mathcal{L}_i$	AIC
Usual	2	-49.85	111.7				
No DM (a)	4	-28.2	64.4	Hybrid (a)	6	-28.2	68.4
No DM (b)	3	-33.75	73.5	Hybrid (b)	5	-21.6	53.2
No DM (c)	2	-1692.65	3386.3	Hybrid (c)	4	-46.05	100.1

Figure 3.7: *In this graphics we report the value of the AIC for each model
considered in this work (see also table 3.6). We cut out of the plot the AIC for
the No DM case (c), since it is too far from the others.*

3.4.2   Amount of actual Dark Matter in hybrid models

In table 3.7 we sum up the mass of the DM halo in the hybrid models and the percentage of actual DM needed in each model up to 35 kpc, calculated as the ratio of the hybrid model over the usual case.

We notice that the case (a) (which we remind is our third best model) is the one that needs the less actual DM (only $\approx$ 15%), case (b) (the one that best describes our data) needs 58.6% of DM, while the case (c) basically needs all of it.

In figure 3.8 we plot the mass of the halos as a function of R for the hybrid models and the usual case, while in 3.9 we plot respectively the percentage of total mass of the galaxy as a function of R: interestingly the (c) case requires more DM at smaller radii ($<$ 15 kpc) than the usual case.

Finally we extrapolate our models up to 300 kpc and in 3.10, we plot the percentage of the total mass of the galaxy up to 300 kpc: we see that in the case (c) the total mass is about 97% of the usual case, in the case (b) about 60% and in case (a) about 30%.

Table 3.7: *The mass of DM halo up to 35 kpc from our fits and % with respect the usual case.*

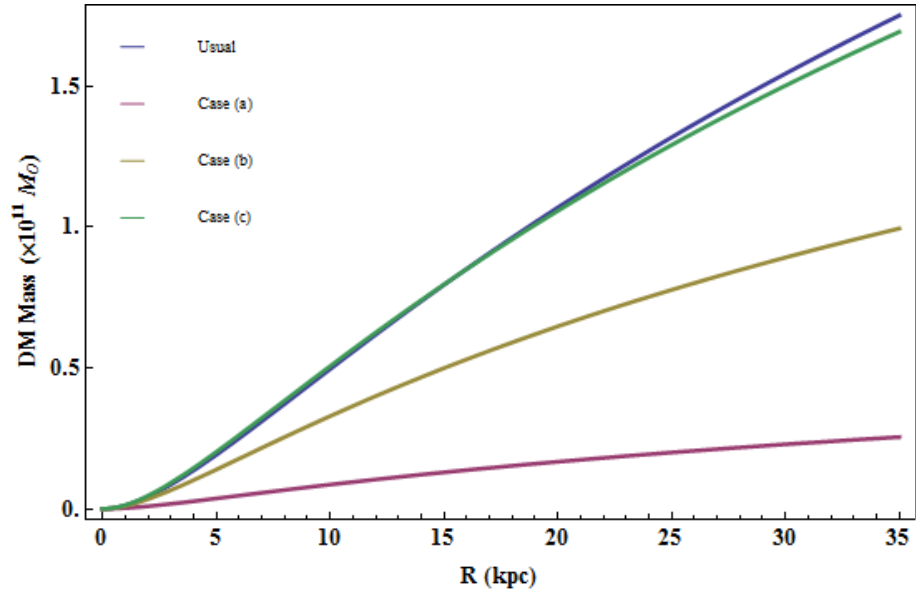| Type of fit (Hybrid models)	With 'real' DM ($\times 10^{11} M_\odot$)	%
Time free ansatz (c)	1.69	96.7%
Linear ansatz (b)	**1.03**	**58.6%**
No priors (a)	0.25	14.6%
Usual case	1.75	(100%)

Figure 3.8: *Mass of the halo as a function of the galactic radius R up to 35 kpc for the hybrid cases and the usual case. In blue the Usual case, in green the case (c), in olive-green the case (b) and in purple the case (a).*

Figure 3.9: *Mass of the halo as a function of the galactic radius R up to 35 kpc for the hybrid cases and the usual case. In blue case (c), in purple case (b) and in in olive green the case (a).*

Figure 3.10: *Percentage of total mass of the galaxy as a function of the galactic radius R up to 300 kpc for the hybrid cases and the usual case. In blue the Usual case, in green the case (c), in olive-green the case (b) and in purple the case (a).*
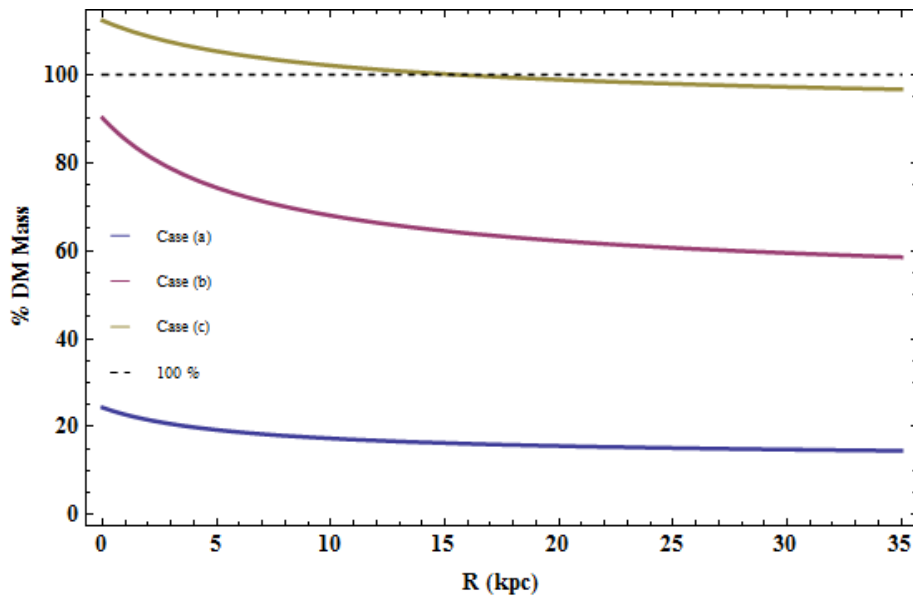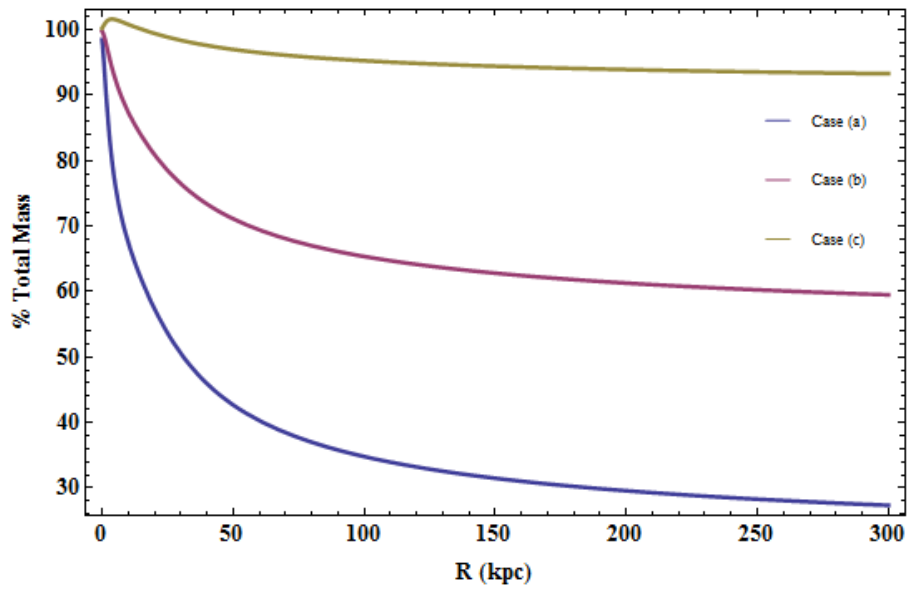
3.5 Effects on PTA

In this section, we estimate the effect of our 0.5 PN term on the PTA using our time free and linear ansatz.

Then we estimate the effect of the average potential of the Milky Way on PTA, assuming that in the Sun neighborhood it is given, essentially, by the stellar disk and the DM halo.

3.5.1 ADM tg

We numerically integrate with *Mathematica 8*™equation (1.30) with the parameters given in tables 3.4 (for the linear ansatz) and 3.5 (for the time free ansatz): we consider the hybrid models (b) and (c) (the actual DM effects are treated in the next section: we will see that they are completely negligible) and the No DM (b).

In this integration one has to keep in mind that the 'r' in the Yukawa-like function is the distance from the center of the Galaxy, while we need to integrate over the distance from the Solar System barycenter 'R' (see equation (1.30) and section 2.2.3); since we are dealing with functions already at PN order, we can use the Euclidean Geometry and, in particular, the Law of Cosines (see figure 2.1 for the definitions):

$$r = \sqrt{R_\odot^2 + R^2 - 2\,R\,r\,\cos\theta}. \tag{3.21}$$

In figures 3.11, 3.12 and 3.13, we plot, as a function of the observation angle, the corrections to the PTA given by our linear and time free ansatz respectively: the source is in the galactic plane and at distances $R = \{0.5, 1, 1.5, 2\}$ kpc.

We see that in the linear ansatz, both in the hybrid 3.11 and in the No DM case 3.13, the integral correction is of the order tens of nanoseconds, while the second correction is of the order of percent.

In the time free case 3.12 corrections are completely out of scale (integral correction is of the order of seconds!): one more reason to consider this model wrong.

Figure 3.11: *Corrections to the time of arrival in PTA with our hybrid linear ansatz: in the upper four plots the integral correction, in the lower four, the part between parenthesis.*

Figure 3.12: *Corrections to the time of arrival in PTA with our hybrid time free ansatz: in the upper four plots the first correction, in the lower four, the part between parenthesis.*

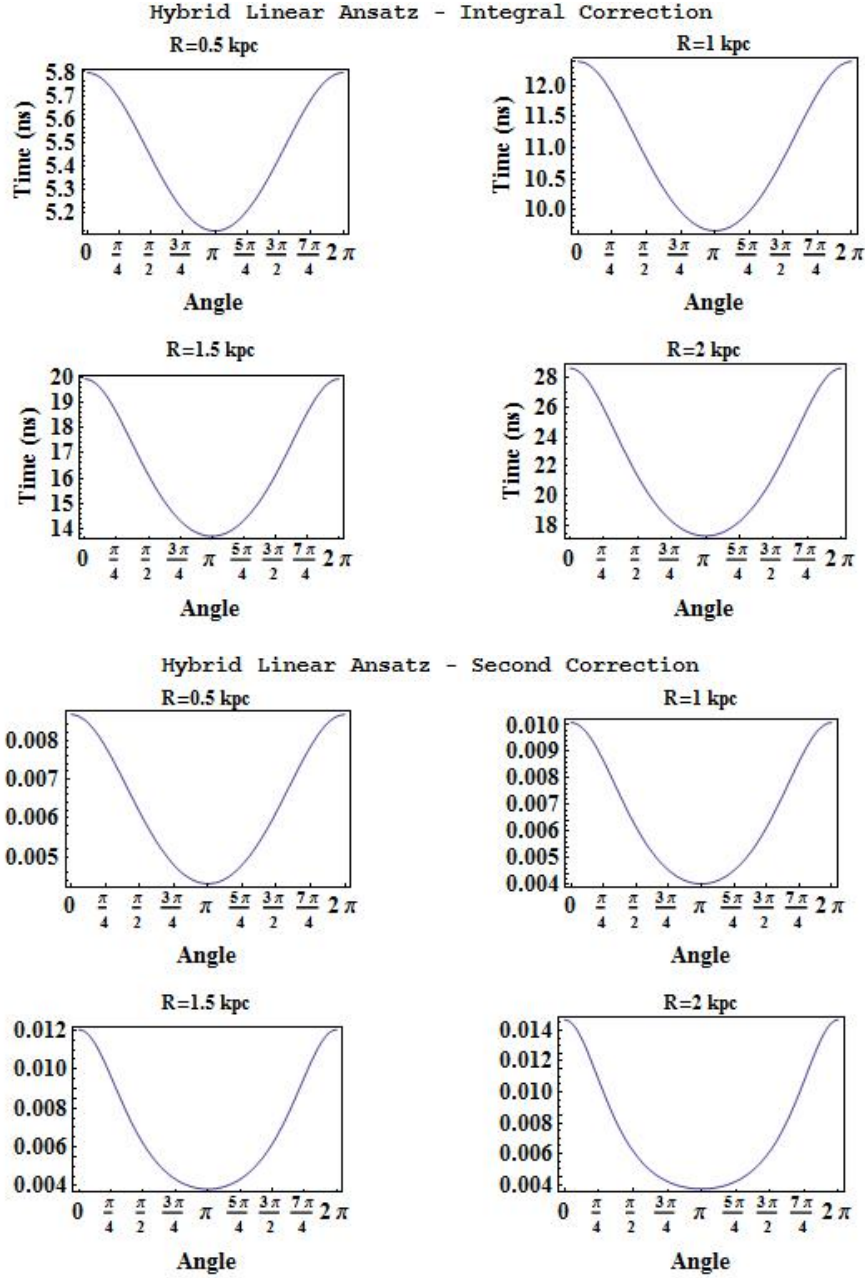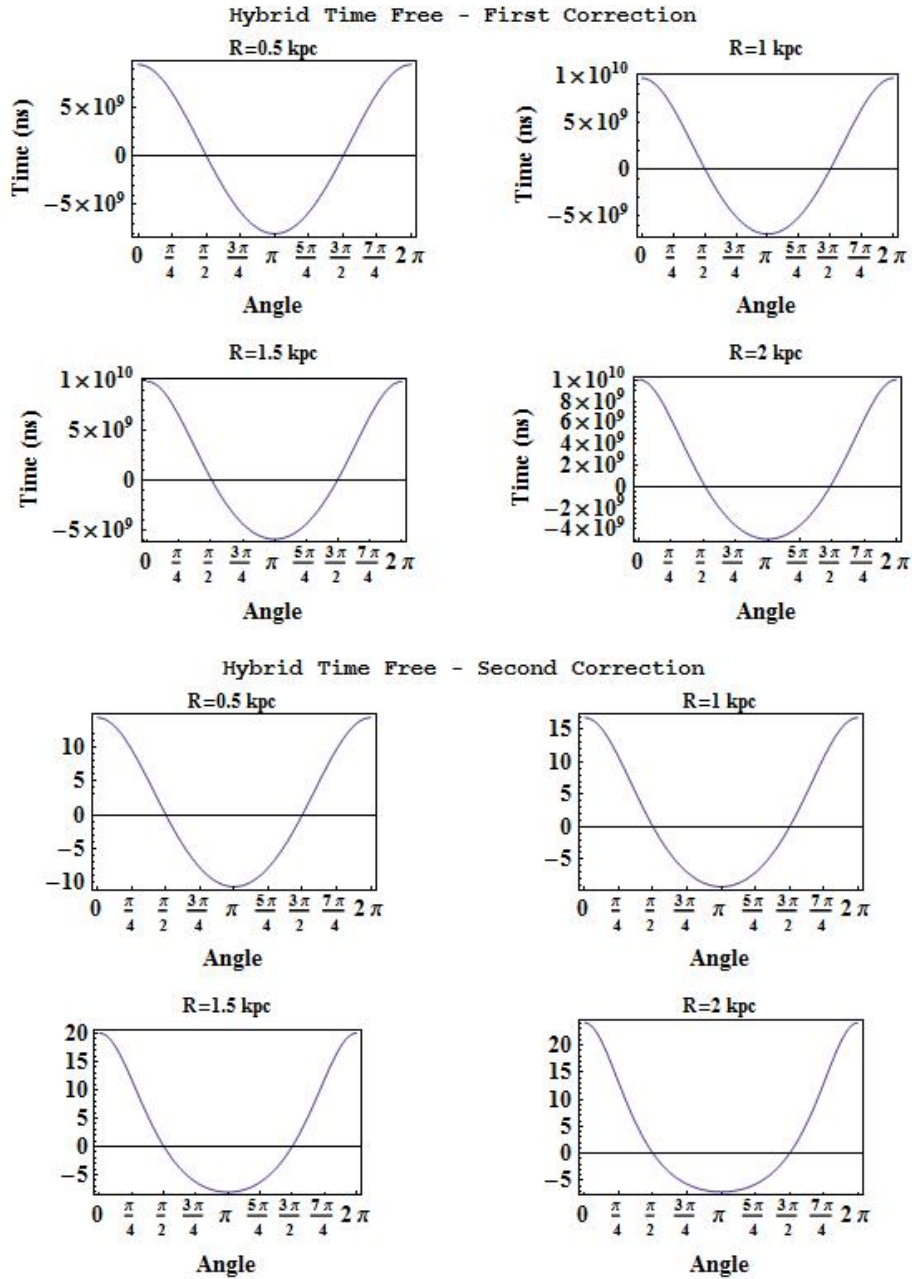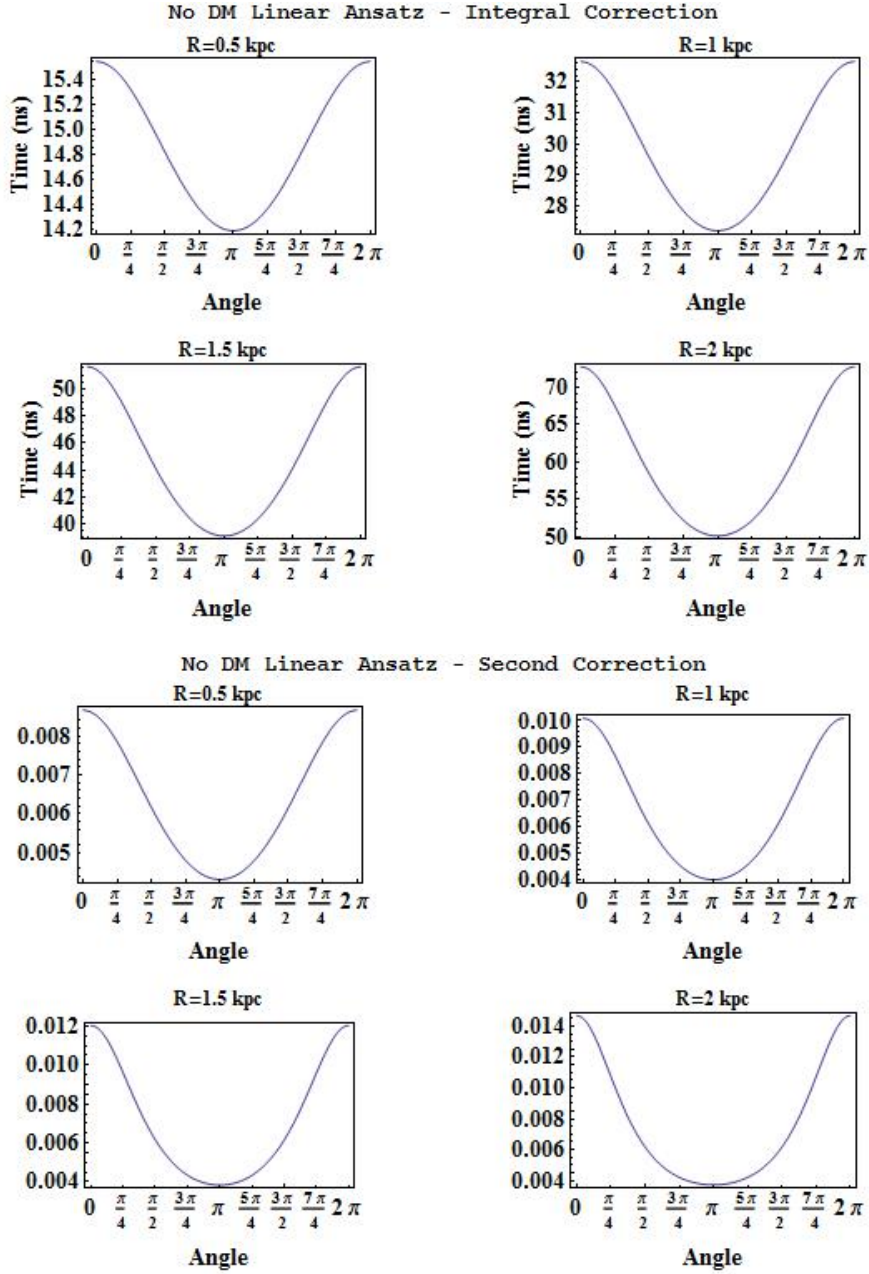**Figure 3.13:** *Corrections to the time of arrival in PTA with our linear ansatz in the No DM case: in the upper four plots the integral correction, in the lower four, the part between parenthesis.*

3.5.2 Effect of DM halo and disk average potential

We consider the effect of the Milky Way DM halo and disk potential on PTA. To do this we have to make a step back to equation (1.20): we now assume that the potential can be written as:[13]

$$-U = \Phi(R, z) = \overline{\Phi}(R, z) + \Phi_{body}(R, z) \qquad (3.22)$$

where $\overline{\Phi}$ is the average (Newtonian) potential of the Galaxy, while Φ_{body} is the (Newtonian) potential of a body. If we neglect the average potential, we go back to equations (1.30) and (1.32); if we consider it, we have another correction of the form:

$$\frac{2}{c^2} \int_0^R dR_1 \int_0^{R_1} dR_2 \, \widehat{k}_\oplus^r \, \partial_r \overline{\Phi} \qquad (3.23)$$

We need a model for the average potential of the Galaxy. Following [155] (chapter 2), we consider a DM halo with a profile of the form:

$$m = \sqrt{R^2 + \frac{z^2}{q_h^2}} \qquad (3.24a)$$

$$\rho_h(R) = \rho_{h0} \left(\frac{m}{a_h} \right)^{-\alpha_h} \left(1 + \frac{m}{a_h} \right)^{\alpha_h - \beta_h} \qquad (3.24b)$$

where ρ_{h0} is the central value of the density, a_h is the scale length.

We also assume, always following [155], that the average potential of the disk is given by a superposition of a thick and a thin disk profile (we assume it is negligible in the neighborhood of a massive body):

$$\rho_d(R, z) = \Sigma_d \exp\left(-\frac{R}{R_d} \right) \left[\frac{\alpha_0}{2z_0} \exp\left(-\frac{|z|}{z_0} \right) + \frac{\alpha_1}{2z_1} \exp\left(-\frac{|z|}{z_1} \right) \right] \qquad (3.25)$$

where $\alpha_0 + \alpha_1 = 1$, they are a measure of the importance, respectively of the thin and thick disk: we will consider the case $\alpha_0 = \alpha_1 = 0.5$.

We further assume that the bulge has negligible effect nearby the Sun.

[155] considers two extreme models: Model I, in which the stellar disk still dominates the potential at the solar radius and beyond, and Model II in which DM dominates at all radii (we can say that Model I is disk dominated and Model II is halo dominated, [155]): we use them both for our estimate; the value of the parameters are listed in 3.8 and are taken from [155].

---

[13]As customary (see [13, 112, 135, 136]) in those paragraphs and in the introduction too, the potential U is actually *minus* the Newtonian potential Φ.

Table 3.8: *Values of the parameters in* (3.24b) *for both Model I and Model II.*

Parameter	Model I	Model II
ρ_{h0} ($M_\odot pc^{-3}$)	0.711	0.266
α_h	-2	1.63
β_h	2.96	2.17
q_h	0.8	
a_h (kpc)	3.83	1.90
Σ_d ($M_\odot pc^{-2}$)	1905	536
R_d (kpc)	2	3.2
z_0	0.3	
z_1	1	

The potentials of the two components are calculated following [155] (chapter 2), then we impose:

$$\overline{\Phi}(R, z) = \Phi_d(R, z) + \Phi_h(R, z). \tag{3.26}$$

and substitute this potential in equation (3.23) and integrate it numerically using *Mathematica 8*™: we only consider the case $z = 0$, since the disk is only few parsec thick.

Just like in the previous section, we have to use the Cosines Law and equation (3.21) to find the correct integration variable. The result of the calculation is reported in figure 3.14 in the case of stars on the galactic equator $(z = 0)$.

We see that the effect is negligible being at most ofthe order of 10^{-15} s $(10^{-6}$ ns) for distances up to 2 kpc from the Sun.
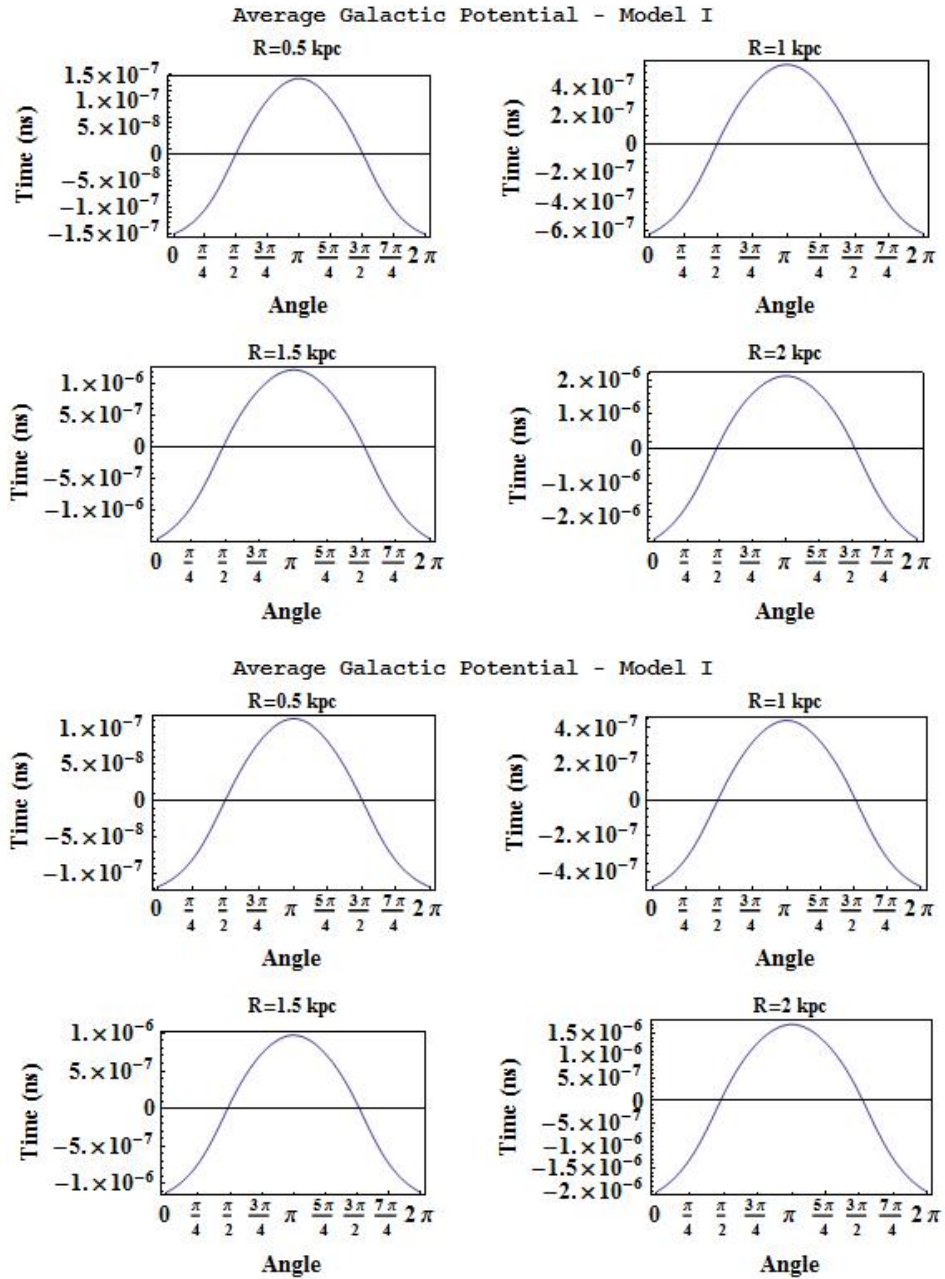
Figure 3.14: *Corrections to the time of arrival in PTA due to the average potential of the Milky Way: upper four plots the Model I, lower four plot Model II.*

3.6   Estimate of the effect of the 0.5 PN term on the radial velocity

In this section we estimate the effect of our 0.5PN correction on the radial velocity using the formulae (2.27) and (2.30) calculated in chapter 2, respectively for the linear and the time free ansatz; we rewrite here those equations for convenience:

$$1 + z = \left(1 + \frac{1}{2} \frac{v^2}{c^2} + \frac{U}{c^2} + \frac{\delta}{c} Y(r) - \delta \frac{|\vec{R}|}{c} v^r \, \partial_r Y(r) \right)_{\text{sor}} \times$$
$$\times \left[1 + \frac{\rho}{c} \left(1 + \delta Y(R) + \delta Y(0) + \left| \vec{R} \right| \delta Y'(R) \right) \right]; \qquad (2.27)$$

$$1 + z = \left(1 + \frac{1}{2} \frac{v^2}{c^2} + \frac{U}{c^2} - \delta' \frac{v^r}{c} \, \partial_r Y(r) \right)_{\text{sor}} \times$$
$$\times \left[1 + \frac{\rho}{c} \left(1 + \delta' Y'(R) - \delta' Y'(0) \right) \right] \qquad (2.30)$$

we want estimate the terms between parentheses in the second lines.

We remind that we use the notation:

$$Y'(r) = \widehat{k}_{\oplus} \cdot \left. \vec{\nabla} Y \right|_r$$

where $\widehat{k}_{\oplus}$ is the direction of observation.

We use the values for δ and δ' and L, given in tables 3.4 for the linear anstz and the hybrid case of 3.5 for the time free ansatz.[14]

Results are shown in figures 3.15 ad 3.16, where we plot the direct correction as a function of the angle of observation θ (see figure 2.1) for the distances from the Solar System barycenter of $R = \{0, 0.5, 1, 1.5, 2\}$ kpc (the source is in the galactic plane)

In the hybrid linear ansatz case 3.15(a), corrections are of the order of $0.3 \div 0.6\%$, corresponding to hundrends of m/s while in the No DM case 3.15(b) are of the order of $1 \div 1.5\%$, correspondig to ≈ 1 km/s.[15]

Once again, the time free ansatz gives corrections completely out of scale 3.16.

---

[14]The No DM time free ansatz describes the results too poorly.

[15]Radial velocity are of the order of 100 km/s [131].

(a)

(b)

Figure 3.15: *We plot the direct corrections to the radial velocity as a function of the angle of observation θ (right ascension) both in the linear (the upper four plots) and in the time free ansatz (the lower four plots) for the distances from the Solar System barycenter equal to R = {0.5, 1.0, 1.5, 2.0} kpc (we consider the case in which the source is in the galactic plane).*
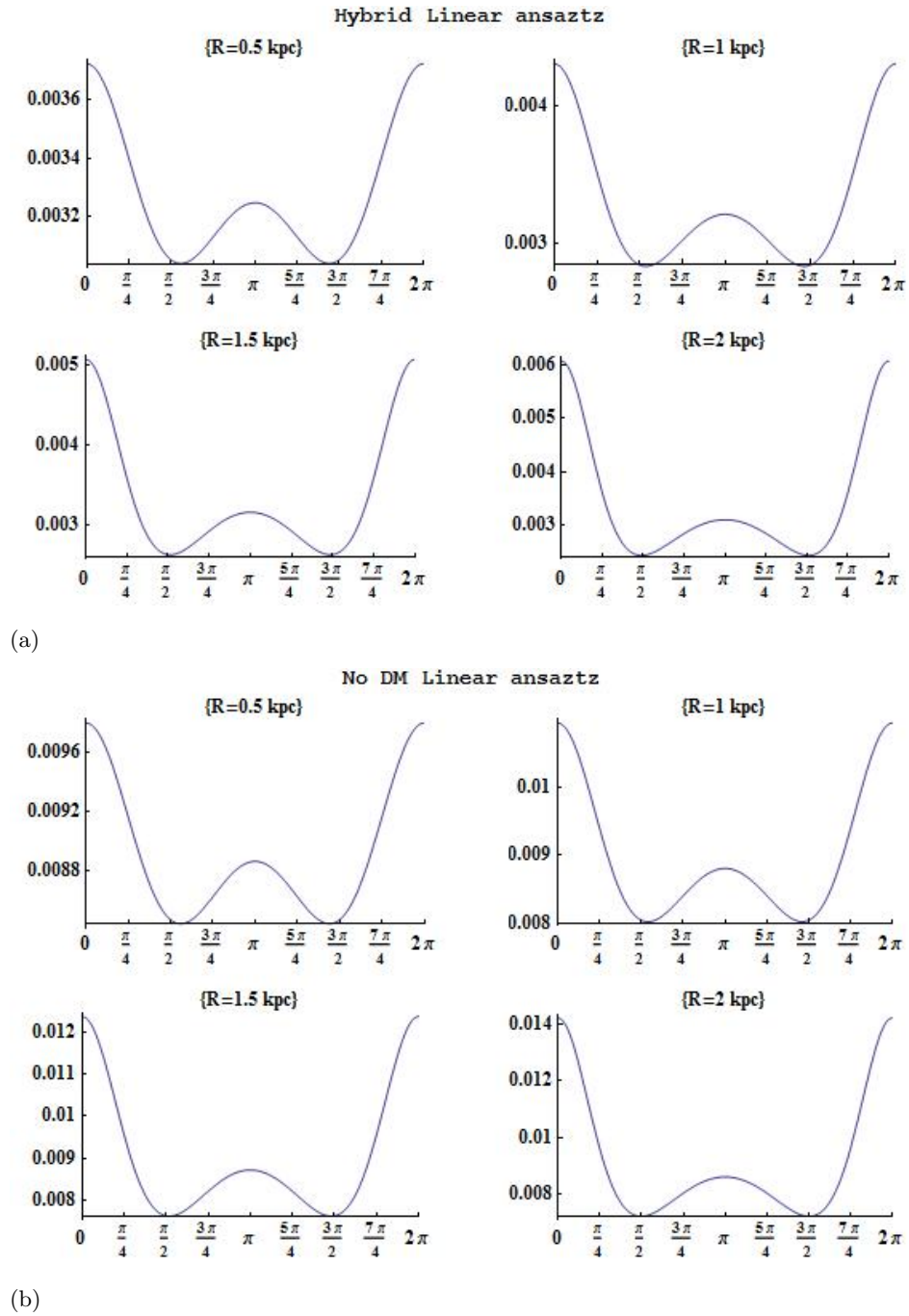
Figure 3.16: *We plot the direct corrections to the radial velocity as a function of the angle of observation θ (right ascension) both in the linear (the upper four plots) and in the time free ansatz (the lower four plots) for the distances from the Solar System barycenter equal to $R = \{0.5, 1.0, 1.5, 2.0\}$ kpc (we consider the case in which the source is in the galactic plane).*
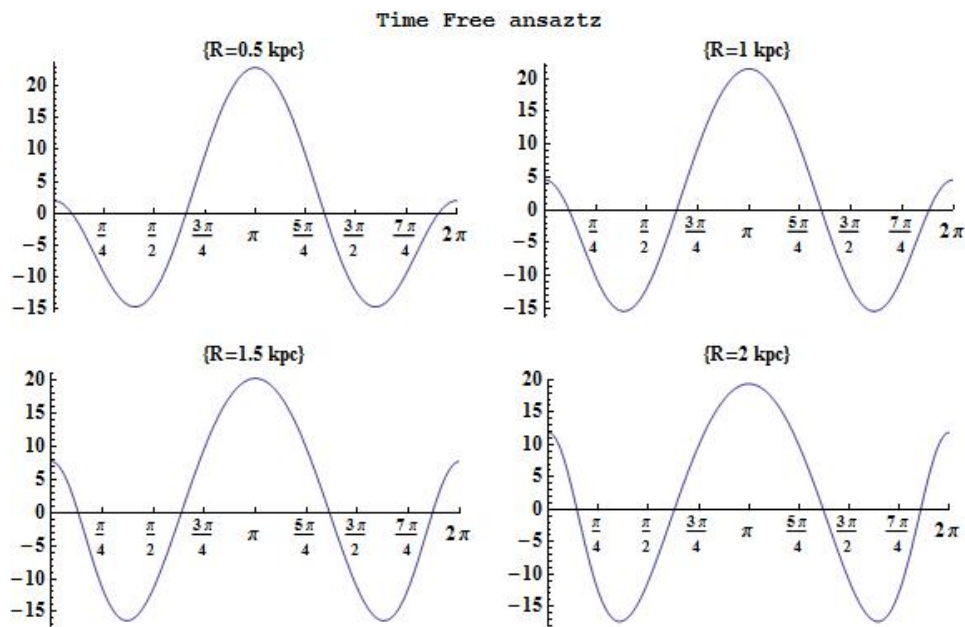
3.7 Summary of the chapter and discussion

In this chapter we considered the three ansatz described in the previous chapter and used them to fit the rotation curve of the M31 galaxy with 7 models:

- The usual model in which the DM is described by a NFW profile;

- Three 'No DM' models in which there is no Dark matter at all its effects are provided by our 0.5PN terms using the three ansatz (no prior, linear ansatz and time free ansatz) described in the previous chapter;

- Three 'Hybrid' models in which there is a DM halo and we also consider the effect of our 0.5PN term.

The results of our fits are described in section 3.3, while in section 3.4 we use the Akaike method [165, 166] to choose the model that best fits our data: it is the Hybrid (b), in which we still need an actual Dark Matter halo, but only about 58% of the usual model and the linear ansatz of chapter 2 is used.

The second and the third best are respectively the No DM (a) and the Hybrid (a): in the former, all the real DM is excluded by hypothesis, while in the latter we need only about 15% of the total Dark Matter halo (up to 35 kpc).

The time free ansatz always gives the worst result.

As already pointed out, the fact that the usual model gives such bad results, might be an indication that the NFW profile is a *naïve* choice: more complicated models might give better results.

In figure 3.10, we extrapolate the total mass of our hybrid models up to 300 kpc: we find that in the case (a) (no prior on Δ) the total mass is only about 30 % of the mass of the usual case; in the case (b) the total mass is about 60% and in the case (c) the total mass is about 97%.

Regardless of which of our models best describes data, the most important result of this chapter (and of this thesis) is that we can dispense with at least 42% of Dark Matter (and of all of it *in the No DM case (a)).*

We then calculated the effects of the 0.5PN term on the PTA (section 3.5) and on redshift (section 3.6).

In the PTA case, we considered equations (2.27) for the linear ansatz and (2.30) for the time free ansatz and numerically calculated the integral and the second corrections for the hybrid and No DM case (b) (linear ansatz) and for the hybrid case (c).[16] Results are given in figures 3.11, 3.12 and 3.13 respectively for the Hybrid (b), Hybrid (c) and No DM (b) models.

As a result of the numerical integration, we find that in case (b) the integral correction is of the order of $\approx 5 \div 30$ ns for the hybrid model (*our best model* fo M31) and $\approx 14 \div 70$ ns in the No DM model. We notice that this is about of the same order of magnitude of the precision one can get in PTA with millisecond pulsars (see section 2.30 and references [140, 141]), therefore this effect *might be observable in the future.*

For PTA we considered also the effect of the average galactic potential. We considered the two extreme models described in [155]: Model I, which is disk dominated and Model II which is halo dominated. We found out that these corrections are of the order of $10^{-7} \div 10^{-6}$ ns; we also notice that these are upper bounds, since we are considering a full Dark Matter halo, so they are completely negligible: all the effects measured in the PTA must be ascribed to the 0.5PN (if any will ever be found).

We already diffusely talked about the problems of spectroscopy and the merits of astrometry in the introduction (see section I.4.2): in chapters 1 and 2, we introduced another direct correction to the radial velocity in the redshift formula; in this chapter we estimated the amount of the correction for the hybrid and No DM case (b) and for the hybrid case (c): results are given in fugures 3.15(a), 3.15(b) and 3.16 respectively.

We see that for the linear ansatz the direct correction to the radial velocity is at most of the order of 1% in the hybrid case (our best model), while in the No DM model they are of the order of $1 \div 1.5$ %: this means that the correction on the radial velocity are of the order of $100 \div 1000$ m/s. We notice that they are comparable the other corrections mentioned in the introduction (see also [131–134]): ruling out the possibility of extracting informations on the 0.5PN term from the redshift as was stated in [102].

In the case (c) all corrections on PTA and redshift are completely out of scale: one more reason to rule out this model.

---

[16]We didn't consider the No DM case (c) because of its poor description of our data: see table 3.6.

One last note on the use of results of fits of M31 in our Galaxy.

The effects of the 0.5PN term on the spectroscopic measurements are not visible for external galaxies (because of the errors: as can be seen in table 3.1 they are of the order of $1 \div 30$ km/s, much higher then the corrections that we estimated for the radial velocity); the precision in measurements in our galaxy make it potentially observable, so these data should be treated carefully. This is true not just for stars, but also for HI regions *et similia*: in these cases there are no corrections due to the convective motions and so on, but our 0.5PN term is linked to the propagation of the light in the galaxy and its effects are unavoidable.

One should therefore use Cepheides and astrometric measurements (such as the Hypparcos catalogue of 180000 stars or GAIA's when it will be available in 2020) when fitting the rotation curve of our Galaxy.

BUT THIS IS WAY OUT OF MY LEAGUE!

So we choose the Andromeda galaxy becase it is similar to ours both in mass and shape (they are both spirals).

CHAPTER 4

OTHER EFFECTS OF 0.5PN

In this chapter we study the effects of the trace of the extrinsic curvature on other observables: the Tully-Fisher relation.

We will then move on to consider a possible connection of the $^3K^1$ with DE.

4.1   The Tully-Fisher relation

The Tully-Fisher relation expresses the link between luminosity L of a spiral galaxy and the velocity v of its stars (usually measured at the optical radius). It was first suggested by R.B. Tully and R.J. Fisher in 1977 [167].

It has the form:

$$4 \log_{10} v = \log_{10} L + \alpha. \tag{4.1}$$

The Tully-Fisher relation has many applications in astrophysics and cosmology: it can be used to measure the Hubble constant (see [69, 167]) and to measure the peculiar motion of galaxies [168].

It is possible that this relation might be only valid at large velocities, since a non-linearity is often observed at small ones (see [169–173], [169], for example fits also quadratic terms in $\log_{10} v$): this non-linearity is usually ascribed to the DM halo [170].

---

[1]Not the PN version!

4.1.1 Derivation of the Tully Fisher relation

The physical basis of the Tully-Fisher relation are the following.

If we assume that the galaxy dynamics is described by Newtonian Physics, then we can write:

$$F_{cfg} = F_{Gr} \qquad \Longrightarrow \qquad \frac{v^2}{r} = \frac{G\,M}{r^2};$$

simplifying the r and taking the square of both members, we have:

$$v^4 = \frac{G^2\,M^2}{r^2}.$$

If we define b the surface brightness of the galaxy, then:

$$b = \frac{L}{4\,\pi\,r^2}; \qquad (4.2)$$

therefore, defining Υ the mass-to-light ratio, we have:

$$v^4 = (4\,\pi\,\Upsilon^2\,G^2\,b)\,L = 10^{\log_{10}\alpha}\,L$$

Taking the logarithm on both sides of the previous equation, we find the linear relation (4.1).

In ADM-tg, we have:

$$\frac{v^2}{r} = \frac{GM}{r^2} - \frac{v}{c}\frac{d^2}{dt^2}{}^3\widetilde{\mathcal{K}}_{(1)}.$$

We bring the 0.5PN term on the LHS, take the square, and retain only $O(c^{-1})$ terms, obtaining:[2]

$$v^4\left(1 + \frac{2r}{c}\frac{1}{v}\frac{d^2}{dt^2}\widetilde{\mathcal{K}}_{(1)}\right) = (4\,\pi\,\Upsilon^2\,G^2\,b)\,L.$$

Taking the logarithm, we find:

$$4\,\log_{10}v + \log_{10}\left(1 + \frac{2r}{c}\frac{1}{v}\frac{d^2}{dt^2}\widetilde{\mathcal{K}}_{(1)}\right) = \log_{10}L + \alpha \qquad (4.3)$$

So the Tully-Fisher relation is *not linear anymore*, in particular at small velocities. The red curve in figure 4.1 describes the qalitative behavoir of this modified Tully-Fisher relation as a function of $\log_{10}v$.

In the usual interpretation (see [170]) the non linearity arises from the DM halo, here they are a consequence of the chosen hypersurface used to describe the 3-space.

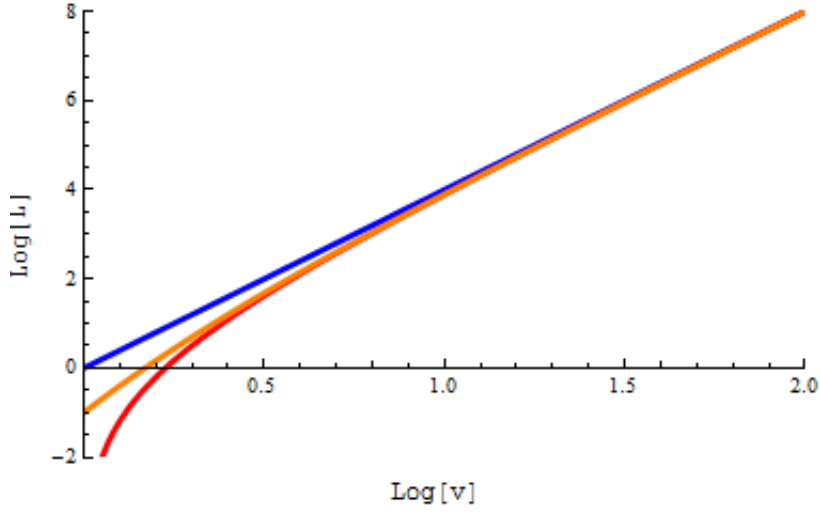
[2]In the RHS we proceed as before.

Figure 4.1: *Qualitative form of the Tully Fisher relation: in blue the original one* (4.1), *in orange the modified, Taylor expanded one* (4.4), *while in red the non expanded one* (4.3). *In each case, we set to zero the off-set* α.

If the 0.5PN term is small enough, we can Taylor expand the second logarithm on the LHS, obtaining:

$$4 \log_{10} v + \frac{2r}{c} \frac{d^2}{dt^2} \widetilde{\mathcal{K}}_{(1)} \frac{1}{v} = \log_{10} L + \alpha$$

(4.4)

$$4 \log_{10} v + \frac{2r}{c} \frac{d^2}{dt^2} \widetilde{\mathcal{K}}_{(1)} 10^{-\log_{10} v} = \log_{10} L + \alpha$$

The qualitative behavoir of this equation as a function of $\log_{10} v$ is given in figure 4.1 (the orange line).

In (4.4), the non-linear term is proportional to $r \dfrac{d^2}{dt^2} \widetilde{\mathcal{K}}_{(1)}$: given a mathematical form for the $^3\widetilde{\mathcal{K}}_{(1)}$ (of the type described in chapter 2), one could, in principle, use the Tully-Fisher relation to fit the needed parameters.

4.1.2 Radial Tully-Fisher

Usually, one measures the velocity at defined radial galactic distance, typically the *optical radius* R_{opt}.[3]

---

[3] The optical radius is the radius which contains about 83% of the light emitted by a spiral galaxy: it is about 3.2 times the scale length of the disk [174].

Following [175], given a model for the spiral galaxy (and therefore, for its velocity field), one can calculate a whole set of Tully-Fisher like relations for different galactic radii, instead of only $r = R_{opt}$ (hence the name *radial Tully-Fisher*) which can be written as:

$$\log_{10} v = \beta_r \log_{10} L + \alpha_r \tag{4.5}$$

In our case, we could consider a model of a spiral galaxy with no DM halo (similar to our Andromeda galaxy model 2 of chapter 3) and study the effect of different ansatz for the 0.5PN term. In principle this too could help constraining the mathematical form of $^3\widetilde{\mathcal{K}}_{(1)}$.

4.1.3   The Hubble parameter

Since when it was proposed in 1977, the Tully-Fisher relation was used for the determination of the Hubble parameter (see [69, 167, 176]: one way for this determination goes as follows [69].[4]

One starts measuring the doppler widening of the Ly_α lines[5] in HI regions[6]; the doppler widening is linked to the velocity field of the galaxy, which in turn is linked to the luminosity by the Tully-Fisher relation. From this, one can fit the distance modulus[7]

It might be intersting to study the effects (if any) of the 0.5PN term on the Hubble parameter using the Tully-Fisher relation.

---

[4]After a suitable calibration (for example, see [13, 69] for a discussion on the *cosmoc distance ladder*).

[5]The Lyman α (Ly_α) lines are the transition line from the $n = 2$ level to the $n = 1$ level in an hydrogen atom (the wavelenght is 1251.67 Å, in the UV part of the electromagnetic spectrum).

[6]Nebulae made of atomic hydrogen.

[7]The distance modulus is given by the difference of the apparent and the absolute magnitude of an object.

The *apparent magnitude* is the measured (logarithm of the) luminosity, while the *absolute magnitude* is the (logarithm of the) luminosity of an object one would measure if it were at the distance of 10pc.

4.2 $^3K^{\mathbf{8}}$ and Dark Energy

We saw that it is possible to describe Dark Matter as a metrology problem: can we do the same with Dark Energy? Yes, as we will now see.[9]

First, one has to notice that ADM tg formalism does not directly apply in the cosmological case,[10] but one could rewrite all the results using kinematical quantities such as *expansion* (θ), *shear* ($\sigma_{\mu\nu}$) and *rotation* ($\omega_{\mu\nu}$) defined through the congruence of the observers and calculated in [107]. These quantities can also be defined in usual ADM gravity: in this way it is possible to extend the ADM tg formalism also to a cosmological context (see [109]).

4.2.1 The link between ^3K and the Hubble parameter

It is known (see for example [177]) that in cosmological context the Hubble parameter $\mathcal{H}$ is proportional to the expansion parameter and it turns out that in ADM tg and in ADM formalism the ^3K is proportional to the expansion too:[11]

$$^3K = \theta = 3\,\mathcal{H} \tag{4.6}$$

so the ^3K is proportional to the Hubble parameter and therefore contains informations about the DE.

4.2.2 The case of Szekeres metrics

As suggested in [109], since ADM tg cannot be used with metric that have some Killing vectors, one should use inhomogeneous and anisotropic models which are generalizations of the FLRW ones, such as the *Szekeres* and *Szekeres-Szafron* ones (see [14, 15, 26, 45, 46, 178–182] and also our appendix A). One can show, see [14, 26, 46, 181, 182], that these models describe non-linear perturbations of a homogeneous and isotropic FLRW model and reduce to the latter when the inhomogeneities are zero.

---

[8]In this section we are not using a PN expansion: this is the *full* trace of the extrinsic curvature.

[9]We already mentioned this possibility in the introduction, page 6.

[10]This is because cosmological metrics are not asymptotically flat (see section I.3.1 and paper [105] for the conditions on the hypersurface in ADM tg).

[11]On the use of the extrinsic curvature tensor and its trace in cosmology, see also [112] exercise 21.16 "*Poor man's way to do cosmology*".

Using the Goode-Wainwright representation of the models (see [181] and appendix A), one can show that the extrinsic curvature tensor and its trace in ADM formalism are given respectively by:[12]

$$^3K_{rs} = \frac{1}{2N} \left[-^3\nabla_r\, N_s - ^3\nabla_s\, N_r + (\partial_\tau + \mathcal{L}_{N_r})\,^3g_{rs} \right] = \frac{1}{2}\, \partial_t\,^3g_{rs} = \quad (4.7)$$

$$= \begin{pmatrix} \dot{S}\,S & 0 & 0 \\ 0 & \dot{S}\,S & 0 \\ 0 & 0 & W^2\left(\dot{S}\,S\,H^2 + S^2\,H\,\dot{H}\right) \end{pmatrix}$$

$$^3K = {}^3g^{rs}\,{}^3K_{rs} = 3\,\frac{\dot{S}}{S} + \frac{\dot{H}}{H} \tag{4.8}$$

Following, [45, 182] among the others, one can define the density contrast δ (ρ is the density field, see the appendix A):

$$\rho = \frac{6\mathcal{M}}{S^3}\left(1 + \frac{F}{H}\right) = \frac{6\mathcal{M}}{S^3}\left(1 + \delta\right) \tag{4.9}$$

Now, substituting everything in (4.8) and remembering equations (4.6) and(A.3), one finds:

$$^3K = \sqrt{\frac{3\,\mathcal{M}}{S^3} - \frac{\kappa}{S^2}} - \frac{1}{3}\frac{\dot{\delta}}{1+\delta} \tag{4.10}$$

$$= \mathcal{H} = \sqrt{\frac{\rho}{S^3} - \frac{\kappa}{S^2} + \frac{\Lambda}{3}}$$

so, by comparison, the additional $\dfrac{\dot{\delta}}{1+\delta}$ term is what in homogeneous models is called Dark Energy: it is linked to the inhomogeneities and their time evolution (see also [183]).

Here is were relativistic metrology comes into play: insisting on the use of homogeneous and isotropic metrics brings up the universe acceleration[13] and, consequently, the DE phenomenon.

On this topic see also [26, 184–188] and references therein.

Within this framework, it is possible to fit also other forms of DE, not just a cosmological constant. Following [189], in [190], authors show that

---

[12]$\mathcal{L}_{N_r}$ is the Lie derivative along the shift, while $^3\nabla$ is the covariant derivative defined in the hypersurface.

[13]In the Szekeres models, the expansion of the universe is regulated by equation (A.3), a Friedman-like equation with no cosmological constant and, therefore, no acceleration.

inhomogeneities can mimick not just the cosmological constant, but also an evolving DE: an underdensity can mimick a phantom DE, while an overdensity mimicks a quintessence DE (see also [28, 191] on this point).

We shall now calculate the confdence level of the flat ΛCDM model and of Szekeres Family II model. To do so, we need the luminosity distance of these models at least at order $O(z^3)$ (calculated in [45]).

4.2.3   Luminosity distance of Family II models

Following [45], one can calculate the Taylor expansion of the luminosity distance and study the cosmographic parameters. Here we only consider the case of the Family II Szekeres model in the hypothesis that at the observer position the structure growth is over:

$$\dot\delta(0) \equiv 0 \quad \Rightarrow \quad \frac{3}{2}\,\sigma(0) = \frac{\dot\delta(0)}{1+\delta(0)} = 0 \tag{4.11}$$

In [45], we used the Sachs equations as a starting point:

$$\begin{cases} \dfrac{d^2\,D_A}{d\lambda} = -\left(|\Sigma|^2 + \dfrac{1}{2}\,R_{\alpha\beta}\,k^\alpha\,k^\beta \right)\,D_A \\[2mm] \dfrac{d\Sigma}{d\lambda} + 2\left(\dfrac{d}{d\lambda}\ln D_A \right)\Sigma = C_{\alpha\beta\mu\nu}\,\epsilon^{*\alpha}\,k^\beta\,\epsilon^{*\mu}\,k^\nu \end{cases} \tag{4.12}$$

where Σ is the shear of the light bundle, $R_{\alpha\beta}$ is the Ricci tensor, $C_{\alpha\beta\mu\nu}$ is the Weyl tensor, k^μ is the null vector tangent to the light path, ϵ^μ is a space-like vector orthogonal to k^μ (the * indicates complex conjugation) and, finally λ is the affine parameter of the null geodesics.

In equation (4.12), we substitute the expansion:

$$D_A(z) = \frac{z}{\mathcal{H}_{\mathcal{O}}} + \frac{z^2}{2}\,\frac{A}{\mathcal{H}_O} + \frac{z^3}{6}\,\frac{B}{\mathcal{H}_O} + O(z^4) \tag{4.13}$$

for the angular diameter distance; finally, using equations (A.31) and (A.32) the luminosity distance is given by:

$$\begin{aligned} D_L(z) &= D_A(z)\,(1+z)^2 \\ &= \frac{z}{\mathcal{H}_O} + \frac{z^2}{2\,\mathcal{H}_O}\,(4+A) + \frac{z^3}{6\,\mathcal{H}_O}\,(6+6A+B) + O(z^4) \end{aligned} \tag{4.14}$$

in this way we can find the coefficients A and B.

At the end of the calculations (carried out in detail in [45]), we find that the luminosity distance is given by [45]:

$$D_L(z) = \frac{D_L^{(1)}}{\mathcal{H}_O} z + \frac{D_L^{(2)II}}{2\,\mathcal{H}_O} z^2 + \frac{D_L^{(3)II}}{6\,\mathcal{H}_O} z^3 + O(z^4), \qquad (4.15)$$

where:

$$D_L^{(1)} = 1; \qquad\qquad (4.16a)$$

$$D_L^{(2)II} = 1 - q_O + \left(\frac{3}{2} \frac{\sigma'}{\mathcal{H}}\Big|_O \right) \cos^2 \alpha$$
$$= 1 - q_{eff}^{II}; \qquad\qquad (4.16b)$$

$$D_L^{(3)II} = 3\,(q_{eff}^{II})^2 + q_{eff}^{II} - j_O - \Omega_O + \left(\frac{3}{2} \frac{\sigma'}{\mathcal{H}}\Big|_O \right) + \left(\frac{3}{2} \frac{\sigma'}{\mathcal{H}}\Big|_O \right) \cos^2 \alpha +$$
$$- 4 \left(\frac{3}{2} \frac{\sigma'}{\mathcal{H}}\Big|_O \right) \cos^2 \alpha \, \frac{1}{\delta} \left[\cos \beta \, \sin \alpha \, \frac{\partial}{\partial x} \delta + \sin \alpha \, \sin \beta \, \frac{\partial}{\partial y} \delta \right]_O,$$
$$(4.16c)$$

where we defined:

- $\mathcal{H}_O$, the Hubble parameter at the observer;

- $q_O = -\frac{\ddot{S}}{S} \frac{1}{\mathcal{H}^2}\bigg|_O$ the deceleration parameter at the observer position;

- $j_O = \frac{\dddot{S}}{S} \frac{1}{\mathcal{H}^3}\bigg|_O$ the jerk parameter;

- $\Omega_O = 1 - \Omega_k$;

- We used polar coordinates and the angle α is the angle between the direction of propagation of the light ray and the $r-$axis, while β is the angle with the $x-$axis (see [45]);

- And a prime $'$ stands for the redshift-derivative.

In equation (4.16b), we defined the effective deceleration parameter:

$$q_{eff}^{II} = q_O - \left(\frac{3}{2} \frac{\sigma'}{\mathcal{H}} \right)_O \cos^2 \alpha$$

and we can also define an effective jerk parameter:

$$j_{eff}^{II} = j_O - \left(\frac{3}{2} \frac{\sigma'}{\mathcal{H}} \right)_O - \left(\frac{3}{2} \frac{\sigma'}{\mathcal{H}} \right)_O \cos^2 \alpha +$$
$$+ 4 \left(\frac{3}{2} \frac{\sigma'}{\mathcal{H}} \right)_O \cos^2 \alpha \, \frac{1}{\delta} \left[\cos \beta \, \sin \alpha \, \frac{\partial}{\partial x} \delta + \sin \alpha \, \sin \beta \, \frac{\partial}{\partial y} \delta \right]_O$$

Following [45], we can relate $\sigma'(0)$ to the local density contrast in the following way:

$$\sigma'\Big|_O = \frac{\partial\sigma}{\partial z}\Big|_O = \frac{\partial\lambda}{\partial z}\frac{\partial\sigma}{\partial\lambda}\Big|_O = \frac{\partial\lambda}{\partial z}\frac{\partial x^\alpha}{\partial\lambda}\frac{\partial\sigma}{\partial x^\alpha}\Big|_O \qquad (4.17)$$

using the definition of σ given in the appendix A and the fact that $F = F(t,r)$, we have:

$$\frac{\partial\sigma}{\partial x} = -\sigma\,\partial_x\,lnH \qquad \frac{\partial\sigma}{\partial y} = -\sigma\,\partial_y\,lnH \qquad (4.18)$$

Since these equations must be evaluated at the observer position (see the definition of the effective jerk parameter), and since we imposed that the growth of structure is over at the observer position ($\sigma(0) \propto \dot\delta(0) \equiv 0$), they are all null; on the contrary, the time and r-derivatives are not, and using the Raychauduri equation (see the appendix, equation (A.6)), we have [45]:

$$\frac{3}{2}\,\sigma'(0) = -\Omega_m\,\mathcal{H}_O\,\delta(0) + \frac{\partial}{\partial r}\frac{\dot F}{H}\frac{k^3}{k^0}\Big|_O =$$

$$= -\Omega_m\,\mathcal{H}_O\,\delta(0) - \frac{3}{2}\frac{\dot\delta_{,r}(0)}{1+\delta(0)}\frac{k^3}{k^0}\Big|_O = \qquad (4.19)$$

$$= -\Omega_m\,\mathcal{H}_O\,\delta(0) - \frac{3}{2}\frac{\dot\delta_{,r}(0)}{1+\delta(0)}\,\cos\alpha$$

where Ω_m is the matter density at the observer position and $\dot\delta_{,r}$ is the derivative in the $r-$direction of the local growing rate of structures at present time: we assume this is 0.

In this way we can rewrite the effective cosmographic parameters as:

$$q_{eff}^{II} = q_O + \frac{3}{2}\,\Omega_m\,\mathcal{H}_O\,\delta(0)\,\cos^2\alpha$$

$$j_{eff}^{II} = j_O + \Omega_O + \frac{3}{2}\,\Omega_m\,\delta(0)\,\left(1+\cos^2\alpha\right) +$$

$$- 6\,\Omega_m\,\cos^2\alpha\,\left[\cos\beta\,\sin\alpha\,\frac{\partial}{\partial x}\,\delta + \sin\alpha\,\sin\beta\,\frac{\partial}{\partial y}\,\delta\right]_O$$

Since in the following we are going to use SNe Ia data, we need the distance modulus [13, 192]:

$$\mu_{th}(y) = 25 - 5\,\log_{10}\left(\frac{\mathcal{H}_O}{c}\right) + \frac{5}{\ln(10)}\left[\ln(y) + \frac{1}{2}\,(3 - q_{eff})\,y + \right.$$

$$\left. - \frac{1}{24}\,\left(-21 + 2\,q_{eff} - 9\,q_{eff}^2 + 4\,j_{eff} + 4\,\Omega_O\right)\,y^2\right] + O(y^3) \qquad (4.20)$$

were we used the redshift (see [193, 194] for example):[14]

$$y = \frac{z}{1+z} \tag{4.21}$$

It can be shown (see [194]) that the ΛCDM distance modulus has the same form as the one given above but with the effective cosmographic parameters substituted by the usual ones.

In the following we shall also use [192, 196]:

$$\hat{\mu}_{th}(y) = \mu_{th}(y) - \left[25 - 5 \log_{10}\left(\frac{\mathcal{H}_O}{c}\right)\right] \tag{4.22}$$

4.2.4   Confidence level

With the luminosity distance given by equations (4.15) and (4.16), one can test the hypothesis that this model is the model that describes the (local)[15] Universe against the null hypothesis that the Universe is described by the flat ΛCDM model.[16]

In order to do this, we fit the luminosity distance (4.15)-(4.16) with the *Union 2.1* SuperNova Compilation, than calculate the confidence level of our model.

References for the Union2.1 Compilation can be found in [197], were also the SNe data are provided; see also papers [198–214] and the NED database [215] for the position of the SNe in the sky. One has to notice that we used polar coordinates, while in astronomy equatorial coordinates are used, therefore one should remember that:

$$\text{declination from literature} = \frac{\pi}{2} - \alpha. \tag{4.23}$$

Following [192, 193, 196], using again a Metropolis-Hastings MCMC, we

---

[14]We use this redshift instead of the usual z, because, as has been pointed out in [195], the z redshift Taylor expansion has a convergence radius of 1 (while we will consider SNe with z redshift up to 3): this problem disappears when using the redshift y, since $y = 1 \mapsto z = \infty$ (other choices are possible).

[15]Only the local Universe, because of the Taylor expansion in redshift.

[16]I thanks the anonimous referee of [45] for this suggestion. See also [26] for an analogous treatment of the Lamaître-Tolman-Bondi spherical symmetric model (they find a confidence level of about 31% for LTB model and 26% for the ΛCDM model.

maximized the likelihood:[17]

$$\mathcal{L} \propto \exp\left[-\frac{1}{2}\left(c1 - \frac{c2^2}{c3}\right)\right] \qquad (4.24\text{a})$$

where (μ is the measured distance modulus, $\hat{\mu}_{th}$ is the theoretical one (4.22) and σ_i^2 are the squared errors of the measured distance modulus):[18]

$$c1 = \sum_{i=1}^{580} \frac{(\mu_i - \hat{\mu}_{th}(i)) \cdot (\mu_i - \hat{\mu}_{th}(i))}{\sigma_i^2} \qquad (4.24\text{b})$$

$$c2 = \sum_{i=1}^{580} \frac{(\mu_i - \hat{\mu}_{th}(i))}{\sigma_i^2} \qquad (4.24\text{c})$$

$$c3 = \sum_{i=1}^{580} \frac{1}{\sigma_i^2} \qquad (4.24\text{d})$$

In our MCMC, we imposed the constraints $D_L(y) > 0$ and $\delta(0) > -1$ in the case of the Szekeres model and also $\mathcal{H}^2 > 0$ in ΛCDM model.

In this case, we considered 20×10^3 elements long chain and we eliminated 25% of the elements at the beginning for the burn in phase, so our final chain was 30×10^3 elements long. The acceptance rate was about 0.3. Again we used the Gelman-Rubin test for the convergence: the $R - 1$ parameters were < 0.002

The errors on parameters are estimated with the Fisher matrix method [161, 216, 217].

If $\mathcal{L}$ is the likelihood and p_i are the considerd parameters, one first calculates the Fisher information matrix F_{ij} at the best fit point (were the likelihood is maximum):

$$F_{ij} = -\frac{\partial^2 \ln \mathcal{L}}{\partial p_i \, \partial p_j}$$

then one inverts it to find the *covariance matrix* C_{ij}. Finally, the errors on parameters are given by:

$$\Delta p_i = \sqrt{C_{ii}},$$

---

[17]As shown in [196], this likelihood is a likelihood marginalized over the Hubble parameter; this sholud be preferred because of the non homogeneous origin of the Union2.1 catalogue [196].

[18]In the following summations, 580 is the total number of SNe in the Union2.1 Compilation.

the squared root of the diagonal elements of the Covariance matrix.[19]

Fit results

The results of our fits are listed in table 4.1:for each model we give the fitted parameters and the corresponding error together with the logarothm of the likelihood.

We see that Szekeres models favours a local underdensity (in accordance with [26, 29–31], but we notice that we did not consider a particular model for the denstiy field). Nevertheless this void is too shallow to erase the acceleration, which has a value consistent with the ΛCDM one.[20]

If we use the value $\Omega_m = 0.31622 \pm 0.0062$ (see [1]), we find that the underdensity is about 30%.

We make some comments on the value of the parameter $j_O + \Omega_O$: in a flat ΛCDM *it has* to be $\equiv 2$,[21] and our best fit value for a Flat ΛCDM is in accordance with the the predicted one (this is in line with other findings [218] that use SNe data, but not with others that also use *Gamma Ray Bursts* [219–221]); in the Szekeres case, the presence of the (inhomogeneities induced) angular dependence changes the value of $j_O + \Omega_O$ taking it to the value of 0.63 ± 0.98 about 1.5σ far from the value of 2:[22] this might suggest that our model prefers different forms of Dark Energy (or a curved spacetime see [37, 222]).

It is known that SNe data alone cannot constraint the value of the spacetime curvature: to solve this issue and find out the value of Ω_k, we have to integrate SNe with, at least, CMB data.

To estimate the confidence level of our model, we use the likelihood-ratio

---

[19]Non diagonal elements of the covariance matrix, C_{ij} are related to the correlation between parameters p_i and p_j.

[20]The fact thtat the void is shallow also justifies *a posteriori* the use of the distance modulus calculated by the Union SNe collaboration supposing an homogeneous and isotropic universe: in a more complete work one should recalculate the distances of the SNe using the Szekeres metric starting anew with the light curve of the SNe.

[21]This is a prediction of the model: $\Omega_O = 1 - \Omega_k = 1$ for the flat metric and $j_O \equiv 1$ for a Dark Energy described by a cosmological constant.

[22]Starting from the definition of j_O and the Friedmann-like equaiton (A.1), it is easy to show that also Λ-Szekeres models (with a cosmological constant as DE) also predict $j_O \equiv 1$ and $j_O + \Omega_O \equiv 2$; for a curved spacetime, we have $j_O + \Omega_O \equiv 2 - 2\Omega_k$.

test (this time models *are* nested):

$$R = -2 \left(\ln \mathcal{L}_{\Lambda CDM} - \ln \mathcal{L}_{Szek.} \right) \tag{4.25}$$

R behaves like a chi-squared distribution with a number of degrees of freedom ($d.o.f.$) given by the difference of the $d.o.f.$ of the two models. In our case:

$$R = 2 \quad \Delta(d.o.f.) = 3. \tag{4.26}$$

Assuming (see [165]) that R follows a χ^2 distribution with 3 d.o.f, we find a probability of 19% for the ratio R to be smaller than 2 (for the correct model to be closer to the null hypothesis): so we are led to favour our model over the ΛCDM with a CL of 81%.

The confidence level for excluding our model is 19%, so there is a strong evidence that our model describes SNe data better than the flat ΛCDM.

Table 4.1: *Results of the fit of the Family II Szekeres cosmological model with arbitrary curvature and for the flat ΛCDM model.*
We also list the logarithm of the likelihood and degrees of freedom (d.o.f.).

Szekeres Family II up to third order				
q_O	$j_O + \Omega_O$	$\Omega_M \delta$	$\Omega_M \delta_x$	$\Omega_M \delta_y$
-0.44 ± 0.11	0.63 ± 0.98	-0.08 ± 0.09	0.03 ± 0.37	-0.52 ± 0.36
$\ln \mathcal{L}_{Szek.}$		-280.35	d.o.f.	575
Flat ΛCDM				
q_O	$j_O + \Omega_O$	$\Omega_M \delta$	$\Omega_M \delta_x$	$\Omega_M \delta_y$
-0.34 ± 0.09	2.18 ± 0.51	$//$	$//$	$//$
$\ln \mathcal{L}_{\Lambda CDM}$		-281.50	d.o.f.	578

4.3   Summary of the chapter and discussion

In this chapter, we considered the effects of the 0.5PN terms on the Tully-Fisher relation and found that it gives a deviation from linearity at small velocities; deviations from linearity are often found in observations and are interpreted as an effect of the DM halo: in our case they become an effect of the extrinsic curvature of the 3-space. We postulated that the study of the radial Tully-Fisher relation might give hints on the mathematical form of the ${}^3\widetilde{\mathcal{K}}_{(1)}$.

We also considered the possibility to explain Dark Energy as an effect of metrology. In line with the literature, we found that the problem is the use of homogeneous and isotropic metric to describe a Universe that is not (at least at small scales) neither homogeneous or isotropic: local structures and their evolution might mimic a Dark Energy driven expansion and/or influence the nature of the Dark Energy itself.

To verify this hypothesis, we considered non-homogeneous and non-isotropic Szekeres Family II cosmological models and calculated the Taylor series expansion of its luminosity distance and fitted the result with SNe data taken from the Union2.1 compilation.

We found that our model has a confidence level of about 80%, indicating that the use of an homogeneous and isotropic metric might be too *naïve*.

We also found (in accordance to the literature) that we live in an undendense region about $25 \div 30\%$ less dense than the average: this value is not enough to get rid of the Dark Energy, in fact the deceleration parameters of Sekeres and ΛCDM have the same values (within the errors), but it can *influence our interpretation of the nature of Dark Energy*. We see in fact that the jerk parameter is different between the flat ΛCDM and the Szekeres model because of the introduction of angular dependence (due to the inhomogeneities) indicating that the value measured in ΛCDM is *contaminated* by the presence of the inhomogeneities and so is the equation of state of Dark Energy.

SUMMARY AND OVERALL CONCLUSION

Così la donna cannone, quell'enorme mistero volò
tutta sola verso un cielo nero, nero si incamminò;
tutti chiusero gli occhi nell'attimo esatto in cui sparì
altri giurarono e spergiurarono che non erano mai stati lì

Francesco de Gregori - La donna cannone

Despite the fact that we have a model, the ΛCDM, that is in excellent agreement with the observational data, our understanding of the Universe is quite poor: only about 5.5% of it (made of baryonic matter and radiation) is known, the rest is *the dark side of the universe*: about 26 % is Dark Matter –a form of matter that does not interact with electromagnetic radiation, but has gravitational effect on the rest of the matter –and about 68% is Dark Energy –which is responsible for the acceleration of the expansion of the universe.

In the introduction we made a review on the possible nature of these forms of matter-energy:

The most widely accepted hypothesis for the nature of DM is that it is made of WIMPs (*Weakly Interactive Massive Particle*); modified form of gravity can also be an explanation (MOND, $f(R)$ theories);

The hypothesis that DE is a consequence of a Cosmological constant due to vacuum energy is the most widely accepted (but has some

flaws); in litterature it is suggested that the accelleration might be due to extended theory of gravity (through scalar fields such as *Galileon* or *Chamaleon*), but also that it is the consequence of the inhomogeneities of the universe.

In this work we did not follow any of those theories: we followed [102, 109], instead, where it is shown that (at least part of the) Dark Matter can be a consequence of the choice of the hypersurface that describes the 3-space embedded in the spacetime: the DM problem becomes a metrology problem.

More specifically, in this work we used the ADM tg formalism, introduced in [102–110]: an Hamiltonian reformulation of General Relativity based on a 3+1 foliation of spacetime using the (co)tetrads as fundamental variables (instead of the metric of the $3 - D$ hypersurface as in ADM gravity). In this formalism it was found that the equations of motion of a massive particle acquires a new term at 0.5PN order ($O(c^{-1})$) dependending on the derivatives of the (non-local) trace of the extrinsic curvature tensor at the PN order ${}^3\widetilde{\mathcal{K}}_{(1)}$ and therefore on the choice of the 3+1 foliation. This additional term can be put in the form of a mass term (the Dark Matter) depending on the choice of the foliation; this means that DM becomes an inertial relativistic effect depending on the conventions used in the measurements: *the conventional use of a flat Euclidean spacetime is the source of the effects known as Dark Matter.*

The aim of this thesis was to study *how much* Dark Matter can be interpreted as an inertial effect and study other possible (observable) effects of the 0.5PN terms on the propagation of light. We also considered the hypothesis that also the Dark Energy phenomenon might be a metrology problem. All in the hypothesis (contrary to what is generally assumed) that the 3-space is non-Euclidean.

To do that, we started from the Time Of Arrival (TOA) of a light ray using the Post Newtonian (PN) expansion of the ADM tg metric given in the introduction (equation (1.25)) with a non null ${}^3\widetilde{\mathcal{K}}_{(1)}$ (thus with a non Euclidean 3-hypersurface) and from that we derived the TOA for a pulsar signal (used in Pulsar Timing Array, PTA), for Very Long Baseline Interferometry (VLBI) and the redshift formula.

We found that the effect of the non-local ${}^3\widetilde{\mathcal{K}}_{(1)}$ on the TOA is twofold: it affects the propagation of the light ray through an integral correction τ_{3K}

which only depends on the non-local York time and its derivatives and a second correction coming from the redefinition of the proper time in the non-Euclidean 3-space (see equation (1.25)).

These corrections propagate in the PTA and in the redshift (and in the radial velocity) not in VLBI, because of its definition:[23] this means that the catalogue already in use for the definition of ICRF are not affected by our 0.5PN term.

We then asked which analytical form for ${}^3\widetilde{\mathcal{K}}_{(1)}$ might be used: we exploited the similarity between ours and $f(R)$ PN metric and made the ansatz that the space dependent part has a Yukawa-like form; for the time dependent part we considered three possibilities:

(a) We made no hypothesis at all on the time dependence and let it be a free function;

(b) We considered a linear ansatz;

(c) We considered a time free ansatz.

As noted in chapter 2, the interpretation of the Yukawa term (and of Dark Matter) is very different in ADM tg and $f(R)$ theories: in the former it is linked to the 3-space curvature and Dark Matter is a relativistic inertial effect, while in the latter the Yukawa term is a real potential wich corrects the Newtonian (they are both of order $O(c^{-2})$) one and Dark Matter is a consequence of the use of a *wrong* theory of gravity.

We used the three ansatz we made, to fit the rotation curve of the Andromeda (M31) galaxy in order to find out how much *real* Dark Matter is actiually needed. We modeled the luminous part of the Andromeda galaxy as a Hernquist bulge+thin disk and considered 7 models for the Dark Matter:

- An actual DM halo with a NFW profile and no Yukawa terms;

- No DM halo, but only Yukawa terms with the three ansatz described above;

- Three hybrid models with both an actual DM halo described by a NFW profile and one of the three ansatz for the Yukawa term.

---

[23]We remind that one has to subtrac the TOA od the same sources measured in two different and distant stations: this subtraction eliminates the dependence on the non-local York time.

As a result, we found that the model that best describes the data we used is the *hybrid model with a linear ansatz* which still requires about 58% of actual Dark Matter.

The second best model is the *model with No DM and no hypothesis on the form of the time dependent part of* ${}^3\widetilde{\mathcal{K}}_{(1)}$ and the third best is the correspondig hybrid model with only 15% if actual Dark Matter.

Thus, we see that *it is possible to eliminate the need for great part of the Dark Matter.*

With the values for the parameters we derived for M31, we estimated also the effects of the ${}^3\widetilde{\mathcal{K}}_{(1)}$ on PTA and redshift; we found that for the linear ansatz (both in the no DM and in the hybrid models) the correction for the PTA are of the order of tens of nanoseconds (possibly observable in the future) and are at the percent level for the redshift (correspondig to corrections to the radial velocity of the order of $100 \div 1000$ m/s).

Corrections for the time free ansatz are completely out of scale (they are of the order of seconds for the PTA!) and therefore rule out these models (which also fitted quite poorly the data of the rotation curve).

On the use in our Galaxy of parameters obtained from a fit of M31: this obviously a questionable choice, but one should not use lightly data from HI regions or obtained spectroscopically in our galaxy, since, as we saw, the propagation of a light ray in a non-flat 3-space implies the appearence of corrections still not well understood (we made a choice for the ${}^3\widetilde{\mathcal{K}}_{(1)}$, but other my be possible and results way change); one should, instead, use Cepheides and astrometrical data.

BUT THIS IS OUT OF MY LEAGUE

Finally, we asked ourselves if also the dark Energy can be an effect due to relativistic metrology. In agreement with literature, we found that the problem is that the ΛCDM is homogeneous and isotropic, while the actual Universe is not (at least at small scales): the use of an isotropic and homogeneous model might affect the measurement giving rise to the DE effects. Anisotropies and inhomogeneities also affects the nature of DE: it might appear to be evolving while it is actually not.

In order to test this hypothesis, we considered the 3rd order Taylor expansion of the Luminosity distance of Szekeres Family II models and used it to fit the SNe data from the Union2.1 compilation.

We found that we live in underdense region, but it is not enough to eliminate the need for Dark Energy (it is too shallow), in fact the deceleration parameter has the same value both in our fit of ΛCDM model and in the Szekeres one; the presence of the inhomogeneities, nevertheless, affects the value of the jerk parameter and through it the equation of state and the *nature* of the Dark Energy, since the introduction of the angular dependence (induced by the inhomogeneities) changes the value of the jerk paramter; actually this might also suggest that the spacetime is –locally –curved, but SNe data are not sensible to the value of Ω_k: to settle this issue other cosmological data are needed, particurarly CMB data.

We also found that the Szekeres family II cosmological model describes SNe data better that the ΛCDM model with a confidence level of 81%.

At the end of this work, we reached the following conclusions:

- Dark Matter can be interpreted as a metrology effect: by considering a non Euclidean 3-space, with our anstaz we could get rid of 42% of it in our best model and of *all of it* in the second best (this is our most important result);

- The curvature of the 3-space gives (possibly observable) correction to TOA of a pulsar signal and to the redshift and radial velocity of a source (probably not observable: there are too many unknown in the redshift formula at the present);

- In the Dark Energy case, we found that we live in a underdense region of the Universe: this can influence our understanding of the nature of Dark Energy but it value is too small to eliminate the need for it, so the use of a homogeneuos and isotropic model (such as the ΛCDM one) inflluences the nature of DE, not the need for it. Work is still needed on this topic to understand the effects of the curvature of spacetime

You are gonna carry that weight

Cowboy Bebop ep. 26
The real folk blues (part 2)

APPENDIX A

THE SZEKERES COSMOLOGICAL MODELS

In this Appendix we give a review on the Szekeres cosmological models and report some long formulae needed in chapter 4.

Other reviews on this subjet are: [14, 15, 26, 45, 46].

A.1   The model

Szekeres cosmological models are solutions of the Einstein's Field equations of the type:

$$ds^2 = dt^2 - e^{-2\,\alpha}\,dr^2 - e^{-2\,\beta}\left(dx^2 + dy^2\right) \qquad (A.1)$$

with irrotational dust as a source (see [14, 15, 26, 46, 178]). One can also include a cosmological constant as a source (see for example [14] and [223, 224]); Szafron [179] (see also [14, 26, 46]) considered radiation and dust as sources.

In their most general form they have no killing vectors [180] and are therefore inhomogeneous.[1]

---

[1]Particular choices for the arbitrary functions can, nevertheless, lead to models with symmetries

There are two families of this metric: the one with $\beta_{,r} \neq 0$ (Family I) and the one with $\beta_{,r} = 0$ (Family II). The function α always depends on all of the variables.

All Friedmann-Lemaître-Robertson-Walker and Lemaître-Tollman-Bondi models can be obtained from the Szekeres ones: in [46], see figures 2.1 and 2.2 for all the subcases of Family II and figure 2.4 for the subcases of Family I models (on this topic see also [14]); also, one should notice that, as proven in [14], for example, Family II can be obtained as the limit for $\beta_{,r} \to 0$ of the Family I.

In literature, there are at least three commonly used representation of the Szekeres models (see [14, 26, 46]): we will consider the Goode and Wainwright one.

Goode and Wainwright's is a representation of the metric for the case $\Lambda = 0$ in which it is evident that the models describe non linear perturbations of the FLRW metrics; it also encompasses properties of both families [181].

In this representation, he metric is given by:

$$ds^2 = dt^2 - S^2 \left[H^2 \, W^2 \, dr^2 + e^{2\nu} \left(dx^2 + dy^2 \right) \right]. \tag{A.2}$$

The function $S(t, r)$ is the solution of the equation:

$$\left(\frac{\dot{S}}{S} \right)^2 = \frac{2\mathcal{M}}{S^3} - \frac{\kappa}{S^2} \qquad \kappa = \{0, \pm 1\}, \tag{A.3}$$

where $\mathcal{M}(r)$ is an arbitrary function linked to the matter density (see later); in case a cosmological constant is present, we have [14, 46, 223, 224]:

$$\left(\frac{\dot{S}}{S} \right)^2 = \frac{2\mathcal{M}}{S^3} + \frac{\Lambda}{3} - \frac{\kappa}{S^2}, \qquad \kappa = \{0, \pm 1\}. \tag{A.4}$$

With or without a cosmological constant, we have:

$$\begin{aligned} H(t, x, y, r) &= A(t, x, y, r) - F(t, r) = \\ &= A(t, x, y, r) - \left[\beta_+(r) \, f_+(t) + \beta_-(r) \, f_-(t) \right], \end{aligned} \tag{A.5}$$

where $f_\pm(t)$ are independent solutions of the (Raychaudhuri) equation:[2]

$$\ddot{F} + 2\frac{\dot{S}}{S} \, \dot{F} - \frac{3\mathcal{M}}{S^3} \, F = 0 \tag{A.6}$$

---

[2]See [14] for their analytical expression in case there is no cosmological constant, and [224] for the case $\kappa = 0$ and $\Lambda \neq 0$.

and the $\beta_\pm(r)$ functions are arbitrary: the choice $\beta_\pm \equiv 0$ leads to Robertson-Walker models (see [14]).

In every case, the density field is given by:

$$\rho = \frac{6\,\mathcal{M}}{S^3}\left(1 + \frac{F}{H}\right) = \frac{6\,\mathcal{M}}{S^3}\,(1 + \delta) \tag{A.7}$$

where we defined the density contrast δ.

Another relation involving the density contrast needed in the calculation in chapter 4 is:

$$\frac{\dot{F}}{H} = -\frac{\dot{H}}{H} = \frac{\dot{\delta}}{1+\delta} \tag{A.8}$$

Finally, we calculate the shear tensor; it is given by[45]:

$$\sigma^r{}_r = \frac{2}{3}\frac{\dot{\delta}}{1+\delta} := \sigma; \tag{A.9}$$

$$\sigma^x{}_x = \sigma^y{}_y = -\frac{1}{2}\,\sigma \tag{A.10}$$

where we defined $\sigma = \dfrac{2}{3}\dfrac{\dot{\delta}}{1+\delta} = \dfrac{2}{3}\dfrac{\dot{F}}{H}$.

These were the common relations between the two families; the two families are defined as follows (in the case there is no Cosmological Constant among the sources):

Family I $(\beta_{,r} \neq 0)$

$\mathcal{M}_{,r}^2 + T_{,r}^2 \neq 0$, and $S = S(t, r)$.[3] Moreover:

$$e^\nu = \frac{f(r)}{a(r)\,(x^2+y^2) + 2\,b(r)\,x + 2\,c(r)\,y + d(r)} \tag{A.11}$$

f is arbitrary and:

$$ad - b^2 - c^2 \;=\; \frac{\epsilon}{4}, \qquad \epsilon = \{0, \pm 1\}; \tag{A.12}$$

$$W^2 \;=\; (\epsilon - \kappa f^2)^{-1}; \tag{A.13}$$

$$\beta_+ \;=\; -\frac{\kappa f \mathcal{M}_{,r}}{3\,\mathcal{M}}, \qquad \beta_- = \frac{f\,T_{,r}}{6\,\mathcal{M}}; \tag{A.14}$$

$$A \;=\; f\,\nu_{,r} - \kappa\,\beta_+. \tag{A.15}$$

---

[3]$T(r)$ is the, position dependent, time of the big bang, see [14].

The seven functions f, a, b, c, d, $\mathcal{M}$ and T are arbitrary, but one should remember that there is the freedom to make a change of coordinates of the form $r \mapsto g(r)$, so, keeping in mind condition (A.12), there are actually five arbitrary functions (see also [181]).

Family II $(\beta_{,r} = 0)$

$\mathcal{M}$ and T are constants, $S = S(t)$ and $W = 1$. Moreover:

$$e^{\nu} = \frac{1}{1 + \dfrac{\kappa}{4} \left(x^2 + y^2\right)} \qquad \kappa = \{0; \pm 1\} \qquad \text{(A.16)}$$

$$A = \begin{cases} e^{\nu} \left\{ a(r) \left[1 - \dfrac{\kappa}{4} \left(x^2 + y^2\right) \right] + b(r)\, x + c(r)\, y \right\} - \kappa\, \beta_{+}(r) & \kappa = \pm 1; \\[4mm] a(r) + b(r)\, x + c(r)\, y + \dfrac{\beta_{+}(r)}{2} \left(x^2 + y^2\right) & \kappa = 0; \end{cases}$$

a, b, c are arbitrary.

The five function a, b, c, $\beta_{\pm}$ are arbitrary, but, with the coordinate freedom reported above, one can see that there are actually four arbitrary functions (see [181]).

A.1.1   Null geodesics and redshift

We will now calculate the null geodesics for the Szekeres models.

If λ is the affine parameter along the geodesics (the observer is set at λ_O), we define the tangent vector:

$$k^{\alpha} = \frac{d\, x^{\alpha}}{d\, \lambda} \qquad \text{(A.17)}$$

then, the definition of null geodesics (for both families) is:

$$\begin{aligned} 0 &= k^{\alpha}\, k_{\alpha} \\ 0 &= (k^0)^2 - e^{2\nu}\, S^2 \left[(k^1)^2 + (k^2)^2 \right] - (HWS)^2\, (k^3)^2 \end{aligned} \qquad \text{(A.18)}$$

$$\frac{dk^{\alpha}}{d\lambda} = -\Gamma^{\alpha}_{\beta\gamma}\, k^{\beta}\, k^{\gamma} \qquad \text{(A.19)}$$

where the first and second line are the null condition.

Using the Christoffel symbols given in [45], we find that the null geodesics are:

Family I

$$\frac{d\,k^0}{d\lambda} = -\mathcal{H}\,(k^0)^2 + \frac{3}{2}\,\sigma\,(HWS\,k^3)^2; \tag{A.20}$$

$$\frac{d}{d\lambda}\left[k^1(e^\nu\,S)^2\right] = \frac{1}{2}\,\frac{\partial}{\partial x}(e^{2\nu}S^2)\left[\left(k^0\right)^2 - (HWS)^2\,(k^3)^2\right] + \tag{A.21}$$
$$- e^{2\nu}S^2\,\left(k^3\right)^2\,\frac{\partial}{\partial x}\,\ln\,(H);$$

$$\frac{d}{d\lambda}\left[k^2\,(e^\nu\,S)^2\right] = \frac{1}{2}\,\frac{\partial}{\partial y}(e^{2\nu}S^2)\left[\left(k^0\right)^2 - (HWS)^2\,(k^3)^2\right] + \tag{A.22}$$
$$- e^{2\nu}S^2\,\left(k^3\right)^2\,\frac{\partial}{\partial y}\,\ln\,(H);$$

$$\frac{d}{d\lambda}\left[k^3\,(HSW)^2\right] = (HWS)^2\left[\left(k^0\right)^2 - \left(k^3\right)^2\,(HWS)^2\right]\,\frac{\partial}{\partial r}\,\ln\left[(e^\nu\,S)\right] + \tag{A.23}$$
$$+ \frac{1}{2}\,\frac{\partial}{\partial r}\,[HWS]^2\,(k^3)^2.$$

Family II

$$\frac{d\,k^0}{d\lambda} = -\frac{d}{d\lambda}\,\ln(S)\,k^0 + \frac{3}{2}\,\sigma\,(HS\,k^3)^2 = \tag{A.24}$$

$$= -\mathcal{H}\,(k^0)^2 + \frac{3}{2}\,\sigma\,(HS\,k^3)^2; \tag{A.25}$$

$$\frac{d}{d\lambda}\left[k^0\,S\right] = \frac{3}{2}\,\sigma\,\left(HSk^3\right)^2; \tag{A.26}$$

$$\frac{d}{d\lambda}\left[k^1\,(e^\nu\,S)^2\right] = \frac{1}{2}\,\frac{\partial}{\partial x}(e^{2\nu}S^2)\left[\left(k^0\right)^2 - (HS)^2\,(k^3)^2\right] + \tag{A.27}$$
$$- e^{2\nu}S^2\,\left(k^3\right)^2\,\frac{\partial}{\partial x}\,\ln\,(H);$$

$$\frac{d}{d\lambda}\left[k^2\,(e^\nu\,S)^2\right] = \frac{1}{2}\,\frac{\partial}{\partial y}(e^{2\nu}S^2)\left[\left(k^0\right)^2 - (HS)^2\,(k^3)^2\right] + \tag{A.28}$$
$$- e^{2\nu}S^2\,\left(k^3\right)^2\,\frac{\partial}{\partial y}\,\ln\,(H);$$

$$\frac{d}{d\lambda}\left[k^3\,(HS)^2\right] = \frac{1}{2}\,(k^3)^2\,\frac{\partial}{\partial r}\,H^2. \tag{A.29}$$

Redshift

We define, as usual, the redshift with the relation:

$$1 + z = \frac{k^0(\lambda)}{k^0(\lambda_O)} \tag{A.30}$$

Finally, from equation (A.24) and the definition of redshift we just gave, we find the following equation needed in chapter 4:

$$\frac{d\,z}{d\lambda} = -\mathcal{H}\,k^0(0)\,(1+z)^2 + \frac{3}{2}\,\sigma\,(HS\,k^3)^2; \tag{A.31}$$

$$\frac{d^2z}{d\lambda^2} = -\frac{d\mathcal{H}}{d\lambda}\,k^0(0)\,(1+z)^2 - 2\,(1+z)\,\left(\mathcal{H}k^0(0)\right)\,\frac{dz}{d\lambda} + \tag{A.32}$$
$$+ \left(\frac{3}{2}\,\frac{\sigma'}{k^0(0)}\right)\,\frac{dz}{d\lambda}\,(k^3\,HS)^2 + \left(\frac{3}{2}\,\frac{\sigma}{k^0(0)}\right)\,\frac{d}{d\lambda}\,(k^3\,HS)^2$$

APPENDIX B

MCMC

In this appendix we review some generalities about Bayesian statistics, MCMC codes and the Gelman-Rubin criterion.

B.1 Bayesian statistics and Likelihood

There are two diferent interpretation of statistics: the Frequentis interpretation and the Bayesian one.

In the frequentist approach the probability is defined as the limit of the frequency of an event:

$$Pr = \lim_{N \to \infty} \frac{n}{N}$$

where n is the number of positive outcomes and N is the number of the trials.

In the Bayesian approach, instead, the probability is a distibution and its calculation is based on the Bayes theorem: the probability that our hypothesis H is true given the data the data is[1]

$$Pr\{H|data\} = \frac{Pr\{data|H\} \, Pr\{H\}}{Pr\{data\}} \tag{B.1}$$

where:

---

[1]We use the standard notation where $P\{A|B\}$ is the conditional probability of having A when B already happened.

- $Pr\{H\}$ is the *prior* distribution of H;

- $Pr\{H|data\}$ is the *posterior* probability (this tells what we want to know: the probability of H given the data);

- $Pr\{data|H\}$ is the *likelihood*: the probability of observing the data given H.

B.2   MCMC codes

A *Markov Chain Monte Carlo*, shortened by MCMC, is a method to obtain the posterior distributions.

A Markov Chain is a chain of elements genereted with a process with no memory (*Markovian*), i.e. a process in which the n-th element is generated knowing only the $(n-1)$-th element. The Monte Carlo part of these kind of codes constitutes the Markovian process.

These methods are guaranteed to converge to an equilibrium distribution (see [159]).

In the Metropolis-Hastings code we used, one samples the n-th element of the chain from a *prior* distribution in which the $(n-1)$-th element is taken to be the mean value (this is a Markovian process, since all information from all the previous elements is lost).

Prior distribution often used in MCMC codes are the Normal distributions (random walk MCMC) and the Uniform distribution.

B.3   Gelman Rubin criterion

The main problem in MCMC codes is to find out if the Markov Chain has converged to the equilibrium distribution and if the code has swept all the region around the maximum of thelikelihood. Many tests are avaliable, we used the Gelman-Rubin one.

The Gelman and Rubin criterion tests whether a chain has converged or not to the equilibrium distribution using a parameter called R (to be defined later in equation (B.2)): if R is close to 1 we have convergence.

It is a matter of convention how close to 1 R should be: usually one takes $R - 1 < 0.1$ [159]. In our models we had $R - 1 \approx 0.01$ except for the case of the no DM (c) where we had $R - 1 \approx 0.1$ for δ'.

B.3.1 The R parameter

This test must be done independetly for each parameter of the model: in the following we will consider the case of a model with a single parameter; the general case is a straightforward extension of this one.

For the application of this criterion one needs a number of chains $n > 2$, each with length m; the whole test, basically, is meant to confront the variance within a chain W and the variance between the chains B.

The within and between chains variance are given respectively by (we define $c_{j,i}$ the j-th element of the i-th chain, and $\bar{c}_i$ is the average value of the i-th chain):

$$W = \frac{1}{m} \sum_{j=1}^{m} \left[\frac{1}{n-1} \sum_{i=1}^{n} (c_{j,i} - \bar{c}_i)^2 \right];$$

$$B = \frac{n}{m-1} \sum_{j=1}^{m} \left[\bar{c}_j - \frac{1}{m} \sum_{i=1}^{m} \bar{c}_i \right]^2.$$

Finally one defines:

$$v\hat{a}r = \left(1 - \frac{1}{m} \right) W + \frac{1}{m} B$$

and then sets:

$$R = \sqrt{\frac{v\hat{a}r}{W}} \tag{B.2}$$

At the beginning of the sampling (the burn in phase), $R \gg 1$, since the code is far from the equlibrium distribution and $B \gg 0$; when the equilibrium is approached, $B \approx 0$ and $R \approx 1$.

CONVENTIONS

We gather here the convenctions and definitions used in this work. Metric signs $(+;-,-,-)$.

Object	Definition
$M_\odot$	Solar mass ($1.9 \ 10^{30}$ kg)
$R_\odot$	Distance of the Sun from the center ofthe Galaxy (7.6 kpc)
G	Gravitational constant ($6.67 \ 10^{-11}$ m^{3}kg^{-1}s^{-2})
L_C	$1.48086826741 \ 10^{-8} \ \pm 2 \ 10^{-17}$
η	Flat Minkowsky metric
x^μ	Cartesian coordinates
σ^A	Radar coordinates
μ	Index of cartesian coordinates; it runs form 0 to 3
A	Index for radar coordinates; it is split into a time coordinate (τ) and space coordinates ($r = \{1,2,3\}$)
(α)	tetrad index; it runs from (0) to (3). Latin letters (a), (b), $\ldots = \{1,2,3\}$
$\bar{a}$	Index for graviton's polarization; it has values 1 and 2;
$^4g_{AB}$	Spacetime metric in radar coordinates
n	Lapse function
n_r	Shift function
$^3e^r_{(\alpha)}$	Triad
$^3e_{(\alpha)r}$	Cotriad
Γ^r	Combination of the $R_{\bar{a}}$: $\Gamma^r = \gamma_{\bar{a}r} \ R_{\bar{a}}$

... continued

Object	Definition
$\gamma_{\bar{a}r}$	Set of coefficients such that:
	$\begin{cases} \sum_{\bar{a}} \gamma_{\bar{a}r}\, \gamma_{\bar{a}s} = \delta_{rs} - \dfrac{1}{3} \\ \sum_{r} \gamma_{\bar{a}r}\, \gamma_{\bar{b}r} = \delta_{\bar{a}\bar{b}} \\ \sum_{r} \sum_{\bar{a}} \gamma_{\bar{a}r} = 0 \end{cases}$
Σ_{τ}	Hypersurface at time τ
$\approx$	In Hamiltonian formalism it means that the equality holds only
	weakly (when all constraint are considered)
$(t, \vec{x})$	Coordinates for BCRS
$(T, \vec{\xi})$	Coordinates for GCRS

ACKNOWLEDGMENTS

BIBLIOGRAPHY

1. Plank collaboration, *Planck 2013 results. XVI. Cosmological parameters* (2013; `arXiv:1303.5076[astro-ph.CO]`).

2. Supernova Search Team Collaboration, *Astrophysical Journal* **116**, 1009 (1998).

3. Supernova Cosmology Project Collaboration, *Astrophysical Journal* **571**, 565 (1999).

4. A. Fressler, R. Hodak, S. Kovalenko, F. Simkovic, *Search for the cosmic neutrino background and KATRIN* (2013; `arXiv : 1304 . 5632[nucl-th]`).

5. E. Giusarma, R. de Putter, S. Ho, O. Mena, *Physical Review D* **88**, 063515 (2013).

6. V. Springel, L. Hernquist, *Monthly Notice of the Royal Astronomical Society* **339**, 312 (2003).

7. A. Friedmann, *Zeitschrift f'ur Physik* **10**, 377 (1992).

8. A. Friedmann, *Zeitschrift f'ur Physik* **21**, 326 (1924).

9. G. Lemaître, *Annales de la Societe Scientifique de Bruxelles* **A47**, 49 (1927).

10. H. Robertson, *Proceedings of the National Academy of Sciences of the United States of America* **15**, 822 (1929).

11. H. Robertson, *Review of Modern Physics* **5**, 62 (1933).

12. A. Walker, *The Quarterly Journal of Mathematics* **6**, 81 (1935).

13. S. Weinberg, *Gravitation and Cosmology: Principles and applications of the General theory of Relativity* (Jhon Wiley & Son, ed. 1, 1972).

14. J. Plebanski, A. Krasiński, *An introduction to General Relativity and cosmology* (Cabridge University Press, Cambridge, ed. 1, 2006).

15. H. Stephani, D. Kramer, M. Maccallum, C. Hoenselaers, E. Helrt, *Exact solutions of Einstein's Field Equations* (Cambridge University Press, Cambribge, ed. 2, 2003).

16. L. Amendola, S. Tsujikawa, *Dark Energy Theory and observations* (Cambribge University Press, Cambridge, ed. 1, 2010).

17. I. J. Aitchinson, *Supersymmetry and MSSM: an elementary introduction* (2005; `arXiv:hep-ph/0505105`).

18. S. Hawking, *Physics Letter B* **134**, 403 (1984).

19. J. Yokoyama, *Physical Review Letter* **88**, 151302 (2002).

20. J. Mukohyama, L. Randall, *Physical Review Letter* **92**, 211302 (2004).

21. G. Kane, M. Perry, A. Zytkow, *Physical Letter B*, 7 (2005).

22. A. Dolgov, F. Urban, *Physical Review D* **77**, 083503 (2008).

23. T. Mattson, *General Relativity and Gravitation* **42**, 567 (2010).

24. V. Marra, PhD thesis, Università di Padova, Dipartimento "Galileo Galilei", 2008.

25. A. Joice, B. Jain, J. Khoury, M. Trodden, *Beyond the Cosmological Standard Model* (2014; `arXix:1407.0059[astro-ph.CO]`).

26. K. Bolejko, A. Krasiński, M.-N. Célérier, *Structures in the universe by exact methods: Formation, Evolution, Interaction* (Cambribge University Press, Cambridge, ed. 1, 2009).

27. V. Marra, A. Notari, *Classical and Quantum Gravity* **28**, 164004 (2011).

28. V. Valkenburg, M. Kunz, M. Valerio, *Physics of the Dark Universe* **2**, 219 (2013).

29. I. Zehavi, R. Kirshner, A. Dekel, *Astrophysical Journal* **503**, 483 (1998).

30. K. Tomita, *Monthly Notice of Royal Astronomical Society* **326**, 287 (2001).

31. K. Tomita, *Astrophysical Journal* **529**, 38 (2000).

32. M. N. Célérier, *Astronomy & Astrophysics* **535**, 63 (2000).

33. H. Iguchi *et al.*, *Progress of Theoretical Physics* **108**, 809 (2002).

34. J. Pasqual-Sánchez, *Modern Physics Letter A* **14**, 1539 (1999).

35. W. Valkenburg, *Journal of Cosmology and Astroparticle Physics* **1201** (2012).

36. A. Romano, *European Journal of Physics C* **72**, 2242 (2012).

37. T. Biswas, A. Notari, W. Valkenburg, *Journal of Cosmology and Astroparticle Physics* **11**, 030 (2010).

38. D. Schwartz, *Accelerated expansion without dark energy* (2002; `arXiv: astroph/0209584`).

39. C. Wetterich, *Physical Review D* **67**, 043513 (2003).

40. T. Buchert, *General Relativity and Gravitation* **32**, 105 (2000).

41. T. Buchert, *General Relativity and Gravitation* **33**, 1381 (2001).

42. C. Clarkson, O. Umeh, *Classical and Quantum Gravity* **28**, 164010 (2011).

43. S. Green, R. Wald, *Physical Review D* **83**, 084020 (2011).

44. S. Räsänen, *Journal of Cosmology and Astroparticle Physics* **0611**, 3 (2006).

45. M. Villani, *Journal of Cosmology and Astroparticle Physics* **0614**, 015 (2014).

46. A. Krasiński, *Inhomogenehous cosmological models* (Cambridge University Press, Cambridge, ed. 1, 1997).

47. T. Jarred, *et al.*, *Astronomical Journal* **119**, 2498 (2000).

48. R. Tully, Y. Courtois Hél'ene end Hoffman, D. Pomarède, *Nature* **513**, 71 (2014).

49. F. Zwicky, *Helvetica Physica Acta* **6**, 110 (1933).

50. F. Zwicky, *Astrophysical Journal* **86**, 217 (1937).

51. A. Vikhlinin, A. Kravtsov, W. Forman, C. Jones, M. Markevitch, *et al.*, *Astrophysical Journal* **640**, 691 (2006).

52. V. Rubin, W. K. Ford Jr, *Astrophysical Journal* **159**, 379 (1970).

53. V. Rubin *et al.*, *Astrophysical Journal* **238**, 471 (1980).

54. V. Rubin *et al.*, *Astrophysical Journal* **289**, 81 (1985).

55. J. F. Navarro, C. S. Frenk, S. D. M. White, *Astrophysical Journal* **463**, 563 (1996).

56. D. Merritt, A. W. Graham, B. Moore, B. Terzić, *The Astronomical Journal* **132**, 2685 (2006).

57. J. Einasto, U. Haud, *Astronomy & Astrophysics* **223**, 89 (1989).

58. P. Schneider, J. Ehelers, E. Falco, *Gravitational lenses* (ed. 1, 1999).

59. M. Bartelmann, P. Schneider, *Physics Report* **340**, 291 (2001).

60. A. F. Boden, M. Shao, D. Van Buren, *The Astrophysical Journal* **502**, 538 (1998).

61. V. Springel *et al.*, *Nature* **435**, 329 (2005).

62. M. Boylan-Kolchin, V. Springel, S. D. M. White, A. Jenkins, G. Lemson, *Monthly Notice of the Royal Astronomical Society* **398**, 1150 (2009).

63. R. E. Angulo *et al.* (2012; `arXiv:1203.3216[astro-ph.CO]`).

64. A. A. Klypin *et al.*, *Astrophysical Journal* **740**, 102 (2011).

65. J. Primack, presented at the Proceedings of the Jerusalem Winter School, ed. by A. Dekel, J. Ostriker.

66. G. Jungman, M. Kamionkowski, K. Griest, *Physics Reports* **267**, 195–373 (1996).

67. K. Griest, M. Kamionkowski, *Physics Reports* **333-334**, 167–182 (2000).

68. G. Bertone, D. Hooper, J. Silk, *Physics Reports* **205**, 279–390 (2005).

69. S. Weinberg, *Cosmology* (Oxford University Press, Oxford, ed. 1, 2008).

70. R. D. Peccei, *Lecture Notes in Physics* **741**, 3 (2008).

71. M. Drewes, *Internationa Journal of Modern Physics E* **22**, 1330019 (2013).

72. M. Loewenstein, A. Kusenko, *The Astrophysical Journal* **714**, 652 (2010).

73. E. Bulbul *et al.*, *The Astrophysical Journal* **789**, 13 (2014).

74. DAMA Collaboration, *The DAMA experiment* (2013; `http://people.roma2.infn.it/~dama/web/home.html`).

75. CDMS Collaboration, *The CDMS experiment* (2014; `http://cdms.berkeley.edu`).

76. PICASSO Collaboration, *The PICASSO experiment* (2011; `http://www.picassoexperiment.ca`).

77. PAMELA Collaboration, *The PAMELA mission* (2006; `http://pamela.roma2.infn.it/index.php`).

78. The AMS Collaboration, *The AMS 02 mission* (2014; `http://www.ams02.org/`).

79. AGILE Collaboration, *The AGILE mission* (2007; `http://agile.rm.iasf.cnr.it/`).

80. The Fermi-LAT telescope, *The Fermi-Large Area Telescope* (2014; `https://www-glast.stanford.edu/`).

81. The LUX Collaboration, *LUX Dark Matterx* (2014; `http://lux.brown.edu/LUX_dark_matter/Home.html`).

82. The ICECUBE Collaboration, *ICECUBE Southpole Neutrino Observatory* (2014; `http://icecube.wisc.edu/`).

83. B. Barnabei *et al.*, *La Rivista del Nuovo Cimento* **26N**, 1 (2003).

84. K. Blum, *DAMA vs. the annually modulated muon background* (2011; `arXiv:1110.0857[astro-ph.HE]`).

85. J. Pradler, *On the Cosmic Ray moun Hypothesis for DAMA* (2012; `arXiv:1205.3675[hep-ph]`).

86. The PAMELA collaboration, *Nature* **458**, 607 (2009).

87. The AMS02 Collaboration, *Physical Review Letters* **110**, 141102 (2013).

88. J. Chang *et al.*, *Nature* **456**, 362 (2008).

89. The AMS Collaboration, *Physics Reports* **366**, 331, (2006).

90. Fermi LAT Collaboration, *Physical Review Letters* **108**, 011103 (2012).

91. I. Cholis, G. Dobler, D. P. Finkebeiner, L. Goodenough, N. Weiner, *Physical Review D* **80**, 123518 (2009).

92. D. Grasso *et al.*, *Astroparticle Physics* **32**, 140 (2009).

93. C. Nathaniel, presented at the Beyond the Standard Model after the first run of the LHC.

94. M. Milgrom, *The Astrophysical Journal* **270**, 365 (1983).

95. M. Milgrom, *The Astrophysical Journal* **270**, 371 (1983).

96. M. Milgrom, *The Astrophysical Journal* **270**, 384 (1983).

97. I. Ferreras, N. E. Mavromatos, M. Sakellariadou, F. Yusaf, *Physical Review D* **86**, 083507 (2012).

98. R. Sanders, *Lecture Notes on Physics* **720**, 375 (2006).

99. J. D. Bekenstein, *Physical Review D* **70**, 083509 (2004).

100. A. Nusser, E. Pointcountreau, *Monthly Notice of the Royal Astronomical Society* **366**, 969 (2006).

101. S. Capozziello, M. De Laurentis, *Physical Report* **509**, 167 (2011).

102. D. Alba, L. Lusanna, *Canadian Journal of Physics* **90**, 1131 (2012).

103. L. Lusanna, *General Relativity and Gravitation* **33**, 1579 (2002).

104. L. Lusanna, S. Russo, *General Relativity and Gravitation* **34**, 189 (2002).

105. R. De Pietri, L. Lusanna, L. Martucci, S. Russo, *General Relativity and Gravitation* **34**, 877 (2002).

106. D. Alba, L. Lusanna, *General Relativity and Gravitation* **39**, 2149 (2007).

107. D. Alba, L. Lusanna, *Canadian Journal of Physics* **90**, 1017 (2012).

108. D. Alba, L. Lusanna, *Canadian Journal of Physics* **90**, 1077 (2012).

109. L. Lusanna, presented at the Black objects in Supergravity - Springer Proceedings in Physics, ed. by S. Bellucci, p. 267.

110. S. Deser, C. Isham, *Physical Review D* **14**, 2505 (1976).

111. R. Arnowitt, S. Deser, C. Misner, *General Relativity and Gravitation* **40**, 1997 (2008).

112. C. W. Misner, K. S. Thorne, J. A. Wheeler, *Gravitation* (W.H. Freeman and company, San Francisco, ed. 1, 1973).

113. E. Poisson, *A relativist's toolkit. The Mathematics of black-hole mechanics* (Cambridge University Press, Cambridge, ed. 2, 2007).

114. P. A. Dirac, *Lectures on Quantum Mechanics* (Dover Publucation Inc., Mineola, New York, ed. 1, 2001).

115. M. Henneaux, C. Teitelboim, *Quantization of Gauge Systems* (Princeton University Press, Princeton, New Jersey, ed. 1, 1994).

116. P. Havas, *General Relativity and Gravitation* **19**, 435 (1987).

117. D. Alba, L. Luca, *Internation Journal of Geometrical Methods and Modern Physics* **7**, 33 (2010).

118. D. Alba, L. Lusanna, *Internation Journal of Geometrical Methods and Modern Physics* **7**, 185 (2010).

119. J. York jr, presented at the Sources of Gravitational Radiation, ed. by L. L. Smarr.

120. A. Qadir, J. Wheeler, presented at the, ed. by E. Gotsoma, G. Tauber.

121. J. Schwinger, *Physical Review* **130**, 1253 (1963).

122. R. M. Wald, *General Relativity* (University of Chicago Press, Chicago and London, ed. 1, 1984).

123. L. Eyer *et al.*, presented at the Proceedings of the XIth Hvar Astrophsical Colloquium, p. 115.

124. R. N. Manchester, *Classical and Quantum Gravity* **30**, 1 (2013).

125. C. Ma, M. Feissel, Eds., IERS technical note 23: Definition and realization of the Internation Celestial Reference System by VLBI astrometry of extragalactic objects, IERS.

126. G. Kaplan, *The IAU Resolutions on Astronomical Reference System, Time Scales, and Earth Rotation: Expalnation and implementation* (U.S. Naval Observatory, Washington, D.C., ed. 1, 2005).

127. K. A. van der Huct, *Proceedings of the twenty-sixth General Assemby, Prague 2006* (Cambridge University Press, Cambridge, ed. 1, 2008).

128. On behalf of the IERS/IVS Working Group, *The Second Realization of the International Celestial Reference Frame by Very Long Baseline Interferometry - IERS techincal note 35*, ed. by D. Fey Alan L.and Gordon, J. S. Jacobs Christopher.

129. S. M. Kopeikin, presented at the Reference Frames and Gravitomagnetism: Proceedings, ed. by J. Pascual-Sanchez, L. Floria, A. San Miguel, F. Vicente.

130. S. A. Klioner, M. H. Soffel, presented at the Proceedings of Symposium "The three-dimensional universe with GAIA, p. 305.

131. L. Lindegren, D. Dravnis, *Astronomy & Atrophysics* **401**, 1202 (2003).

132. D. Dravnis, D. Gulberg, L. Lindegren, S. Madsen, presented at the Precise stellar Radial velocities, ASP conference series, ed. by J. B. Hearnshaw, C. D. Scarfe, vol. 463, p. 41.

133. L. Lindegren, D. Dravnis, S. Madsen, presented at the Precise stellar Radial velocities, ASP conference series, ed. by J. B. Hearnshaw, C. D. Scarfe, vol. 463, p. 73.

134. S. Madsen, L. Lindegren, D. Dravnis, presented at the Precise stellar Radial velocities, ASP conference series, ed. by J. B. Hearnshaw, C. D. Scarfe, vol. 463, p. 77.

135. R. Hellings, *Astronomical Journal* **91**, 650 (1986).

136. R. Hellings, *Astronomical Journal* **92**, 1446 (1986).

137. I. I. Shapiro, *Physical Review Letters* **13**, 789 (1964).

138. R. N. Manchester, J. H. Taylor, *Pulsars* (W.H. Freeman and company, San Francisco, ed. 1, 1977).

139. D. Lorimer, M. Kramer, *Handbook of Pulsar Astronomy* (Cambridge University Press, Cambridge, ed. 1, 2005).

140. C. J. Moore, *The sensitivity of pulsar timing array* (2014; `arXiv: 1408.0739[gr-qc]`).

141. G. Hobbs *et al.*, *Classical and Quantum Gravity* **27**, 084013 (2010).

142. D. Backer, R. W. Hellings, *Annual Review of Astronomy and Astrophysics* **24**, 537 (1986).

143. A. Gontier, M. Feissel, C. Ma, presented at the IERS technical note 23: Definition and realization of the Internation Celestial Reference System by VLBI astrometry of extragalactic objects.

144. The Event Horizon Telescope Collaboration, *The Event Horizon Telescope* (2014; `http://www.eventhorizontelescope.org/`).

145. S. A. Klioner, S. M. Kopejkin, *Astrophysical Journal* **104**, 897 (1992).

146. D. Madison, S. Chatterjee, J. Cordes, *The Astrophysical Journal* **777**, 104 (2013).

147. J. Verbiest, M. Bailes, W. van Straten, G. Hobbs, R. Edwards, *et al.*, *Astrophysical Journal* **679**, 675 (2008).

148. S. Capozziello, M. de Laurentis, *Annalen der Physik* **524**, 545 (2012).

149. S. Capozziello, M. Franviglia, *General Relativity and Gravitation* **40**, 357 (2008).

150. S. Capozziello, M. de Laurentis, presented at the, ed. by K. Rosquist, Jantzen, R. T., R. Ruffini.

151. S. Mendoza, X. Hernandez, J. C. Hidalgo, T. Bernal, *Monthlt Notice of the Royal Astronomical Society* **411**, 226 (2011).

152. S. Capozziello, E. de Filippis, V. Salzano, *Monthly Notice of the Royal Astronomical Society* **394**, 947 (2009).

153. A. de Felice, S. Tsujikawa, *Living Reviews in Relativity* **13**, 1 (3 2010).

154. M. J. Reid, *Annual Reivew of Astronomy and Astrophysics* **31**, 345 (1993).

155. J. Binney, S. Tremaine, *Galactic Dynamics* (Princeton Univerity Press, Princeton, New Jersey (USA), ed. 2, 2008).

156. J. Geehan, M. Fardal, A. Babul, P. Guhathakurta, *Monthly Notice of Royal Astronomical Society* **366**, 996 (2006).

157. C. Carignan, L. Chemin, W. K. Huchtmeier, F. J. Lockman, *Astrophysical Journal Letters* **641**, 109 (2006).

158. R. Salow, T. Statler, *The Astrophysical Journal* **611**, 245 (2004).

159. B. A. Berg, *Markov Chain Monte Carlo simulations and their statistical analysis* (World Scientific, Florida State University, USA, ed. 1, 2004).

160. W. M. Bolstad, *Understanding computational Bayesian Statistics* (Wiley, ed. 1, 2010).

161. L. Verde, *A practical guide to Basic Statistical Techniques for Data Analysis in Cosmology* (2008; `0712.3028[astro-ph]`).

162. J. Kormendy, *Astrophysical Journal* **325**, 128 (1988).

163. L. Widrow, K. Perret, S. Suyu, *The Astrophysical Journal* **588**, 311 (2003).

164. R. Walterbros, R. Kennicutt, *Astronomy & Astrophysics* **198**, 61 (1987).

165. K. P. Burnham, D. R. Anderson, *Model selection and multimodel inference: A practical information-theoretic approach* (Springer, ed. 2, 2002).

166. H. Akaike, *Automatic control, IEEE Transaction* **19**, 716 (1974).

167. R. Tully, R. J. Fisher, *Astronomy & Astrophysics* **54**, 661 (1977).

168. M. Giovanelli, presented at the, ed. by S. Bonometto, J. Primack, A. Provenzale.

169. M. Aaronson, J. Huchra, J. Mould, P. Schechter, R. Tully, *The Astrophysical Journal* **258**, 64 (1982).

170. M. Persic, P. Salucci, *Monthly Notice of the Royal Astronomical Society* **248**, 325 (1991).

171. J. Mould, M. Han, G. Bothun, *The Astrophysical Journal* **347**, 112 (1989).

172. S. Gurovich *et al.*, *Publications of the Astronomical Society of Australia* **21**, 412 (2004).

173. S. McGaugh, J. Schombert, G. Bothum, W. de Blok, *Astrophysical Journal* **533**, L99 (2000).

174. M. Persic, P. Salucci, S. Fulvio, *Monthly Notice of the Royal Astronomical Society* **281**, 27 (1996).

175. I. Yegorova, P. Salucci, *Monthly Notice of the Royal Society* **377**, 507 (2007).

176. R. Giovanelli *et al.*, *The Astrophysical Journal* **477**, L11 (1997).

177. G. Ellis, *General Relativity and Gravitation* **41**, 581 (2009).

178. P. Szekeres, *Communications of Mathematical Physics* **41**, 55 (1974).

179. D. Szafron, *Communications of Mathematical Physics* **18**, 1673 (1977).

180. W. Bonnor, A. Sulainan, N. Tomimura, *General Relativity and Gravity* **8**, 549 (1977).

181. S. Goode, J. Wainwright, *Physical Review D* **26**, 3315 (1982).

182. M. Ishak, A. Peel, *Physical Review D* **85**, 083502 (2012).

183. M.-N. Célérier, *Astronomy & Astrophysics* **353**, 63 (2000).

184. K. Kainulainen, V. Marra, *Physical Review D* **83**, 127301 (2009).

185. K. Kainulainen, V. Marra, *Physical Review D* **84**, 063004 (2011).

186. K. Kainulaiken, V. Marra, presented at the Invisible Universe: Proceedings of the conference, vol. 1241, p. 1043.

187. W. Valkenburg *et al.*, *Physics of The Dark Universe* **2**, 219 (2013).

188. V. Marra *et al.*, *Monthly Notice of the Royal Astronomical Society* **431**, 1891 (2013).

189. C. Zunckel, C. Clarkson, *Physical Review Letters* **101**, 181301 (2008).

190. A. E. Romano, A. S. Starobinski, M. Sasaki, *The European Physical Journal* **72**, 2242 (2012).

191. I. Ben-Dayan, M. Gasperini, G. Marozzi, F. Nugier, G. Veneziano, *Physical Review Letters* **110**, 021301 (2013).

192. K. Bamba, S. Capozziello, S. Nojiri, S. D. Odintsov, *Astrophysics and Space Science* **342**, 155 (2012).

193. M. Demianski *et al.*, *Monthly notice of the Royal Astronomical Society* **426**, 1396 (2012).

194. K. Bamba, S. Capozziello, S. Nojiri, S. D. Odintsov, *Astrophysics and Space Science* **342**, 155 (2012).

195. C. Cattoen, M. Visser, *Classical and Quantum Gravity* **24**, 5985 (2007).

196. R. Amanhullah *et al.*, *The Astrophysical Journal* **716**, 712 (2010).

197. The Union Collaboration, *The Union2.1 compilation* (2012; `http://supernova.lbl.gov/Union/`).

198. R. Amanullah *et al.*, *Astronomy & Astrophysics* **486**, 375 (2008).

199. P. Astier *et al.*, *Astronomy & Astrophysics* **447**, 31 (2006).

200. B. J. Barris *et al.*, *The Astronomical Journal* **602**, 571 (2004).

201. G. Folatelli *et al.*, *The Astronomical Journal* **139**, 120 (2010).

202. M. Hamuy *et al.*, *Astronomical Journal* **112**, 2398 (1996).

203. M. Hicken *et al.*, *The Astronomical Journal* **700**, 1097 (2009).

204. S. Jha *et al.*, *The Astronomical Journal* **131**, 527 (2006).

205. R. Knop *et al.*, *The Astrophysical Journal* **598**, 102 (2003).

206. M. Kowalski *et al.*, **686**, 749 (2008).

207. K. Krisciunas *et al.*, *The Astronomical Journal* **130**, 2453 (2005).

208. G. Miknaitis *et al.*, *The Astrophysical Journal* **666**, 674 (2007).

209. S. Perlmutter, *the Astrophysical Journal* **517**, 565 (1999).

210. A. G. Riess *et al.*, *The Astrophysical Journal* **659**, 98 (2007).

211. A. Riess *et al.*, *The Astronomical Journal* **117**, 707 (1999).

212. A. Riess *et al.*, *The Astrophysical Journal* **607**, 665 (2004).

213. N. Suzuki *et al.*, *The Astrophysical Journal* **746**, 85 (2012).

214. J. L. Tonry *et al.*, *The Astrophysical Journal* **594**, 1 (2003).

215. NASA, JPL, CalThec, ipac, *NED* (2014; `http://ned.ipac.caltech.edu/`).

216. R. Fisher, *Journal of the Royal Statisitcal Society* **98**, 39 (1935).

217. D. Coe, *Fisher Matrix and confidence ellipses: a Quick-start guide and software* (2009; `0906.4126-[astro-ph.IM]`).

218. D. Rapetti *et al.*, *Monthly Notice of the Royal Astronomical Society* **375**, 1510 (2007).

219. S. Capozziello, R. Lazkok, V. Salzan, *Physical Review D* **84**, 124061 (2011).

220. E. Pedipalumbo *et al.*, *Monthly Noticel of the Rosyal Astronomical Society* **441**, 3643 (2014).

221. S. Capozziello, L. Izzo, *Astronomy & Astrophysics* **490**, 31 (2008).

222. T. Clifton, P. Ferreira, J. Zuntz, *Journal of Cosmology and Astroparticle Physics* **07**, 029 (2009).

223. J. Barrow, J. Stein-Schables, *Physical Letters A* **103**, 315 (1984).

224. N. Meures, M. Bruni, *Physical Review D* **83**, 123519 (2011).